2004

Derivation of wheat yield and rangeland productivity in the northern Great Plains using MODIS algorithms

Matthew Clark Reeves
The University of Montana

Maureen and Mike
MANSFIELD LIBRARY

The University of

Montana

Permission is granted by the author to reproduce this material in its entirety, provided that this material is used for scholarly purposes and is properly cited in published works and reports.

Please check "Yes" or "No" and provide signature

Yes, I grant permission   X

No, I do not grant permission   _____

Author's Signature: _____

Date: July 27, 2004

Any copying for commercial purposes or financial gain may be undertaken only with the author's explicit consent.

8/98

Derivation of Wheat Yield And Rangeland Productivity In The Northern Great Plains using MODIS algorithms

by

Matthew Clark Reeves

B.S. Washington State University, 1995

M.S. Arizona State University, 1999

Presented in partial fulfillment of the requirements for the degree of

Doctor of Philosophy

The University of Montana

July 2004

Approved by:

_____
Committee Chairperson

_____
Dean, Graduate School

8-27-04
_____
Date

UMI Number: 3139041

INFORMATION TO USERS

The quality of this reproduction is dependent upon the quality of the copy submitted. Broken or indistinct print, colored or poor quality illustrations and photographs, print bleed-through, substandard margins, and improper alignment can adversely affect reproduction.

In the unlikely event that the author did not send a complete manuscript and there are missing pages, these will be noted. Also, if unauthorized copyright material had to be removed, a note will indicate the deletion.

UMI®

Agricultural and Rangeland Productivity Patterns in the Northern Great Plains Estimated With MODIS Vegetation Data

Committee Chair Dr. Steven W. Running

Abstract

   Agricultural and rangeland land uses occupy large areas in the western United States. An estimated 23 million ha of rangeland and pasture and 6.5 million ha of croplands exist in Montana alone. Ground based reconnaissance provides more accurate measures of crop and rangeland vegetation productivity but is impractical for such large areas. Remote sensing has been promoted as a diagnostic tool for analyzing vegetation productivity given its' synoptic, objective and timely coverage. The Moderate Resolution Imaging Spectrometer (MODIS) provides land products in addition to imagery. This study was conducted to evaluate the efficacy of selected MODIS algorithms for deriving wheat yield and characterizing intra - and inter - annual rangeland vegetation dynamics. This task was completed in three steps. Each step necessarily builds on knowledge gained during the progression of the research. First, I compare MODIS - derived vegetation productivity with measures of above - ground green biomass in the Little Missouri National Grasslands. Second, county, climate district and state level wheat yield is derived from MODIS gross primary productivity (GPP) and compared with observed yield from the same spatial domains. Third, I formulate a spring wheat yield model for Montana driven by MODIS vegetation data. Results demonstrate that although MODIS vegetation products have some improved characteristics over earlier platforms (e.g AVHRR and ETM+) they are still restricted by the same limitations of relating coarse resolution remote sensing data to ground based biophysical phenomena identified decades earlier. As a result, areas needing further research are identified and suggestions for further evaluating rangeland vegetation and wheat yield using MODIS algorithms are provided.

Acknowledgements

There are many who deserve credit and thanks as contributors to my education, sanity and quality of life during this five - year ordeal. First I thank my advisor Dr. Steve Running and my committee members Dr.'s Lloyd Queen, Rama Nemani, Mark Jensen and Don Bedunah for providing support and direction. Youngee Cho, the real boss, kept me out of trouble and I appreciate our pleasantly distracting conversations. I thank Carl and Jim and the Pixel Ranch gang for providing suggestions. Dr.'s Zhao and Heinsch deserve special mention for the many hours of scientific conversation, which gave me inspiration for new ideas. I owe a great deal of my success to the computer guys, Saxon Holbrook, Andrew Neuschwander, Andy Michaelis, and Chad Bowker, who made computers, easy, fun, and dependable. My family also deserves credit for their encouragement, continued love and support and raising me to have enough confidence to get this done. Finally, I thank my wonderful wife Sonja, for putting up with me and acting as a source of inspiration and encouragement.

Reproduced with permission of the copyright owner. Further reproduction prohibited without permission.

Table of Contents

List of Tables

List of Figures

CHAPTER 4

CHAPTER 1

REMOTE SENSING of RANGELAND AND AGRICULTURAL VEGETATION

Overview

The goal of this dissertation research is to explore the potential of MODIS derived vegetation productivity for quantitatively characterizing rangeland and agricultural patterns on the Northern Great Plains. This document is organized into five chapters, ordered chronologically, to demonstrate progressive understanding of MODIS products and potential implications of the research. The common thread linking each of these stand alone chapters is the exploration of this new satellite data stream and a critical evaluation of appropriate spatial scale for applying MODIS vegetation data within the context of my research.

Statement of Problem

In the western United States we are blessed with an, albeit decreasing, abundance of agricultural and rangeland landscapes. Montana alone hosts nearly 23 million ha of pasture and rangeland and roughly 6.5 million ha of croplands (Fisher et al. 1998). Most of the rangelands in the west occur in relatively remote areas making quantification of vegetation productivity exceptionally challenging, despite the need for such data. Different authors use different criteria for determining the spatial extents of rangelands, though Global estimates for rangeland are as high as 50 – 70% of the total land surface (Holechek et al. 1989). Vogelmann et al. (2001) estimate that shrublands and grasslands are 34% of the total area in the conterminous USA (Hunt et al. 2003).

The situation is different for crops because producers have reasonably good estimates of crop yield, and therefore are not necessarily dependent upon yield estimates,

particularly from satellite imagery. But, for the purposes of drought mitigation, crop insurance and averting disastrous crop failures, it is important to understand regional crop production patterns. This is especially the case in developing countries that have few, if any, regularized yield monitoring systems.

Ground based assessment techniques, such as plot level biomass measurement, or more recently, in the case of crops, yield monitors on crop harvesting machinery remain the most reliable method for characterizing vegetation productivity. However, given the large expanses of crop and rangeland in the western United States, comprehensive ground based reconnaissance at regular temporal and spatial intervals is impractical.

This is problematic as time is a critical factor for evaluating rangelands and crops because drought conditions can significantly alter ecological conditions and economic returns from a region. Although finer resolution spaceborne sensors, such as the widely used Landsat Enhanced Thematic Mapper plus (ETM+) provide sufficient resolution for detailed spatial analyses, they provide limited spatial and temporal coverage. Often, during the growing season, ETM+ data may be un-useable due to clouds given the sensors repeat frequency of 16 days. In contrast, timely, synoptic coverage is the forte of the MODIS vegetation products, making them an attractive tool for monitoring regional crop and rangeland productivity despite their 1-km spatial resolution. Unfortunately, in spite of the widely recognized need for regular monitoring of crop and rangeland resources, few studies to date have focused on using MODIS vegetation data from a managerial perspective, though many have used other forms of remotely sensed imagery. This is partly due to the infancy of the MODIS data stream and partly from the nature of University research in general. Hence the central focus of this research is investigating

the role of MODIS vegetation products for evaluating selected aspects of agricultural and rangeland landscapes in the Northern Great Plains.

The conclusions supported as a result of this research are similar for both systems in that, I provide suggestions for appropriate spatial scales and what kind of questions can suitably be answered with MODIS vegetation data. While not exhaustive, this research provides much needed insight to the behavior and suitability of MODIS vegetation data for evaluating crop and rangeland systems from a realistic, and at times, critical standpoint.

Background

Rangeland Remote Sensing

One of the first research activities was to examine the usefulness of MODIS vegetation productivity data for range management. Even after completing this dissertation, that task remains largely unsatisfied. The reasons for this are many and beyond the scope of a single document. However, two overriding factors have prevented operational use of nearly any remote sensing data for the purposes of range management owed largely to the mismatch in the information needed by managers and the information that can realistically and practically be derived from remote sensing (Hunt et al. 2003).

First, most management decisions are based on factors which are not resolved using most practical means of remote sensing, especially form a satellite perspective. For example, utilization of key species at the allotment (or finer) level often instigates removal of livestock from an area. This level of detail is not detectable in most forms of remote sensing data, particularly spaceborne instruments. This is not to say however, that given enough time, money and appropriate objectives, one could not devise scientifically

and managerially interesting products based on remote sensing. As Tueller (1989)

suggests, remote sensing *does* hold significant promise as an analysis tool for rangelands,

but not to the degree those in the in the industry would like to think. Second, smaller

grazing allotments can usually be characterized more quickly and accurately by

traditional ground based reconnaissance methods on an individual basis. Herein lays the

conundrum. Although we can more accurately characterize key rangeland components

using ground based methods it is nearly impossible to evaluate all grazing allotments in a

region using these techniques. This exemplifies the need for alternate means of data

collection, which remote sensing can help provide.

Major concerns facing range managers are invasive weeds, time of greenup,

utilization, vegetation species composition, vegetation productivity, and rangeland health.

A wide variety of satellite remote sensing platforms differing in repeat frequency, spatial

resolution and radiometric precision are available for use as tools to asses the vegetative

state of rangelands and have been used to examine rangeland condition (Pickup et al.

1994), desertification (Dregne and Tucker 1988,Nicholson et al. 1998) productivity

(Anderson et al. 1993,Pickup 1996) and stocking rate (Oesterheld et al. 1998). Other

studies have successfully mapped noxious weed infestations using higher spectral and

spatial resolution imagery. For example, the Airborne Visible Infrared Imaging

Spectrometer (AVIRIS) has been used to identify leafy spurge infestations (Williams and

Hunt 2002) on rangelands in north eastern Wyoming. The fine spatial scale required for

appropriately addressing rangeland vegetative characteristics is usually accompanied by

limited repeat frequency. For example, it is difficult, if not impossible to get a temporal

growth profile from Ikonos, AVIRIS, ETM+ or ASTER data. In contrast, many

management schemes require information for large areas within an extended temporal framework, as in the case of biomass utilization or trends in production. So we have the puzzling difficulty of large landscapes with detailed monitoring requirements and remote sensing platforms which are generally ill-suited to address most site specific concerns unless time, money and personnel are unlimited. To this end, addressing the top concerns of the range management community using merely remote sensing data is, for most purposes, pushing the technology beyond practical limits and certainly exceeds the scope of this dissertation. However, given that a major research focus of NTSG has been the derivation and ,more recently, application of the MODIS vegetation productivity data stream; I wanted to simultaneously determine the usefulness of these data for assessing rangeland vegetation and the appropriate degree of spatial aggregation for applying these data in rangeland environments.

Monitoring biomass conditions has been a key subject of past research endeavors in rangeland environments. In particular, the AVHRR has been extensively used to evaluate rangeland biomass (Justice and Hiernaux 1986, Prince and Tucker 1986, Tucker et al. 1986, Nicholson et al. 1998). The NDVI has been the most common application of AVHRR data for assessing the state of vegetation. The NDVI is calculated as (NIR-RED)/(NIR+RED) where NIR is the reflectivity of the near infrared waveband and RED is the reflectivity of the red waveband from a remote sensing instrument (Justice et al. 1985). The popularity and wide use of AVHRR NDVI is owed partly to its simplistic formulation and inherent link to biophysical rates and largely because until recently AVHRR was the instrument of choice for collecting coarse resolution imagery for large regions due to its twice daily coverage and synoptic view (Peters et al. 2002).

Although NDVI is linked to many vegetative traits such as vegetation cover (Schmidt and Gitelson 2000), photosynthetic capacity (Asrar et al. 1992) and biomass (Prince and Tucker 1986, Box et al. 1989, Wylie et al. 1995), it is not itself a biophysical measure and must therefore be indirectly related to a vegetative characteristic vicariously. These vicarious linkages are most often expressed as regression formulas whose application is spatially and temporally limited to data used in the formulation. In particular, this means that quantitative assessment of rangeland productivity is only possible in a retrospective empirical manner (e.g. Prince and Tucker (1986) and Wylie et al. (1995).

Thus, there is niche for a regional rangeland vegetation productivity monitor that can be applied in a timely manner and is not solely dependent on empiricism yet provides a reasonably accurate depiction of regional rangeland vegetation patterns. To facilitate this endeavor, the MODIS leaf area index (LAI)/fraction of photosynthetically active radiation (FPAR) data are combined with meteorological inputs and used to produce daily estimates of gross and net primary productivity (GPP and NPP) and net photosynthesis (PSN_{net}) in a simplified plant growth algorithm. Few if any studies, however, have sought to examine the performance of MODIS vegetation products in rangeland environments. This is largely due to the infancy and historical instability of the data stream.

The Terra and Aqua MODIS sensors were successfully deployed by NASA on 18, December 1999 and 4 May, 2002 respectively. Several decades of improved communications, hardware, software, data storage capacity, and satellite engineering enable the MODIS instrument to provide enhanced monitoring capabilities. A suite of

satellites has been used to measure and monitor biophysical constituents of the earth's

surface, each exhibiting different characteristics. The MODIS sensor, however, is unique

because it combines both the spatial and spectral resolution of several satellites on a

single platform. MODIS exhibits greater radiometric resolution than traditional sensors

providing a broader range of measurement and therefore increased sensitivity to small

changes in spectral reflectivity. The MODIS offers 36 spectral channels, as compared to

five on the AVHRR instrument, seven on Landsat TM or eight on ETM+. These

characteristics provide new capability for terrestrial remote sensing intended for global

change research for which MODIS generates a suite of standard products designed to

remove the burden of most data processing requirements (Justice et al. 1998). Although

Landsat systems offer greater spatial resolution (30 meter) they exhibit a revisit time of

16 days. With clouds they often yield only two to three scenes per growing season.

Changes in surface conditions are sufficiently rapid to make high-temporal-frequency

coverage a requisite for monitoring vegetation, particularly in semi-arid regions for which

the MODIS primary productivity estimates (eight-day summations) are uniquely suited

(Reeves et al. 2001). The combination of improved sensor characteristics and high

temporal frequency of data collection makes MODIS a logical choice for monitoring

regional patterns of rangeland and agricultural vegetation alike.

Remote Sensing of Wheat Growth and Yield

Crops provide a powerful testbed for evaluating the reliability of remote sensing

based vegetation metrics because of our wealth of knowledge of crop growth and

extensive data base of yield provided the USDA Published estimates Database (PEDB).

Since I had no background in agricultural systems or crop modeling, I was originally

excited by the opportunity of using the extensive data base of yield to compare with modeled predictions. However, I soon learned that having an abundance of observations is a double-edged sword. On one hand, observations provide an excellent means of testing model theory, design and overall performance. On the other hand, this makes the modeling endeavor more risky from the standpoint of publication, as it usually brings model weaknesses to the forefront. This is in sharp contrast to models for natural environments, or global vegetation models, where there are few if any observations for validation. Despite the academic risk of this environment and my original lack of knowledge of developing crop models, I faithfully maintained this endeavor for the course of my Ph.D. education.

Part of the difficulty developing a regional yield monitoring system is a lack of comparable models to provide background information. Traditionally, wheat yield models have been broad scale and retrospective or extremely, intricate, point based simulators of wheat yield. With the exception of the USDA Foreign Agricultural Service (FAS), broad scale models have, almost exclusively, used AVHRR NDVI to derive empirical, statistical relationships between NDVI and crop yield. However, information surrounding the details of both USDA foreign large scale wheat yield forecasting is difficult to obtain. Nevertheless, it appears that, the FAS uses 25 mile X 25-mile meteorological data to drive a simple water balance model. Application of this and other strictly empirical models (e.g. Brocklehurst 1977, Gao et al. 1993) is limited to areas where the regression equations were formulated. More recently Labus et al. (2002), derived a very simplistic experiment in which growing season NDVI was regressed with yield for different climate districts in Montana. While these retrospective analyses

provide insight to past performance and suffice for calibration, they do little to aid the need for near real time yield information.

On the other extreme, several field-level, cultivar specific wheat growth models are currently available. The most widely used are CERES-wheat (Ritchie and Otter 1985) and Sirius (Jamieson et al. 1998). These models essentially "grow" a wheat kernel from emergence to maturity by simulating complex physiological interactions between the wheat plant and surrounding environment. Management, weather, soil and crop genetic data are required to achieve accurate yield calculations yet are difficult if not impossible to obtain for a region. Due to their complex nature intricate, point level models are not suitable for regional estimates of yield and are consequently not widely used by organizations that might benefit from this information. For these reasons, I perceive a niche for a model that uses remote sensing data and is a compromise between large-scale empirical relationships and extremely small-scale, highly detailed, physiologically complex field level models.

The concept of using satellite remote sensing data for analyzing crop yield and as an input to crop models is not new. Use of satellite remotely sensed data for crop production research has generally fallen into one of four categories; First, and most simplistic is relating temporal integration of imagery (usually AVHRR NDVI) to yield in statistical models. This approach was used by Wiegand et al. (1979), Tucker et al. (1981), Benedetti and Rossini (1993), Gupta et al. (1993) and Doraiswamy and Cook (1995) and others previously mentioned. The second application of remotely sensed data is derivation of critical model parameters which are difficult to estimate using other means across the landscape using traditional techniques. This includes, but is not limited

to, estimating surface temperature for improving evapotranspiration estimates (Moran et al. 1994), computing crop emergence (Badwhar 1980), estimating crop moisture deficit (Doraiswamy and Thompson 1982, Moran et al. 1994) and soil moisture status. In the second method, a time series of remotely sensed measurements is used as calibration data for the crop model. For example, Doraiswamy et al. (2003) used Landsat TM and AVHRR NDVI to adjust simulated NDVI derived from EPIC (Erosion Productivity Impact Calculator) and SAIL (Verhoef 1984) a one-dimensional radiative transfer model. The adjustment of simulated NDVI was ultimately used to calibrate LAI as predicted by EPIC. The final approach, which was used in this research, involves computation of key biophysical crop parameters from remote sensing data and directly feeding them into the model. Crop parameters successfully used in this method are measures of light interception with the canopy, principally leaf area index (LAI). This approach has not been used on a regular basis because LAI is usually estimated with regression techniques that are not stable through space and time and must therefore be re-evaluated for different regions, rendering them nearly useless for practical, wide-scale implementation. However, one of the key variables derived from MODIS data is fraction of photosynthetically active radiation absorbed by the plant canopy (FPAR). Thus, it seemed logical to utilize these data as a direct input to a simple wheat yield model, the formulation of which is discussed in Chapter 4.

The research presented in this dissertation fills a gap in the current body of knowledge of crop yield assessment and rangeland vegetation productivity as estimated with MODIS data. As demonstrated, past research has focused on similar regions, but not with MODIS vegetation products, and not usually with management implications in

mind. The ultimate findings of this research provide valuable insight to future users of these vegetation products, as it advances our understanding of the problems and merits of linking remotely sensed data to vegetation productivity in both crop and rangeland environments. Specifically, when developing this research I sought to move beyond simply modeling vegetative and grain yield by applying statistical models.

Objectives

This research seeks to answer four basic questions. To what extent does the MODIS vegetation productivity product emulate trends in rangeland vegetation? Can wheat yield be accurately estimated for entire regions using only the MODIS vegetation product suite? If not, what changes can be made to the modeling environment and input data stream to improve yield estimates? and, what is the appropriate spatial domain for characterizing regional rangeland productivity and wheat yield from MODIS data? In order to improve our understanding of the performance and usefulness of MODIS vegetation data in a managerial context this research will:

1) Describe the spatial and temporal relationship between MODIS vegetation productivity estimates and scaled, plot based measures of above-ground green biomass in a heavily grazed rangeland setting (Chapter 2).

2) Explore the usefulness and feasibility of using standard MODIS products for estimating regional wheat yield without the use of retrospective empirical analyses (Chapter 3).

3) Develop a regional spring wheat yield monitor for Montana by exploiting the strengths and subverting the weaknesses of the process developed in Chapter three.

To achieve these objectives I relate seasonal MODIS net photosynthesis (PSN$_{net}$) to above – ground green biomass (AGGB) for the 2001 and 2002 growing seasons. The relations during the 2001 growing season were much better than in 2002. At this stage I conducted an in-depth analysis to determine the cause of the different results between the years and found years with much higher than normal growing season precipitation (2001) followed by a very dry year (2002) makes remote sensing of AGGB difficult. In addition, I characterize the inter-annual variation in net primary productivity of rangelands for 2001 through 2003. Significant differences in NPP ($P \leq 0.05$) were observed between years owed mainly to the significant ($P \leq 0.05$) decline in growing season precipitation during the same time. These large differences provided an excellent test bed for a first look at the behavior of MODIS vegetation productivity products in rangeland environments.

Next, in Chapter three, I integrate MODIS GPP estimates over an apparent growing season and compute yield at the county, climate district and state levels. Yield estimates were compared with observations aggregated over the identical spatial domains. Progressive levels of spatial aggregation provide increasingly better predictive ability for Montana and North Dakota. Critical examination revealed several factors inhibiting accurate wheat yield estimation for counties.

Finally, in Chapter four, these inhibiting factors were partially ameliorated and wheat yield was estimated for counties of Montana using a process based phenomenological wheat yield model driven by MODIS FPAR. Results were greatly improved over those demonstrated in Chapter three, but still indicated that spatial aggregation provides more reliable yield estimates.

Literature Cited

Amir, J. and Sinclair, T.R., 1991, A model of the temperature and solar-radiation effects on spring wheat growth and yield. *Field Crops Research*, **28**, 47-58.

Anderson, J.A., Hanson, J.D. and Haas, R.H., 1993, Evaluating Landsat Thematic Mapper derived vegetation indices for estimating above-ground biomass on semiarid rangelands. *Remote Sensing of Environment*, **45**, 165-175.

Asrar, G., Myneni, R.B. and Choudhury, B.J., 1992, Spatial heterogeneity in vegetation canopies and remote sensing of absorbed photosynthetically active radiation: A modeling study. *Remote Sensing of Environment*, **41**, 85-103.

Badwhar, G.D., 1980, Crop emergence date determination from spectral data. *Photogrammetric Engineering and Remote Sensing*, **46**, 369-377.

Benedetti, R. and Rossini, P., 1993, On the use of NDVI profiles as a tool for agricultural statistics: The case study of wheat yield estimate and forecast in Amilia Romagna. *Remote Sensing of Environment*, **45**, 311-326.

Box, E.O., Holben, B.N. and Kalb, V., 1989, Accuracy of the AVHRR vegetation index as a predictor of biomass, primary productivity and net CO_2 flux. *Vegetatio*, **80**, 71-89.

Brocklehurst, P.A., 1977, Factors controlling grain weight in wheat. *Nature*, **266**, 348-349.

Doraiswamy, P.C. and Cook, P.W., 1995, Spring wheat yield assessment using NOAA AVHRR data. *Canadian Journal of Remote Sensing*, **21**, 43-51.

Doraiswamy, P.C., Moulin, S., Cook, P.W. and Stern, A., 2003, Crop yield assessment from remote sensing. *Photogrammetric Engineering and Remote Sensing*, **69**, 665-674.

Doraiswamy, P.C. and Thompson, D.R., 1982, A crop moisture stress index for large areas and its application in the prediction of spring wheat phenology. *Agricultural Meteorology*, **27**, 1-15.

Dregne, H.E. and Tucker, C.J., 1988, Desert encroachment. *Desertification Control Bulletin*, **23**, 243-251.

Fisher, F.B., Winne, J.C., Thornton, M.M., Tady, T.P., Ma, Z., Hart, M.M. and Redmond, R.L., 1998. Montana land cover atlas, University of Montana, Missoula, MT.

Gao, B., Heidebrecht, K. and Goetz, A., 1993, Derivation of scaled surface reflectances from AVIRIS data. *Remote Sensing of Environment*, **44**, 165-178.

Gupta, R.K., Prasad, S., Rao, G.H. and Nadham, T.S.V., 1993, District level wheat yield estimation using NOAA/AVHRR NDVI temporal profiles. *Advances in Space Research*, **13**, 252-256.

Holechek, J.L., Pieper, R.D. and Herbel, C.H., 1989, Range Management Principles and Practices, (Englewood Cliffs: Prentice-Hall Inc.).

Hunt, E.R., Jr., Everitt, J.H., Ritchie, J.C., Moran, M.S., Booth, D.T., Anderson, G.L., Clark, P.E. and Seyfried, M.S., 2003, Applications and research using remote sensing for rangeland management. *Photogrammetric Engineering and Remote Sensing*, **69**, 675-693.

Jamieson, P.D., Porter, J.R., Goudriann, J., Ritchie, J.T., Keulen, H.v. and Stol, W., 1998, A comparison of the models AFRCWHEAT2, CERES-Wheat, Sirius, SUCROS2

and SWHEAT with measurements from wheat grown under drought. *Field Crops Research*, **55**, 23-44.

Justice, C.O. and Hiernaux, P.H.Y., 1986, Monitoring the grasslands of the Sahel using NOAA AVHRR data: Niger 1983. *International Journal of Remote Sensing*, **7**, 1475-1497.

Justice, C.O., Townshend, J.R.G., Holben, B.N. and Tucker, C.J., 1985, Analysis of the phenology of global vegetation using meteorological satellite data. *International Journal of Remote Sensing*, **6**, 1271-1318.

Justice, C.O., Vermote, E., Townshend, J.R.G., Defries, R., Roy, D.P., Hall, D.K., Salomonson, V.V., Privette, J.L., Riggs, G., Strahler, A., Lucht, W., Myneni, R.B., Knazikhin, Y., Running, S.W., Nemani, R.R., Wan, Z., Huete, A.R., Leeuwen, W., Wolfe, R.E., Giglio, L., Mueller, J.P., Lewis, P. and Barnesly, M.J., 1998, The Moderate Resolution Imaging Spectroradiometer (MODIS): Land Remote Sensing for Global Change. *IEEE Transactions on Geoscience and Remote Sensing*, **36**, 1228-1248.

Labus, M.P., Nielsen, G.A., Lawrence, R.L. and Engel, R., 2002, Wheat yield estimates using multi-temporal NDVI satellite imagery. *International Journal of Remote Sensing*, **23**, 4169-4180.

Moran, M.S., Clarke, T.R., Inoue, Y. and Vidal, A., 1994, Estimating crop water deficit using the relation between surface-air temperature and spectral vegetation index. *Remote Sensing of Environment*, **49**, 246-263.

Nicholson, S.E., Tucker, C.J. and Ba, M.B., 1998, Desertification, drought, and surface vegetation: An example from the west African Sahel. *Bulletin of the American Meteorological Society*, **79**, 815-829.

Oesterheld, M., DiBella, C.M. and Kerdiles, H., 1998, Relationship between NOAA-AVHRR satellite data and stocking rate of rangelands. *Ecological Applications*, **8**, 207-212.

Peters, A., Walter-Shea, E.A., Ji, L., Vina, A., Hayes, M. and Svoboda, M.D., 2002, Drought monitoring with NDVI-based standardized vegetation index. *Photogrammetric Engineering and Remote Sensing*, **68**, 71-75.

Pickup, G., 1996, Estimating the effects of land degredation and rainfall variation on productivity in rangelands: an approach using remote sensing and models of grazing and herbage dynamics. *Journal of Applied Ecology*, **33**, 819-832.

Pickup, G., Bastin, G.N. and Chewing, V.H., 1994, Remote sensing based condition assessment for nonequilibrium rangelands under large-scale commercial grazing. *Ecological Applications*, **4**, 497-517.

Prince, S.D. and Tucker, C.J., 1986, Satellite remote sensing of rangelands in Botswana 2. NOAA AVHRR and herbaceous biomass. *International Journal of Remote Sensing*, **7**, 1555-1570.

Reeves, M.C., Winslow, J.C. and Running, S.W., 2001, Mapping weekly rangeland vegetation productivity using MODIS algorithms. *Journal of Range Management*, **54**, A90-A105.

Ritchie, J.T. and Otter, S., 1985. Description and performance of CERES-Wheat: A user-oriented wheat yield model. In ARS Wheat Yield Project, edited by W.O. Willis), pp. 159-175.

Schmidt, H. and Gitelson, A., 2000, Temporal and spatial vegetation cover changes in Israeli transition zone: AVHRR-based assessment of rainfall impact. *International Journal of Remote Sensing*, **21**, 997-1010.

Tucker, C.J., Holben, B.H., Elgin, J.H. and 3, J.E.M., 1981, Remote sensing of total dry-matter accumulation in winter wheat. *Remote Sensing of Environment*, **11**, 171-189.

Tucker, C.J., Justice, C.O. and Prince, S.D., 1986, Monitoring the grasslands of the Sahel 1984-1985. *International Journal of Remote Sensing*, **7**, 1571-1581.

Tueller, P.T., 1989, Remote sensing technology for rangeland management applications. *Journal of Range Management*, **42**, 442-452.

United States Department of Agriculture (USDA) National Agricultural Statistics Service (NASS)., 2003, USDA Published Estimates Database. *http://www.nass.usda.gov:81/ipedb/*.

Verhoef, E., 1984, Light scattering by leaf layers with application to canopy reflectance modeling: The sail model. *Remote Sensing of Environment*, **16**.

Vogelmann, J.E., Howard, S.M., Yang, L., Larson, C.R., Wylie, B.K. and Driel, N.V., 2001, Completion of the 1990s national land cover data set for the conterminous united states from Landsat Thematic Mapper data and ancillary data sources. *Photogrammetric Engineering and Remote Sensing*, **67**, 650-662.

Wiegand, C.L., Richardson, A.J. and Kanemasu, E.T., 1979, Leaf area index estimates for wheat from LANDSAT and their implications for evapotranspiration and crop modeling. *Agronomy Journal*, **71**, 336-342.

Williams, A.P. and Hunt, E.R., 2002, Estimation of leafy spurge cover from hyperspectral imagery using mixture tuned matched filtering. *Remote Sensing of Environment*, **82**, 446-456.

Wylie, B.K., Dendra, I., Pieper, R.D., Harrington, J.A., Reed, B.C. and Southward, G.M., 1995, Satellite-based herbaceous biomass estimates in the pastoral zone of Niger. *Journal of Range Management*, **48**, 159-164.

CHAPTER 2

APPLYING IMPROVED ESTIMATES OF MODIS PRODUCTIVITY TO
CHARACTERIZE GRASSLAND VEGETATION DYNAMICS

Abstract

The Moderate Resolution Imaging Spectroradiometer (MODIS)-derived

vegetation productivity was tested in the grasslands of western North Dakota to

determine its ability to characterize fluctuations in above-ground green biomass and

provide regional perspectives of inter-annual vegetation dynamics. Above ground green

biomass was measured at 2200 vegetation quadrats (0.5 m^2) in 2001 and 2130 quadrats in

2002. These observations were spatially disjunct which required interpolation between

quadrats. Interpolation models were constructed using high resolution satellite imagery

and accumulated growing degree days. The interpolations were applied to large spatial

aggregations (about 185,000 ha). Regionally scaled biomass measurements were

subsequently compared with MODIS net photosynthesis (PSN_{net}) estimates at three times

during the growing seasons of 2001 and 2002. The relationships between MODIS PSN_{net}

estimates and scaled above-ground green biomass improved steadily during the

progression of each growing season, and reached a maximum ($r^2 = 0.77$ and 0.57 in 2001

and 2002, respectively) near peak greenness. Above-ground green biomass was more

tightly coupled in 2001 because of the relative abundance of green biomass compared

with 2002. Inter-annual variability in grassland vegetation is characterized through

analysis of MODIS derived net primary productivity (NPP) for the years 2001 to 2003.

MODIS NPP estimates showed a significant decline ($P \leq 0.05$) from 2001 to 2003, partly

induced by a significant decline ($P \leq 0.05$) in growing season precipitation.

Introduction

Though ground-based measurement is the most reliable method for assessing site-specific vegetative conditions, long-term planning and administrative needs, such as county and state level drought mitigation, may be more appropriately addressed by a consistent, regional overview which ground-based reconnaissance is unlikely to provide. Remote sensing may offer a sample measure of productivity at regional scales and has been promoted as a diagnostic tool for these purposes (White et al. 1997, Sannier et al. 1998, Steininger 2000, Reeves et al. 2001, Tucker et al. 2001). The Moderate Resolution Imaging Spectroradiometer (MODIS) instrument allows for regional monitoring through generation of global, weekly (eight-day) net photosynthesis (PSN_{net}) and annual estimates of net primary productivity (NPP). Because of the recent launch of the instrument few, if any, studies have evaluated the performance of regional MODIS vegetation productivity estimates in grassland environments. Therefore, the objective of this study is to test the efficacy of the MODIS as a monitoring tool by directly comparing productivity estimates with field measurements of biomass in North Dakota grasslands and then analyzing inter- and intra-annual dynamics as estimated from PSN_{net} and NPP for the years 2001 to 2003. First MODIS PSN_{net} was compared with scaled above - ground green biomass (AGBB) by scaling biomass observations for each of 12 mapping units in the Little Missouri National Grasslands (LMNG) for 2001 and 2002. Second, total precipitation from 1 January to peak greenness was quantified for each mapping unit in the LMNG for 2001 to 2002. Third, I compared time integrated MODIS productivity estimates from 1 January through the composite period containing the date of AGGB prediction with

scaled biomass observations. Finally, I characterized inter-annual variation of NPP in relation to differing amounts of growing season precipitation.

Background

Grassland environments are relatively simple laboratories for relating MODIS productivity to AGGB because large inter - annual fluctuations of AGGB are common, and dominance of herbaceous biomass allows for collection of biomass. In addition, herbaceous vegetation tends to respond more quickly to precipitation than other types of vegetation (Lauenroth 1979).

Field above-ground biomass is often used as an indicator of the pattern and magnitude of variation of natural carbon fixation (Zheng et al. 2003). This makes aboveground biomass a logical attribute to relate with MODIS PSN_{net} for regional studies, though conceptually MODIS primary productivity estimates can only be quantitatively validated by comparison with flux tower measurements. Tower-based estimates of productivity represent a spatial average of carbon flux over a tower "footprint". The "footprints'" dimensions depend on wind speed, wind direction, surface roughness, and atmospheric stability (Turner et al. 2003). The variably sized, usually small (< 1-km^2) footprint of flux towers, combined with low tower density in grassland environments, make validation of MODIS products challenging. Moreover, most management schemes rely more on biomass dynamics than carbon flux measurements.

Study Area

The Little Missouri National Grasslands (LMNG) located in North Dakota (figure 1), a 809,380 ha area managed primarily by the USDA Forest Service for grazing by domestic and wild animals, was the study area. Portions of the LMNG were converted to

nearly homogenous stands of crested wheat grass (*Agropyron cristatum*) in the early to

mid-1900's, though these stands receive no artificial fertilization or irrigation. Climate of

the LMNG is continental and semi-arid and Cleland et al. (1997) provides a detailed

description of the LMNG geo-climatic setting. Annual average precipitation varies from

360 to 410 mm, with 70% occurring between April and September (Whitman 1978). In

2001 the LMNG region was notably wetter during the growing season (1 April to 1

September) and drier in 2002 and 2003 than the 50-year mean (figure 2). Potential

natural vegetation of the LMNG is typical of the mixed grass prairie in the Northern

Great Plains (Jensen et al. 2001) and is predominantly a wheatgrass-needlegrass

(*Pascopyrum-Nasella*) association (Jensen et al. 2001). Dominant species include

western wheatgrass (*Pascopyrum smithii* (Rydb.) A. Löve), green needlegrass (*Nassella*

viridula (Trin.)), needle and thread grass *Hesperostipa comata* (Trin.) & Rupr.), blue

grama (*Bouteloua gracilis* (H.B.K.)Lag.) and threadleaf sedge (*Carex filifolia*).
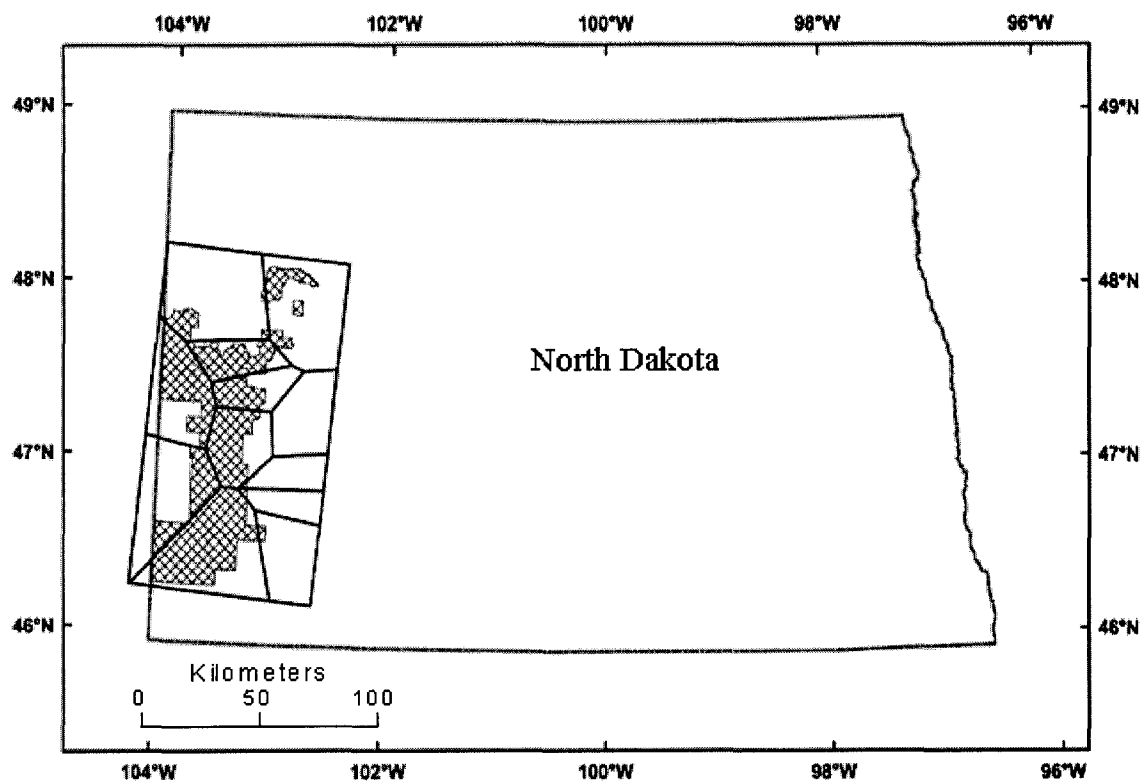
Figure 1. Location of the Little Missouri National Grasslands (cross hatched region) in North Dakota and the spatial arrangement of the zones of meteorological influence (Thiesson polygons).
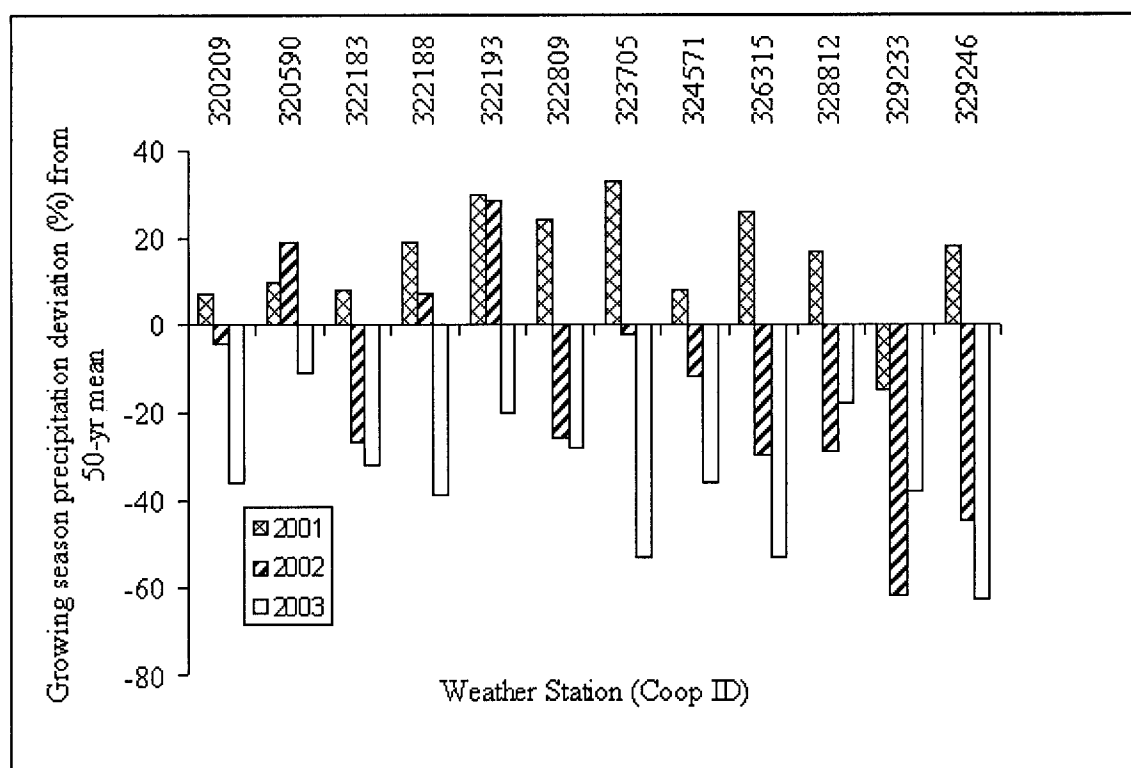
Figure 2. Difference between 2001 to 2003 growing season precipitation and the 50-year mean at 12 weather stations within and adjacent to the Little Missouri National Grasslands.

Methods

The ultimate goal of this research was to compare MODIS vegetation productivity to AGGB. This required the following methodological steps: 1) area pre-stratification for the biomass sampling procedure, 2) acquiring high resolution satellite data and converting them to normalized difference vegetation index (NDVI), 3) Identifying the appropriate scale for comparing AGGB, 4) creating biomass scaling models (for interpolating between spatially disjunct biomass observations and 5) comparing scaled biomass measures to MODIS PSN_{net} and NPP.

2

Collecting Biomass Observations

For sampling purposes, the study area was classified in four strata including native and seeded grasslands with high productivity (3 and 38 percent of study area, respectively) and native and seeded grasslands with low productivity (9 and 50 percent of study area, respectively). This was possible because of a suite of biophysical variables developed by Jensen et al. (2001) permit detailed sampling and masking procedures. Based on this I tried to allocate our sampling resources accordingly. This ensured that grazing allotments were selected that represented the different areas within the LMNG to describe spatial and temporal trends in AGGB (kg ha^{-1}).

AGGB was measured for 473 transects across 3 time periods (27 – 31 May, 13 – 17 June, and 13 – 17 July) during the 2001-growing season in the LMNG. Sites were selected based on federal ownership and accessibility and observed strata. For each site, a transect was established perpendicular to and started at least 50-meters from fence-lines to avoid the influence of roads or channeled livestock trails that typically run along fence-lines. Transect length was randomly determined and varied from 250 to 500 meters. Beginning and ending locations for each transect were recorded with a global positioning system (gps). At 25-m intervals a 0.5-m^2 quadrat was clipped at 1-cm stubble height, placed in a paper bag, and the percentage of living vegetation was estimated. A total of 2200 quadrats were clipped in the 2001-growing season.

The mean allotment size for the LMNG is 342 ha, making it difficult to strike a balance between sufficient sampling intensity for a given allotment while sampling enough allotments to cover the range of variability expected across the differing environments within the LMNG. Based on this premise the sampling procedure for 2002

was modified, hoping that a pixel based approach (3 X 3 pixel average NDVI versus plot level biomass) would provide a more accurate depiction of the range of variability within and between allotments that were sampled. Above-ground green biomass was measured in the 2002 growing season at 426 sites over 3 time periods (20 – 23 May, 14 – 17 June, and 10 – 13 July) using the area weighted sampling designed in 2001. At each site, a sampling microsite (45 x 45 m) was established. Microsites were homogeneous in species composition and biomass. A range of biomass levels from nearly bare ground around prairie dog towns, to heavily vegetated allotments were sampled to ensure that I could capture as much of the productivity continuum as possible.

Within each microsite, above-ground biomass was clipped within five randomly located-0.5 m^2 quadrats to a 1-cm stubble height, placed in a paper bag, and the percentage of living vegetation was estimated. A total of 2130 quadrats were clipped during the 2002-growing season. All herbaceous biomass collected was subsequently dried at 65 C° for at least 48 hours and weighed. The average AGGB per site was calculated as the total dry weight multiplied by the percent of green vegetation from each sampled quadrat during each sampling period for both years of the study.

Scaling Biomass Observations

The disparate resolution between MODIS vegetation data and the vegetation quadrats combined with large distances between sampling areas required interpolation between biomass observations. Large distances (> 40 km) precluded the use of geostatistical techniques for interpolation. Instead I chose to scale biomass observations using Advanced Spaceborne Thermal Emission and Reflection Radiometer (ASTER) and Enhanced Thematic Mapper Plus (ETM+) NDVI. This required identification of the

appropriate spatial scale for analysis. In other words each vegetation quadrat could be related to the accompanying ASTER or ETM+ NDVI image pixel, or some spatial aggregation of both pixels and quadrats. Before scaling, it was necessary to first acquire and then process the ETM+ and ASTER imagery into NDVI.

Three relatively cloud free Level -1G Landsat Enhanced Thematic Mapper (ETM+) scenes (path 34/row 27) were acquired over the Little Missouri National Grasslands for 19 May, 22 June, and 22 July 2001. All scenes were registered to UTM zone 13 North and exhibited less than 10% cloud cover. A dark object subtraction was applied to reduce path radiance. All scenes were cloud-and water-masked, co-registered, and converted from digital counts to radiance (W m^{-2} sr^{-1} nm^{-1}). To minimize between scene variability, radiance values were converted to at-sensor reflectance as described by Markham and Barker (1986). Bands 3 (RED) and 4 (NIR) were used to derive NDVI computed as (NIR – RED)/(NIR + RED)   (1)

where NIR and RED are the spectral responses for the near-infrared and red wavebands respectively. For visible and NIR channels, ASTER has a spatial resolution of 15 meters while ETM+ has a resolution of 30 meters and both sensors measure radiance in the identical RED wavelength (0.63 – 0.69 µm) and nearly identical NIR bands (0.78 – 0.86 and 0.75 – 0.79 µm for ASTER and ETM+ respectively).

In 2002 no cloud free ETM+ data were available, so instead 22 ASTER L2 surface reflectance images of the LMNG were obtained. These ASTER scenes collectively covered the temporal range of 13 May, 5 June, 30 June, and 9 July 2002. All 22 ASTER scenes were geo-registered to UTM zone 13 North. NDVI was subsequently computed for each ASTER image.

Following image pre-processing, to ensure that the pixels analyzed corresponded to the habitats sampled, all grassland habitats that were not sampled during the biomass collection procedure were removed. A 30-meter spatial resolution image depicting grassland habitats throughout the LMNG was obtained from Jensen et al. (2001) and used to isolate the spectral response of grassland vegetation for creation of the above-ground biomass-scaling models. Badlands, shrublands and agricultural lands were removed. Following the masking procedure a series of tests were performed to establish the strongest relationship between biomass measurements and NDVI for the biomass interpolation (scaling) procedure.

These tests included: 1) pixel to sample point comparison (point in cell extraction), 2) 7 x 7 and 3 x 3 zonal mean for 2001 and 2002 data respectively, 3) average NDVI within each grazing allotment, and 4) average NDVI by zone of meteorological influence (described below). I chose a 7 x 7- pixel area surrounding each transect in 2001 and a 3 x 3-pixel area around each microsite in 2002. The 7 x 7-pixel kernel (210 x 210 meters) was chosen because the average length of sample transects was about 200 meters, while the 3 x 3 pixel kernel was chosen because this ensures a ± 2 pixel boundary around each field site in 2002. Another level of aggregation included spatially averaging NDVI within each grazing allotment. As a final method of relating biomass to NDVI, a zone of meteorological influence was established through creation of Thiesson polygons (figure. 1) around weather stations found within and adjacent to the study area.

Ordinary least-squares regression (Zar 1995) was used to determine the strength of the relationship between average biomass and average NDVI within each of these spatial domains. While spatially averaging all plots within each Thiesson polygon

reduces the sample size available for analyses, it also reduces variability between geographically similar plots while emphasizing regional differences.

The identical spatial aggregations were performed on MODIS PSN$_{net}$. This was done to see if scaling the biomass observations provided better results than just analyzing the raw, plot-level biomass data aggregated without interpolation. If multiple vegetation quadrats occurred within the boundary of a 1-km^2 MODIS pixel they were averaged together.

In addition to NDVI, daily meteorology was acquired for use as explanatory variables in the forthcoming biomass scaling models. Daily precipitation and minimum and maximum temperature were obtained from the National Climate Data Center (NCDC) database of surface meteorology for the years 2001 to 2003 for each Thiesson polygon. These data were screened such that if $\geq 5\%$ of the observations in any meteorological category were missing in any year, then the station was not used. This resulted in 12 complete stations and corresponding Thiesson polygons for 2001-2003 growing seasons (figure 1).

Stepwise regression was used to determine the most appropriate significant ($P \leq$ 0.05) regression model for scaling biomass observations. The model initially included the meteorological variables, NDVI and their interactions for each Thiesson polygon. A tolerance of 0.01 was selected for avoiding variables exhibiting a high degree of colinearity during the forward-stepping regression process.

Processing and Computing Improved MODIS Vegetation Productivity

The standard MODIS productivity algortithm produces anomalous and artificial productivity boundaries due to the coarse resolution (1° X 1.25°) daily meteorological

data required by the algorithm (Heinsch et al. 2003). In addition cloud contamination can render artificially low productivity estimates due to missing or inaccurate estimates of LAI and FPAR.

To ameliorate these effects MODIS productivity estimates were reprocessed for 2001 - 2003. To accomplish this task, MODIS land cover and LAI/FPAR data for the MODIS tiles H10V04 and H11V04 were obtained from the Earth Observing System Data Gateway for 2001 to 2003. Both the land cover and LAI/FPAR are 1-km^2 spatial resolution products. The primary productivity estimates used in this study were computed from the standard Collection 4 LAI/FPAR and land cover products but used modified daily meteorological records and the updated biome properties look up table (BPLUT) found in Heinsch et al. (2003).

The original meteorological data used for standard computation of MODIS productivity estimates comes from the NASA Goddard Space Flight Center (GSFC) Data Assimilation Office (DAO) (Atlas and Lucchesi 2000) and includes daily estimates of minimum and average temperature, solar radiation, and vapor pressure deficit (VPD). These meteorological data are only available at $1.25° \times 1°$ spatial resolution. This ensures that within the spatial extent of each DAO cell, every 1-km^2 MODIS pixel will inherit identical DAO characteristics. The disparate resolution of these inputs to the MODIS productivity algorithm produces noticeable, artificial boundaries in the end products, particularly the eight-day composite PSN$_{net}$. As a result the DAO data were spatially smoothed, thereby taking out the artificial boundaries. In addition, due to clouds the LAI/FPAR product was temporally filled where necessary.

The LAI/FPAR product is ultimately derived from atmosphere corrected surface reflectance data and contains quality assurance layers within each file. The quality assurance layer provides a means of screening all pixels that are not desirable for analysis, either as a result of sensor and algorithm performance, atmospheric conditions, or cloud contamination. Screening criteria used to filter LAI/FPAR used in this study are included in Table 1. If any LAI/FPAR pixel did not pass the quality screening criteria, its value was determined through linear interpolation between the previous period's value and the next period to pass the screening process. The resulting productivity estimates derived from these temporally and spatially smoothed inputs are identical to the standard MODIS products in all other aspects.

Table 1. Quality control criteria used for screening MODIS LAI/FPAR data for 2001 to 2003.

QC flag description[1]	Screening criteria
MODLAND_QC	≤ 1
DEADDETECTOR	0
CLOUDSTATE	0 or 3
SCF_QC	≤ 3

[1]A detailed explanation of these criteria can be found in (Heinsch et al. 2003).

Vegetation Productivity Algorithm

The MODIS productivity algorithms used in this study are summarized below. For examining inter-annual variation in primary productivity I used NPP:

$$NPP = \sum_{Period=1}^{46} PSNnet - R_{mlw} - R_{gleaf} - R_{gfroot} - R_{glw} - R_{gdw} \tag{2}$$

where NPP is the estimate of annual net primary productivity, PSN_{net} is the eight-day summation of net photosynthesis (there are 46 periods in a year), R_{mlw} is the maintenance respiration for the live woody component, R_{gleaf} is the growth respiration for leaves,

R_{gfroot} is the growth respiration for fine roots, R_{glw} is the growth respiration for live woody

tissue, and R_{gdw} is the growth respiration for dead wood.

Net photosynthesis is computed as:

$$PSN_{net} = GPP - Rm\_leaf - Rm\_froot \tag{3}$$

where PSN_{net} is the eight-day summation of net photosynthesis (kg C m^{-2}), GPP is the

eight-day summation of gross primary productivity, Rm_leaf is the maintenance

respiration for leaves, and Rm_froot is the maintenance respiration of fine roots. Gross

primary productivity is computed as:

$$GPP = \varepsilon * PAR * FPAR \tag{4}$$

where GPP is the eight-day summation of gross primary productivity (kg C m^{-2}), ε is the

radiation use efficiency (kg C MJ^{-1} photosynthetically active radiation (PAR)), and FPAR

is the fraction of absorbed PAR. Since one objective of this paper was to examine the

performance of MODIS productivity in relation to observed seasonal AGGB, I chose

PSN_{net} instead of GPP, which is theoretically further removed from observed biomass

(i.e. no accounting for respiration in GPP).

All MODIS land products were converted from their native HDF-EOS data

format to flat binary and reprojected from the Sinusoidal projection to Lamberts

Azimuthal Equal Area (center of longitude –100°, reference latitude 45°). Following the

reprojection, tiles were merged and scaled (kg C m^{-2}) to form a seamless representation

of the study area. Primary productivity estimates were spatially subset to include only

grassland vegetation. The analysis mask for this process was derived from MODIS land

cover type 2 data (Strahler et al. 1996). The MODIS land cover mask indicated about

72% of the region was occupied by grassland vegetation. The Type 2 land cover is

comparable to the International Geosphere-Biosphere Program (IGBP) global land cover

data set (Hansen and Reed 2000).

Analyzing Intra-and Inter-Annual Productivity Dynamics

All MODIS grassland pixels passing the quality control criteria (Table 1) were

averaged within each Thiesson polygon to obtain a single mean estimate of time

integrated PSN_{net} from the start of the year to each date of biomass prediction. Net

primary productivity was aggregated in a similar fashion. Since each Thiesson polygon

was a different size, NPP means were computed on an area-weighted basis. The strength

of the relationship between regionally scaled biomass measurements and MODIS PSN_{net}

was determined using ordinary least squares regression in each of 3 time periods for the

entire LMNG in 2001 and 2002. Detection of significant ($P \leq 0.05$) inter-annual

differences between regionally averaged NPP means from 2001, 2002, and 2003 was

accomplished using a one-way ANOVA and the Tukey test (Zar 1995) for separating

means. Trends in NPP were compared with growing season precipitation trends for the

same spatial and temporal domain.

Results

The results of the biomass scaling operation are presented first. This includes the

relationships between different levels of spatial aggregation and high resolution NDVI as

well as the results of the forward stepwise regression analysis used to build the biomass

scaling models. Next, the relationships between scaled and un-scaled AGGB and

MODIS PSN_{net} are examined. Finally the inter-annual trends in NPP and precipitation

are quantified and compared.

Biomass scaling Models

No strong relationships were found between either ETM+ or ASTER NDVI and

clipped plot biomass for any aggregation method except the zone of meteorological

influence (Table 2). This finding was anticipated because at regional scales grassland

biomass is dominated primarily by local climate conditions, especially precipitation

during the growing season (Lauenroth 1979). Grazing is also a factor in the region but

usually for smaller areas. For example, over the span of 100 miles, the dominant driver

of biomass should be the abiotic environment and precipitation, while allotment to

allotment variability tends to be more closely aligned with herbivory. Only four of the

Thiesson polygons are dominated by the Little Missouri National Grasslands. This is not

a problem because the Little Missouri National Grasslands were used as a sampling area

to represent the grassland biomass of the region. This analysis however requires some

sort of scalar to infer productivity outside of the sampling area.

Table 2. Relationship (r^2) between sample measures of above-ground green biomass and ETM+ (2001) and ASTER (2002) NDVI. Dates are sample period midpoints.

Date	Point in cell (n)	Zonal pixel mean[1] (n)	Allotment Mean (n)	Thiesson polygon Mean (n)
2001				
28 May	0.00 (158)	0.11[*](46)	0.16[*](26)	0.49[*] (12)
15 June	0.26[*] (129)	0.15[*] (40)	0.23[*] (29)	0.62[*] (12)
15 July	0.20[*] (186)	0.25[*] (53)	0.28[*] (36)	0.81[*] (12)
2002				
22 May	0.10 (122)	0.03 (48)	0.07 (33)	0.39[*] (9)
16 June	0.15[*] (142)	0.21[*] (59)	0.25[*] (35)	0.57[*] (9)
12 July	0.23[*] (162)	0.28[*] (65)	0.22[*] (35)	0.68[*] (9)

[1]In 2001 a 7 x 7 zonal mean was used. In 2002 a 3 x 3 zonal mean was used.
[*]($P \leq 0.05$).

Since Thiesson polygons provided the best relationships, they were subsequently

used as the spatial aggregate to build scaling models for interpolating biomass. The final

scaling models used NDVI and thermal time resulting in

$$\text{BIOMASS}_{AG01} = \text{NDVI}_{ETM+} (212.6) + \text{gdd}_{sum}(-0.003) - 33.8 \tag{5}$$

where BIOMASS_{AG01} is the estimated AGGB within each Thiesson polygon in 2001,

NDVI_{ETM+} is the average ETM+ NDVI for a given polygon, gdd_{sum} is the summation of

thermal time $(\text{TAVG}_{daily}\text{-}0°C)$ from 1 January 2001 to the date of ground sampling where

TAVG_{daily} is the daily average temperature. In 2002, a similar model was constructed for

scaling biomass observations:

$$\text{BIOMASS}_{AG02} = \text{NDVI}_{ASTER} (266.7) + \text{gdd}_{sum} (-0.009) - 57.9 \tag{6}$$

where BIOMASS_{AG02} is the estimated AGGB within each Thiesson polygon in 2002,

NDVI_{ASTER} is the average ASTER NDVI for a given polygon and gdd_{sum} is the

summation of thermal time $(\text{TAVG}_{daily}\text{-}0°C)$ from 1 January 2002 to the date of sampling.

Stepwise regression indicated that inclusion of precipitation did not improve

overall model predictability due to high colinearity with NDVI (Table 3).

Table 3. Results of stepwise regression for scaling model parameter selection 2001 and 2002. Only the retained significant variables are summarized*.

Model iteration[1]	Adjusted R^2	SEE[2]	Partial correlation coefficient	t − value*
2001				
1) ETM+ NDVI	0.81	5.40	0.90	9.55
2) ETM+ NDVI	0.89	4.19	0.89	8.89
GDDsum x ETM+NDVI			-0.66	-3.78
2002				
1) ASTER NDVI	0.82	5.66	0.89	9.80
2) ASTER NDVI	0.87	4.65	0.88	8.06
GDDsum x ASTER NDVI			-0.60	-3.20

[1]GDD_{sum} is the summation of growing degree days.
[2]n = 22 for 2001 and n = 21 for 2002.
*P ≤ 0.05.

Cross-validation proved that the scaling models worked sufficiently well for describing

spatial patterns of vegetation throughout the grassland region (figure 3), though a higher

degree of bias was observed in the 2002 model.

Regionally scaled AGGB produced at peak greenness was estimated as 1054 ± 36

(SEM) and 980 ± 44 (SEM) kg ha^{-1} for 2001 and 2002 respectively. Unscaled biomass

(quadrat data for AGGB) during peak greenness was 1021 ± 42 (SEM) and 996 ± 57

(SEM) kg ha^{-1} for 2001 and 2002, respectively. These values compare favorably with

results from 11 years of biomass observations by Hanson (1976) who reported an 11-year

mean of 1012 kg ha^{-1} in a similar grassland environment in Montana. The site evaluated

by Hanson (1976) received an annual average of 330 mm of precipitation and had similar

species composition to the current study area.
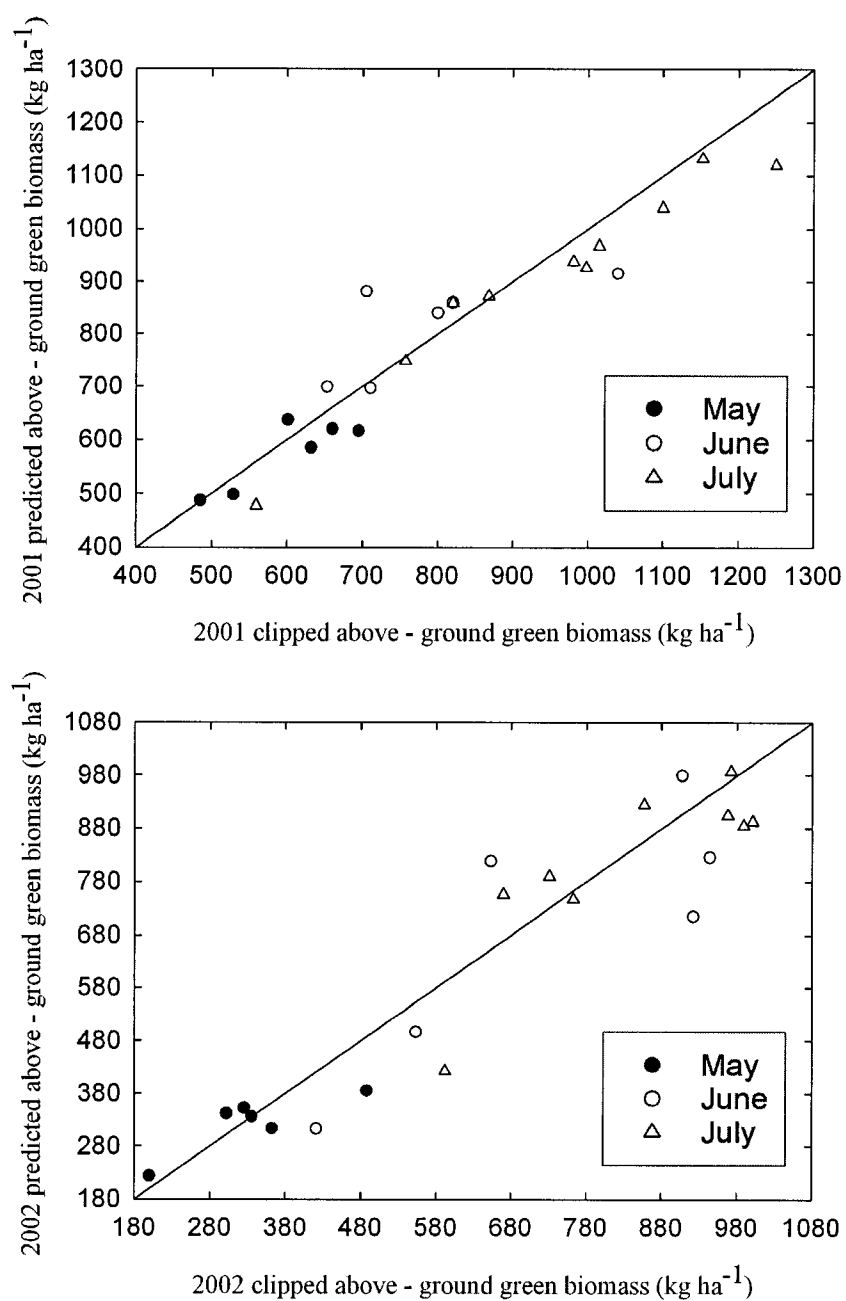
Figure 3. Cross validation results of the biomass scaling models for 2001 and 2002.

Improved Estimates of Primary Productivity

The results of the spatially smoothed climatalogical (DAO) input on weekly

PSN$_{net}$ are noticeable in North Dakota and the region surrounding the LMNG (figure 4).

Figure 4A depicts the artificial boundary from the DAO influence. The improved

estimates of productivity were visually and quantitatively superior. In July, the

relationship between MODIS PSN$_{net}$ and AGGB was improved from r-square 0.54 to

0.77 and 0.51 to 0.57 in 2001 and 2002 respectively using the enhanced productivity

product.
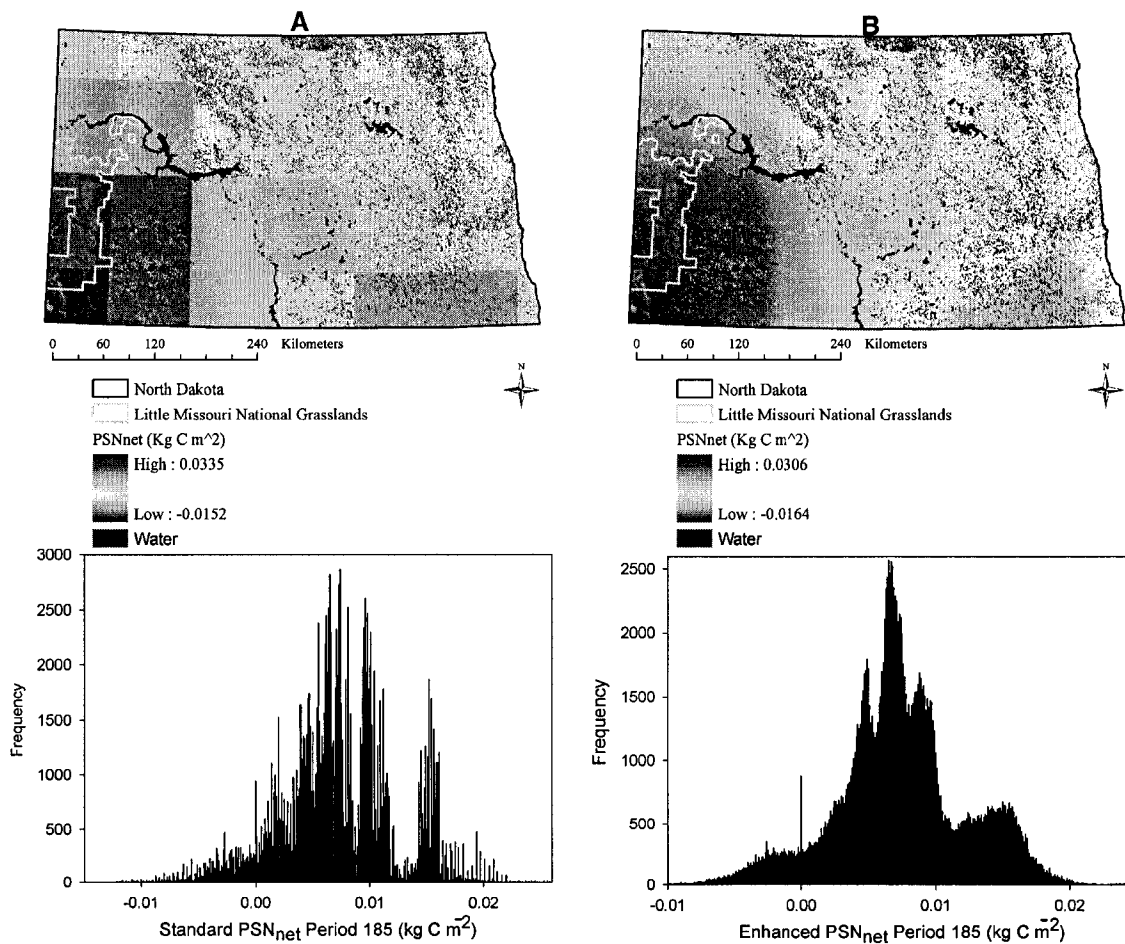
Figure 4. Comparison between standard MODIS derived PSN$_{net}$ (4A) and the enhanced
version that contains spatially smoothed meteorology and temporally filled
LAI/FPAR (4B). Images are PSN$_{net}$ (kg C m^{-2}) from composite period 185, 2001.
Improvements are easily seen in both the images and histograms.

Though these results provide evidence that the improved MODIS productivity

estimates are more appropriate for monitoring AGGB in grassland environments, it is still

impossible to assess whether these improved productivity estimates provide more

accurate estimates of carbon sequestration at regional scales. Such a comparison is

beyond the scope of the current study. All subsequent analyses were performed using the

improved MODIS productivity estimates.

Comparing Net Photosynthesis Estimates to Green Biomass

Net photosynthesis from MODIS was compared with the scaled and un-scaled

above ground green biomass. Table 4 demonstrates the relatively poor relationship

between MODIS PSN$_{net}$ and un-scaled aggb.

Table 4. Relationship (r^2) between sample measures of above-ground green biomass and
accumulated PSNnet from MODIS. Dates are the beginning of the MODIS
productivity composite periods.

Date	Point in cell (n)	Zonal pixel mean[1] (n)	Allotment Mean (n)	Thiesson polygon Mean (n)
2001				
25 May	0.00 (51)	0.09 (42)	0.12 (26)	0.37* (12)
10 June	0.11 (45)	0.16* (38)	0.19* (29)	0.43* (12)
12 July	0.13* (68)	0.19* (52)	0.20* (32)	0.62* (12)
2002				
17 May	0.09 (41)	0.03 (35)	0.07 (33)	0.31* (9)
10 June	0.12 (44)	0.09 (38)	0.16* (31)	0.34* (9)
12 July	0.18* (56)	0.16* (48)	0.18* (35)	0.41* (9)

[1]In 2001 a 7 x 7 zonal mean was used. In 2002 a 3 x 3 zonal mean was used.
*($P \leq 0.05$).

Regionally aggregating using only grassland pixels produced PSN$_{net}$ estimates,

which varied spatially in a similar pattern to scaled AGGB (figure 5). As expected, the

strength (r^2) of the relationships between scaled AGGB and MODIS PSN$_{net}$ were highest

during peak greenness in 2001 and 2002. This finding was anticipated because during

peak greenness the MODIS sensor receives relatively more vegetation signal than

background. The proportional increase in PSN$_{net}$ was higher from June to July than was

observed in AGGB during the same time period.
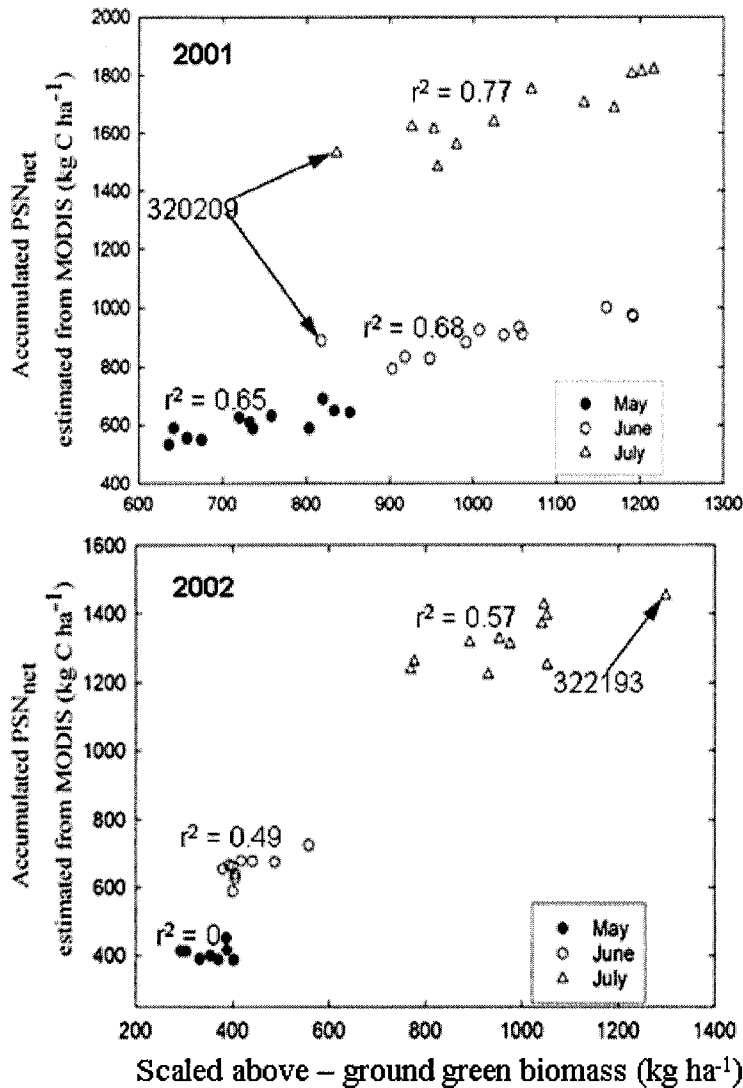
Figure 5. Accumulated MODIS PSN$_{net}$ estimates for 2001 and 2002 compared with
scaled above-ground green biomass from a similar period. For 2001 the
composite periods of accumulation for MODIS PSN$_{net}$ were from 1 – 137 for
May, 1 – 161 for June and 1 – 193 for July. For 2002 the periods of accumulation
for MODIS PSN$_{net}$ were for composite periods 1 – 145 for May, 1 – 161 for June
and 1 – 193 for July. 2001 scaled above-ground green biomass estimates were for
28 May, 15 June and 15 July. 2002 scaled biomass estimates were for composite
22 May, 16 June and 12 July. Note the aberrantly high productivity of Thiesson
polygon 322193.

The relation between MODIS PSN_{net} and AGGB was stronger in 2001 than 2002 due to greater precipitation, which ultimately led to a greater FPAR signal. This was especially evident in May 2002 where no correlation was found between MODIS PSN_{net} estimates and scaled AGGB.

The response of MODIS PSN_{net} to precipitation fluctuations is evident when comparing the 2001 and 2002 growing seasons. For example, Thiesson polygon 322193 (figure 5) exhibited aberrantly high biomass and commensurately high PSN_{net} during 2002 due to much higher than normal growing season precipitation in the same polygon (figure 2).

Inter-Annual NPP Trends

The analysis of variance of regional NPP for 2001 to 2003 revealed a highly significant ($P \leq 0.0001$) decreasing trend in productivity. Table 5 reveals that 2001 was significantly ($P \leq 0.05$) more productive than either 2002 or 2003. Similarly, the 2001 growing season precipitation was significantly higher ($P \leq 0.05$) than either 2002 or 2003. These differences are clearly visible in the NPP images for the 3 years analyzed (figure 6). Growing season precipitation was high in 2001 (figure 2),

Table 5. Regional mean NPP and growing season precipitation for the Little Missouri National Grasslands and adjacent area.

Variable	Year		
	2001	2002	2003
Precipitation (mm)[1]	383 (19)$_a$*	291 (23)$_b$	235 (7)$_b$
NPP (kg C ha^{-1})[1]	3000 (42)$_a$	2437 (57)$_b$	2296 (34)$_b$

[1]Values in parentheses are SEM.
*Means in the same row followed by the same subscript are not significantly different ($P \leq 0.05$).

while 2002 and 2003 were relatively dry in relation, thereby providing ideal test beds to

determine the usefulness of MODIS productivity products for assessing inter-annual

differences in productivity.
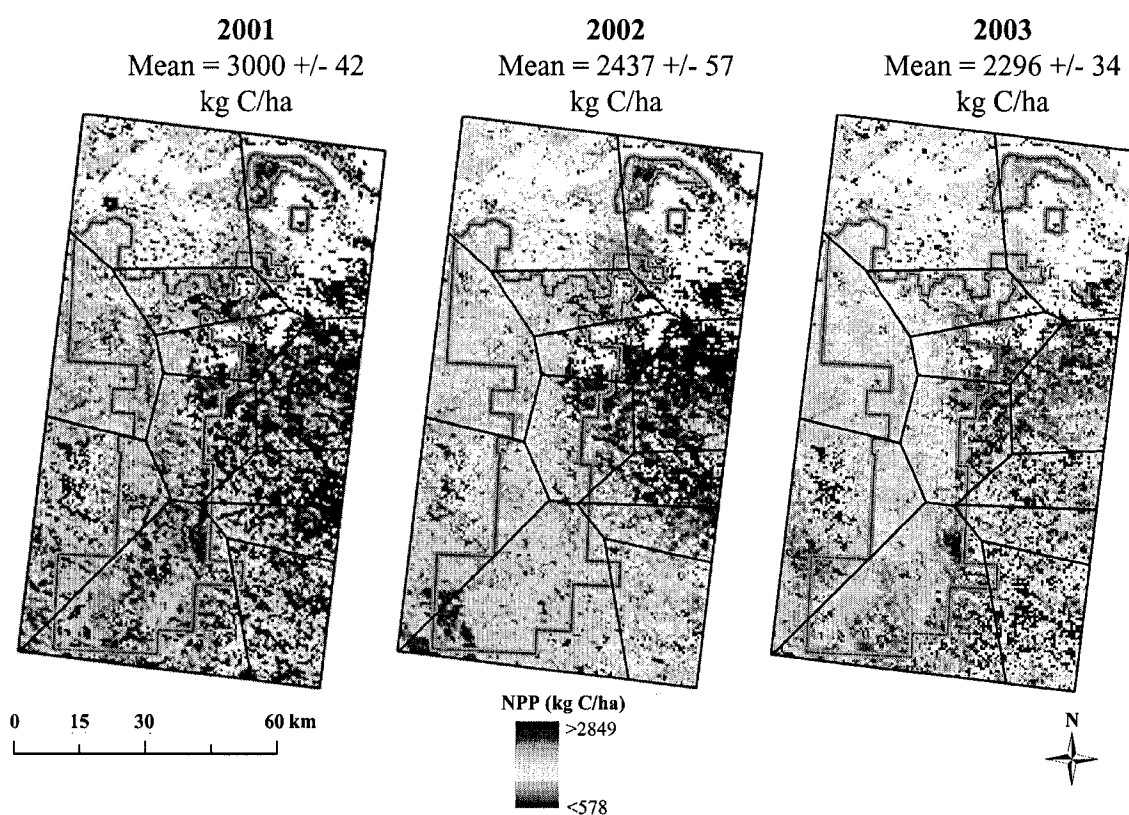
Figure 6. Mean and SEM of net primary productivity for the entire Little Missouri
National Grasslands (LMNG) for 2001 to 2003. Only grassland pixels are
represented. Polygons are Thiesson polygons around 12 weather stations. Gray
line represents the administrative boundary of the LMNG.

Discussion

The highest degree of association between biomass and NDVI occurred during

the July sampling periods (near peak greenness) for both years of the study. Above-

ground green biomass observations were obtained only three times during the growing

seasons of 2001 and 2002, thus, using clipped plot data, it is not possible to know exactly

when peak greenness occurred throughout the LMNG though, in each year for the periods

examined, biomass observations were highest in July. Although many studies have utilized end-of -season standing crop measurements for relating biomass to remote sensing data, for monitoring growing season vegetation conditions, a continuous sampling design (i.e. multiple sampling periods in the growing season) is superior to measuring only the end-of-season standing crop when seasonal variation needs to be quantified. End-of -season standing crop measurements can overestimate annual productivity on perennial grasslands because, inevitably, the biomass measure at a given plot will include dead vegetation from the previous year and, to a much lesser degree, the current growing season. In contrast, if herbivory is significant, End-of -season standing crop measurements can underestimate the current year's growth. Scurlock et al. (2002) provide an excellent overview of the assumptions associated with most techniques for evaluating primary productivity of grasslands.

In addition to identifying the time period with the strongest links between MODIS PSN_{net} and AGGB, this study also discovered an appropriate spatial domain for analysis. Only the Thiesson polygons (average size about 185,000 ha) provided suitable results. At smaller spatial aggregates biomass could not be reliably scaled using the high resolution satellite imagery and meteorological observations. There are several likely reasons why there were weak linkages between NDVI and clipped biomass in all comparisons except the Thiesson polygons. First, while clipping remains the most objective method of measuring biomass on small plots, estimating the amount of green vegetation within a sampling quadrat is difficult. For example, what the human eye detects as "green" might, in reality, be nearly non-photosynthetic, distorting the NDVI/green biomass relationship. Second, especially at the end of the growing season,

there might be a substantial amount of senesced vegetation, within a plot frame, whose

canopy resides over the top of relatively green vegetation. This green vegetation would

be separated and weighed but due to the effects of the senesced vegetation in the upper

canopy, the NDVI signal would remain low. Finally, there is a poorer correlation

between NDVI derived from upwelling radiance than between NDVI derived from

atmosphere corrected data and biomass (Shoshany et al. 1995, Turner et al. 1999), which

would have only affected the 2001 scaling model. While I initially assumed that ASTER

NDVI would be more closely related to AGGB, the presence of large amounts of

senescent vegetation in 2002 resulted in ASTER NDVI being less correlated with

biomass. ASTER L2 surface reflectance data are radiometrically calibrated and

atmospherically corrected. The advantage of ASTER surface reflectance data over

ETM+ data is that they are immediately useful for quantifying biophysical traits of the

earth's surface. Atmosphere corrected sensor data provide a more reliable dataset for

characterizing most vegetative traits (Turner et al. 1999). The disadvantage of ASTER

data is the smaller spatial coverage (about 470,610 ha scene^{-1}) compared with that of

ETM+ (about 4,854,299 ha scene^{-1}).

The resulting scaled biomass observations were more closely related to MODIS

PSN_{net} (Figure 5) than to un-scaled biomass (Table 4). Scaled biomass had the distinct

advantage of being masked using the grassland habitat map by Jensen et al. (2001) while

the un-scaled biomass necessarily unmasked. In either case it was difficult to relate

MODIS PSNnet (a measure of carbon sequestration) to AGGB.

Larger differences were observed within the MODIS PSNnet data than in the

AGGB. For example, in 2001 zone (Thiesson polygon) 320209 exhibited a 2.2%

increase in AGGB but a 69% increase in PSN_{net} (figure 5). The disparity between

observed AGGB and PSN_{net} between these two periods might suggest that a potentially

higher proportion of carbon was being allocated to roots or maintenance respiration,

which is plausible since maintenance respiration is estimated as a function of air

temperature in the algorithm (Running et al. 2000). This indicates that estimating

biomass using MODIS productivity estimates will usually not be appropriate at the scales

examined in this study because it is not feasible to quantify the root to shoot ratio (though

estimates could be made (Scurlock et al. 2002)) for entire regions of grassland vegetation.

Despite this limitation, MODIS PSN_{net} estimates at regional scales can indicate spatial

patterns that are not discernable on the ground, thus bolstering the potential strength of

eight-day summations of PSN_{net} as a monitoring tool. Another explanation for the

dramatic increase in PSN_{net} is inflation of the FPAR response by the contamination of the

LAI/FPAR signal by crops.

Although the MODIS derived PSN_{net} estimates were confined to represent only

grassland pixels, it is likely that a number of these pixels contained mixtures of both

grassland and crop vegetation. This is because developed annual crops are not

intermingled with standing dead residue from the previous year, thereby proportionally

increasing the vegetation signal. In this situation crops could possibly boost FPAR, and

therefore PSN_{net}, while the scaled AGGB only represented grassland vegetation, thereby

distorting the AGGB/PSN_{net} relationship. The situation is further complicated during

years where unfavorable growth conditions predominate. In a similar study, Wylie et al.

(1995) reported better relations between satellite data and biomass during favorable years

($r^2 = 0.8$ and 0.7) versus non-favorable years ($r^2 = 0.25$ and 0.67). More restricted ranges

of biomass (as in this study) will usually reduce the r-square statistic due to its sensitivity to the range of the independent variable (Wylie et al. 1995). However, if a broad range of biomass is examined, the relationship between NDVI and biomass will generally be greater. For example, Wylie et al. (2002), related biomass to Thematic Mapper NDVI over a broad range of biomass and grassland types resulting in a strong relationship ($r^2 =$ 0.85). Using MODIS PSN_{net} estimates to compare with such large differences in biomass will undoubtedly produce more favorable results when in contrast with regions of small differences in productivity.

Regionally averaged Inter-annual trends in NPP were identical to precipitation over the same spatial aggregate. The similar trends between NPP and growing season precipitation are important as they indicate that MODIS can be used for regional grassland assessment, especially where objective coverage from a synoptic perspective is a priority. While the inter-annual NPP analysis is based on a large regional average (about 2,750,000 ha), the accuracy and precision of primary productivity estimates at a particular point is, for some purposes, less useful than temporal trends of NPP (Zheng et al. 2003). To this end, MODIS vegetation productivity products provide a regular, unbiased source of information for evaluating grassland productivity.

Conclusions

The reliability of productivity estimates for monitoring grassland biomass fluctuations is improved during years where plant growth conditions are more favorable. Use of MODIS data for characterizing regional vegetation patterns may be more useful for addressing administrative, rather than managerial needs given a course resolution and regional perspective of the MODIS vegetation products.

This study presents a framework for linking small-scale field observations to improved MODIS PSN$_{net}$ estimates while simultaneously providing needed insight to the response of MODIS productivity estimates to grassland biomass fluctuations. However, the large number of ground samples needed to calibrate the proposed scaling models still makes similar research a significant investment, especially when the goal is monitoring through time as opposed to a single point in the growing season. Despite this cost, with the exception of the ETM+ imagery, all data used to construct the model for both years of the study were freely available. Both ASTER and ETM+ provided sufficient spectral and spatial detail for constructing the scaling models at the scale of Thiesson polygons used in this study (about 185,000 ha). The comparison between scaled and un-scaled AGGB and MODIS data demonstrates the importance of interpolating between plots for regional remote sensing studies.

The relatively higher correlation between improved MODIS PSN$_{net}$ and scaled AGGB in 2001 compared with 2002 indicates that years with beneficial growing conditions, and therefore higher biomass levels, provide more reliable results. This was clearly demonstrated in both visual comparison (figure 4) and quantitatively. Monitoring will be especially difficult if there is a significant amount of senesced vegetation in the upper canopy. In addition, monitoring should be conducted at peak greenness to enhance the probability of successful monitoring. The similarity between differences in precipitation and integrated MODIS PSN$_{net}$ during peak greenness is encouraging and offers evidence that MODIS is a potentially valuable tool for evaluating moisture driven grassland biomass fluctuations within a given year. Similarly, the inter-annual differences in NPP agreed with differences in growing season precipitation in the

45

same period. Despite demonstrating the utility of MODIS data for characterizing varying

levels of grassland biomass, this study was limited in scope and applicability because it

was restricted to northern mixed grass prairie. If the study were designed to characterize

relations across different expressions of grassland vegetation (e.g., transition from

shortgrass prairie to sagebrush-steppe communities), a broader range of vegetation

productivity, and therefore MODIS derived productivity estimates, would have been

observed, making the findings more universally applicable.

Literature Cited

Atlas, R.M. and Lucchesi, R., 2000. File Specification for GEOS-DAS Gridded Output, Data Assimilation Office, Goddard Space Flight Center, Greenbelt Maryland.

Baker, J.T., Pinter, P.J., Regenato, R.J. and Kanemasu, E.T., 1986, Effects of temperature on leaf appearance in spring and winter wheat cultivars. *Agronomy Journal*, **78**, 605-13.

Box, E.O., Holben, B.N. and Kalb, V., 1989, Accuracy of the AVHRR vegetation index as a predictor of biomass, primary productivity and net $CO2$ flux. *Vegetatio*, **80**, 71-89.

Choudhury, B.J., 1987, Relationships between vegetation indices, radiation absorption, and net photosynthesis evaluated by a sensitivity analysis. *Remote Sensing of Environment*, **22**, 209-233.

Cleland, D.T., Avers, P.E., Mcnab, W.H., Jensen, M.E., Bailey, R.G., King, T. and Russel, W.E., 1997. National hierarchical framework of ecological units. In Ecosystem management: applications for sustainable forest and wildlife resources, edited by M.S. Boyce and A. Haney (New Haven: Yale University Press), pp. 181-200.

Hansen, M.C. and Reed, B., 2000, A comparison of the IGBP DISCover and University of Maryland 1 km global land cover products. *International Journal of Remote Sensing*, **21**, 1365-1373.

Hanson, C.L., 1976, Model for predicting evapotranspiration from native rangelands in the Northern Great Plains. *ASAE Transactions*, **19**, 471-477.

Heinsch, F.A., Reeves, M.C., Bowker, C.F., Votava, P., Kang, S., Milesi, C., Zhao, M., Glassy, J., Jolly, W.H., Kimball, J.S. and Nemani, R.R., 2003. User's Guide: GPP and NPP (MOD17A2/A3) Products NASA MODIS Land Algorithm V. 2.0, University of Montana, Missoula, MT.

Jensen, M.E., Dibenedetto, J.P., Barber, J.A., Montagne, C. and Bourgeron, P.S., 2001, Spatial modeling of rangeland potential vegetation environments. *Journal of Range Management*, **54**, 528-536.

Lauenroth, W.K., 1979. Grassland Primary Production: North American grasslands in perspective. In Perspectives in grassland ecology, edited by N.R. French (New York: Springer-Verlag), pp. 3-24.

Markham, B.L. and Barker, J.L., 1986, Landsat MSS and TM post-calibration dynamic ranges, exo-atmosphere reflectances and at-satellite temperatures. *EOSAT Landsat Technical Notes*, 3-8.

Reeves, M.C., Winslow, J.C. and Running, S.W., 2001, Mapping weekly rangeland vegetation productivity using MODIS algorithms. *Journal of Range Management*, **54**, A90-A105.

Running, S.W., Thornton, P.E., Nemani, R. and Glassy, J.M., 2000. Global terrestrial gross and net primary productivity from the Earth Observing System. In Methods in Ecosystem Science, edited by O. Sala, R. Jackson and H. Mooney (New York: Springer Verlag), pp. 44-57.

Sannier, C.A.D., Taylor, J.C., Plessis, W.D. and Campbell, K., 1998, Real-time vegetation monitoring with NOAA-AVHRR in southern Africa for wildlife management and food security assessment. *International Journal of Remote Sensing*, **19**, 621-639.

Scurlock, J.M.O., Johnson, K. and Olson, R.J., 2002, Estimating net primary productivity from grassland biomass dynamics measurements. *Global Change Biology*, **8**, 736-753.

Shoshany, M., Lavee, H. and Kutiel, P., 1995, Seasonal vegetation cover changes as indicators of soil types along a climatological gradient: a mutual study of environmental patterns and controls using remote sensing. *International Journal of Remote Sensing*, **16**, 2137-2151.

Steininger, M.K., 2000, Satellite estimation of tropical secondary forest above-ground biomass: data from Brazil and Bolivia. *International Journal of Remote Sensing*, **21**, 1139-1157.

Strahler, A., Townshend, J., Muchoney, D., Borak, J., Friedl, M., Gopal, S. and Hyman, A., 1996, MODIS land cover and land-cover change Algorithm Theoretical Basis Document (ATBD), version 4.1. *http://modis.gsfc.nasa.gov/data/atbd/land_atbd.html*, 102.

Tucker, C.J., Slayback, D.A., Pinzon, J.E., Los, S.O., Myneni, R.B. and Taylor, M.G., 2001, Higher Northern Latitude NDVI and Growing Season Trends from 1982 to 1999.

Turner, D.P., Cohen, W.B., Kennedy, R.E., Fassnacht, K.S. and Briggs, J.M., 1999, Relationships between leaf area index and Landsat TM spectral vegetation indices across three temperate zone sites. *Remote Sensing of Environment*, **70**, 52-68.

Turner, D.P., Ritts, W.D., Cohen, W.B., Gower, S.T., Zhao, M., Running, S.W., Wofsy, S.C., Urbanski, S., Dunn, A.L. and Munger, J.W., 2003, Scaling gross primary production (GPP) over boreal and deciduous forest landscapes in support of MODIS GPP validation. *Remote Sensing of Environment*, **88**, 256-270.

White, M.A., Thornton, P.E. and Running, S.W., 1997, A continental phenology model for monitoring vegetation responses to inter-annual climatic variability. *Global Biogeochemical Cycles*, **11**, 217-234.

Whitman, W.C., 1978. Analysis of grassland vegetation on selected key areas in southwestern North Dakota. A report on a project of the North Dakota Regional Environmental Assessment Program Contract No. 7-01-2., Department of Botany, North Dakota State University, Fargo, N.D.

Wylie, B.K., Dejong, D.D., Tieszen, L.L. and Biondini, M.E., 1996, Grassland canopy parameters and their relationships to remotely sensed vegetation indices in the Nebraska Sand Hills. *Geocarto International*, **11**, 39-52.

Wylie, B.K., Dendra, I., Pieper, R.D., Harrington, J.A., Reed, B.C. and Southward, G.M., 1995, Satellite-based herbaceous biomass estimates in the pastoral zone of Niger. *Journal of Range Management*, **48**, 159-164.

Wylie, B.K., Meyer, D.J., Tieszen, L.L. and Mannel, S., 2002, Satellite mapping of surface biophysical parameters at the biome scale over the North American grasslands A case study. *Remote Sensing of Environment*, **79**, 266-278.

Zar, J.H., 1995, Biostatistical Analysis, (Upper Saddle River, New Jersey: Prentice-Hall).

Zheng, D., Prince, S. and Wright, R., 2003, Terrestrial net primary production estimates for 0.5° grid cells from field observations-a contribution to global biogeochemical modeling. *Global Change Biology*, **9**, 46-64.

CHAPTER 3

EVALUATING THE USE AND LIMITATIONS OF MODIS PRODUCTIVITY DATA
FOR ESTIMATING WHEAT YIELD OF THE NORTHERN GREAT PLAINS

Abstract

Gross primary productivity (GPP) estimates derived from the Moderate Resolution

Imaging Spectroradiometer (MODIS) are converted to wheat yield and compared with

observed yield for counties, climate districts and entire states for the 2001 and 2002

growing season in Montana and North Dakota. Analyses revealed that progressive levels

of spatial aggregation generally improved the relations between estimated and observed

wheat yield. However, only state level yield estimates were sufficiently accurate ($\leq 5\%$

deviation from observed yield). The statewide yield results were encouraging because

they were derived without the use of retrospective empirical analyses, which constitutes a

new opportunity for timely wheat yield estimates for large regions. Additionally, this

study identifies six practical limits to estimating wheat yield using MODIS GPP

including: (1) positional accuracy within and between successive MODIS GPP estimates,

compared to a spatially dynamic, agriculturally dominated landscape; (2) spatially and

temporally invariant physiological parameters in the GPP algorithm; (3) coarse resolution

GPP and meteorological data; (4) insufficient land cover masks for delineating different

crop types; (5) no current method for determining growing season length without

retrospective analaysis and, (6) lack of spatially explicit cultivar data, which called for

broad assumptions regarding harvest index and root:shoot ratio.

As a result, I recommend 1) a more appropriate, regionally specific land cover classification, 2) more localized meteorology and 3) adaptation of physiological parameters to represent wheat.

Introduction

Chapter two demonstrates the strength of MODIS vegetation data for evaluating regional rangeland biomass in Western North Dakota. Rangelands are often spatially intermingled with agricultural landscapes and can be difficult to adequately differentiate using coarse satellite data. Despite this difficulty, agriculture provides unrivaled economic benefit to the Northern Great Plains. In particular, wheat is the largest crop in terms of acreage and economic gain. In 2003, the total wheat crop in Montana and North Dakota was worth 1.7 billion dollars (USDA 2003).

For decades scientists have sought to develop regionally applicable estimators of wheat yield (Weigand et al. 1979, Tucker et al. 1980, Hatfield 1983, Laguette et al. 1998, Labus et al. 2002), and growth, using models formulated from remote sensing data. With a few exceptions most broad scale remote sensing models have used the Advanced Very High Resolution Radiometer (AVHRR) Normalized Difference Vegetation Index (NDVI) to derive, empirical relationships between NDVI and yield (Benedetti and Rossini 1993, Gupta et al. 1993, Labus et al. 2002). The simplicity of NDVI and its inherent link to photosynthetic activity, make NDVI a popular tool for monitoring crop activity (Benedetti and Rossini 1993), and therefore yield (Doraiswamy and Cook 1995). However, while retrospective analyses provide insight into past performance, these do little to satisfy the need for timely yield information. Application of these empirical NDVI models (e.g., Brocklehurst 1977, Rao et al. 1993) is limited to the regions and time

frames for which the regression equations were formulated. This means that regression models must be carefully re-evaluated each season, limiting their practical utility. Furthermore, these empirical models simply link NDVI, a direct measure of radiation absorption and reflectance, to wheat yield solely on the basis of indirect inference. Unlike crops whose yield consists of total above-ground production, wheat yield is contained in storage organs and is very sensitive to adverse meteorological conditions at critical growth stages, including flowering and grain filling. This means that although above-ground biomass may be high and quantified using NDVI, actual grain yield may not be commensurately large. Thus, there is niche for a regional wheat yield monitor that can be applied in a timely manner and is not solely dependent on empiricism yet provides an accurate depiction of spatially explicit regional crop growth and yield. To facilitate this endeavor, the Moderate Resolution Imaging Spectroradiometer (MODIS) data are combined with meteorological inputs and used to produce daily estimates of gross primary productivity (GPP) in a plant growth algorithm. These GPP estimates can potentially be used for computing the seasonal growth and final yield of wheat for large regions without the need for retrospectively constructing empirical relationships between remote sensing data and observed yield.

To date, few if any studies have sought to estimate wheat yield from the MODIS GPP product, partly due to the infancy of the MODIS data stream and largely because of the difficulties associated with converting GPP to wheat yield for entire regions. For example, in agriculturally dominated environments in Montana and North Dakota, land cover variability is of smaller scales than can be resolved using the 1-km^2 spatial resolution MODIS land cover product. As a result a MODIS 1-km^2 pixel may include

more than one field, with potentially more than one crop or agricultural practice. In addition, the MODIS GPP algorithm was purposely designed for global applicability and includes only a generic set of "crop" physiological parameters.

One of the most challenging tasks in converting MODIS GPP to wheat yield is determining which pixels of a particular MODIS scene to use and the appropriate spatial domain for aggregation. Because large-scale aggregation minimizes landscape heterogeneity it seems intuitive that wheat yield estimates made over progressively larger regions will be increasingly more accurate (Benedetti and Rossini 1993, Doraiswamy and Cook 1995). My study was designed to 1) assess the potential of MODIS GPP for estimating wheat yield in Montana and North Dakota and 2) define the practical limits within which wheat yield can be sufficiently estimated using these data. To achieve these objectives MODIS GPP data were integrated over different time periods within the 2001 and 2002 growing seasons and converted to wheat yield using simple harvest index logic, across three spatial domains including counties, climate districts and states. This research is the first of its kind because it provides potential users of MODIS productivity data with valuable insight to what can realistically be expected using only standard MODIS products for assessing wheat yield in the Northern Great Plains.

Study Area

The study area consists of Montana and North Dakota (figure 1). Most wheat in Montana and North Dakota (97 and 99% respectively) is grown under dryland conditions (i.e. without irrigation) (USDA 2003). In Montana, most agricultural lands are located in the eastern portion of the state while in North Dakota these are distributed throughout (figure 2).
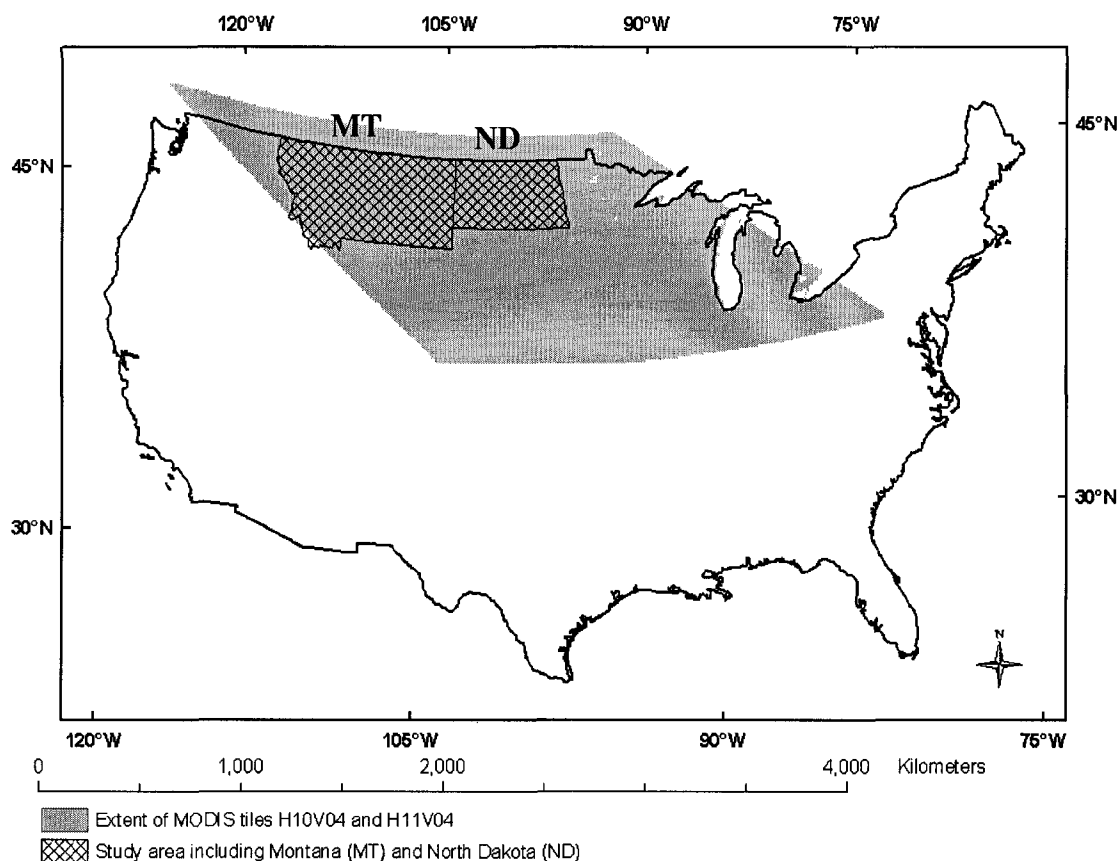
Figure 1. Spatial extent of study area including Montana (MT) and North Dakota (ND) and MODIS land tiles H10 V04 and H11 V04.

For this study, analysis was confined to counties with ≥ 12,000 ha of wheat planted in 2001 and 2002 (figure 3) (USDA 2003). The major wheat growing regions within the study area have continental, semi-arid weather patterns, characterized by cold winters and hot, dry summers. Regional precipitation during the growing season (1 April to 1 September) fluctuates (based on the 50-year mean) from 140-270 mm in Montana and 224-369 mm in North Dakota. Figure 4 demonstrates that the wheat growing regions within North Dakota are generally wetter than in Montana. As a result, greater wheat yields are usually observed in North Dakota. During the 2001 growing season (defined as 1 April to 1 September) North Dakota received 9% more precipitation than the 50 year

mean, while Montana received 12% less. In 2002 the situation was reversed, and

Montana received an amount of precipitation almost equal to the 50-year mean while

North Dakota was nearly 3% below the 50-year mean.
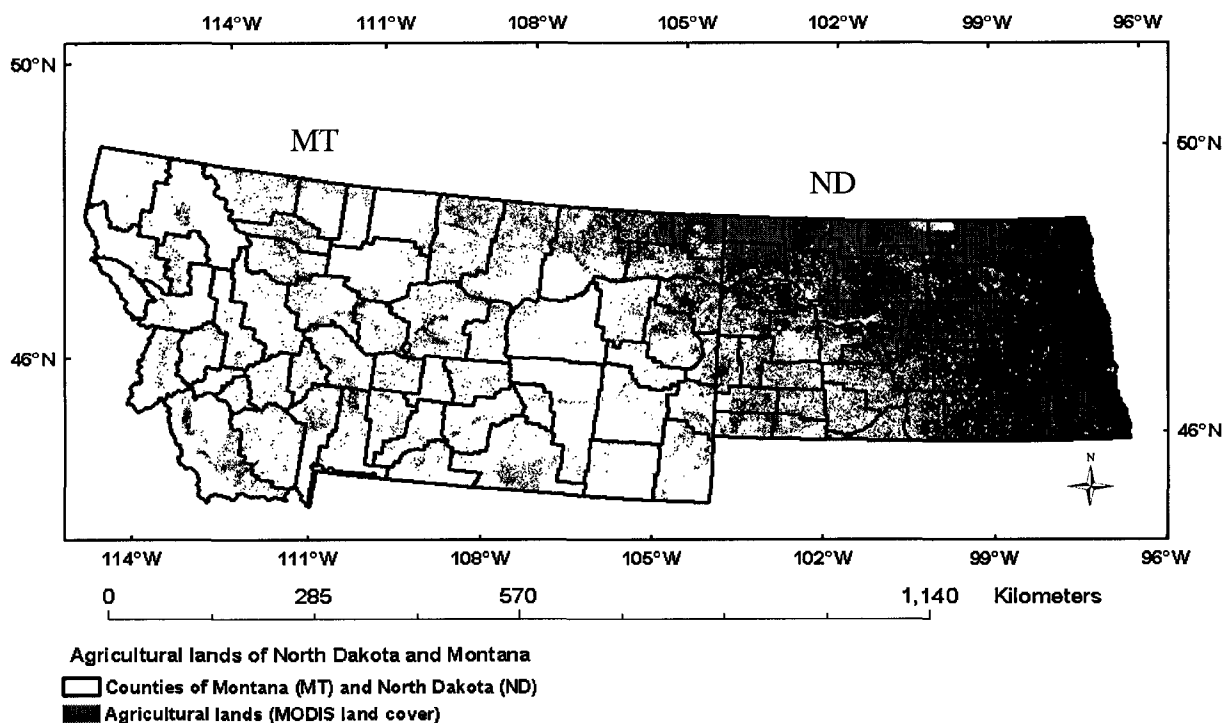
Figure 2. Distribution of agricultural land use (all crops) within North Dakota (ND) and
Montana (MT). Agricultural lands were delineated from other land use types
using the MODIS Type 2 land cover product (University of Maryland
Classification).
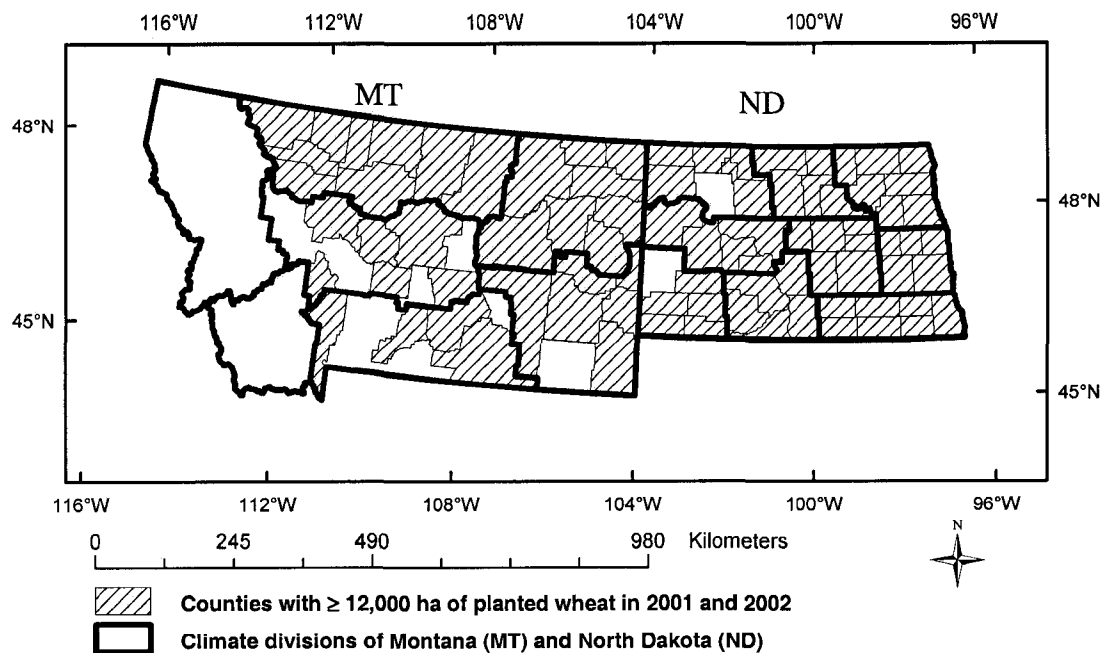
Figure 3. Counties and climate districts with ≥ 12,000 ha of planted wheat in 2001 and 2002 within the states of Montana (MT) and North Dakota (ND).
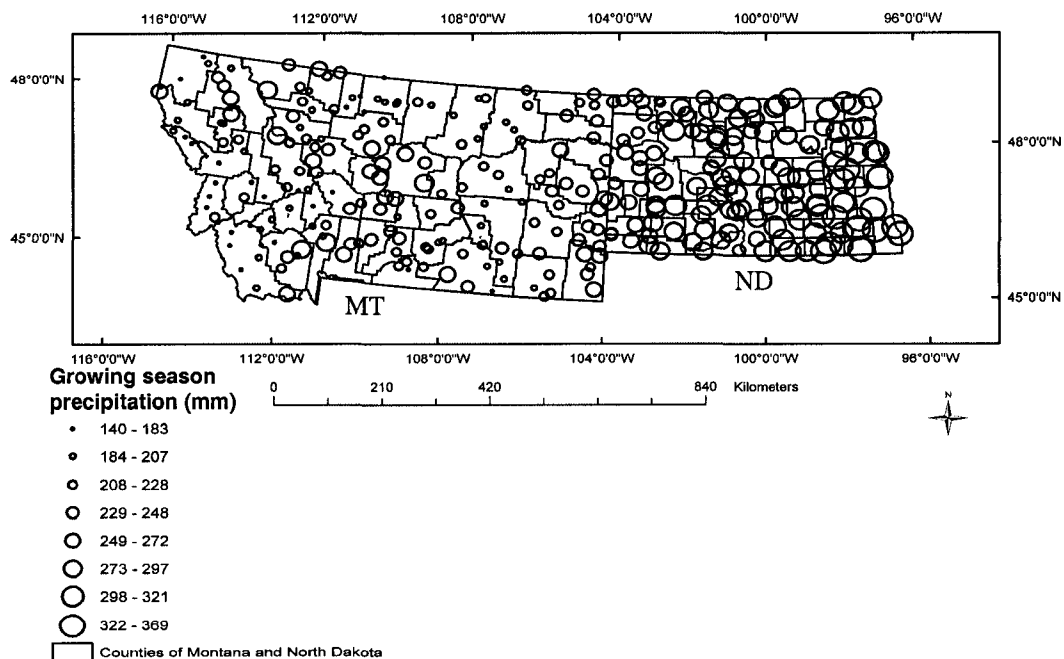
Figure 4. Fifty year mean growing season (1 April -1 September) precipitation at selected weather stations in Montana and North Dakota.

Methods

Procuring and Processing MODIS Data

The MODIS Collection 4 land cover (Friedl et al. 2002), and GPP (Running et al. 2000) from tiles H10 V04 and H11 V04 (figure 1) were used in this study. The spatial location of all MODIS tiles can be found in Heinsch et al. (2003) and elsewhere on the World Wide Web. The MODIS tiling scheme breaks the earth into 10° by 10° sections. Each tile is referenced using horizontal (H) and vertical (V) notation. The starting point for this grid in a Sinusoidal projection is the upper left corner. It follows that tile H10 V04 is the tenth tile from the left (west side of the system) and the fourth tile from the top (north side of the system).

The MODIS productivity algorithm is based on the logic of Montieth (1972, 1977) who suggested that the productivity of a well-watered and fertilized annual crop (one year growth cycle) is linearly related to the amount of absorbed photosynthetically active radiation (APAR). The amount of APAR depends on the quantity of solar radiation reaching a site and the ability of the vegetation to absorb that radiation. Monteith's formulation includes a maximum radiation use efficiency (ε_{max}) that is attenuated by the influence of environmental factors postulated to reduce growth efficiency (Running et al. 2000) including temperature and vapor pressure deficit (VPD). Daily GPP estimates are easily computed in the MODIS productivity algorithm from this logic using:

$$GPP = \varepsilon * PAR * FPAR \tag{1}$$

where GPP equals daily gross primary productivity (kg C m^{-2}), ε is the realized radiation use efficiency, PAR is photosynthetically active radiation and FPAR is the fraction of

absorbed PAR. Further information on the MODIS vegetation productivity algorithm can be found in Running et al. (2000) and in Heinsch et al. (2003).

Eight-day summations of gross primary productivity were obtained for the 2001 and 2002 growing season. The summation is computed by adding all eight days of productivity estimates (kg C m^{-2}). Three eight-day composite periods (153-177) were missing in June 2001 due to sensor malfunction, thus linear interpolations were used to fill in GPP for these missing periods. Precipitation occurring during the missing periods would not have induced a significant amount of error in the analysis since this would have been manifested as increased FPAR in subsequent periods provided the precipitation events were sufficiently intense. Since interpolating the GPP data themselves would have produced relatively inaccurate estimates, linear interpolation on the MODIS-derived FPAR was performed from the periods before and after the missing data. Gross primary productivity was subsequently re-calculated for the missing periods.

All MODIS land products have quality assurance data affiliated with each pixel for every composite period. The quality assurance layer provides a means for screening all pixels that are not suitable for analysis, either as a result of sensor or algorithm performance or atmospheric conditions. In this study, only the best quality GPP pixels were retained for further analysis (Table 1). If a pixel was missing for any given eight-day period (due to clouds, sensor malfunction or any other reason), GPP was recomputed with the MODIS productivity algorithm from interpolated FPAR. Fraction of photosynthetically active radiation was estimated for poor quality or missing periods through linear interpolation as described above. All MODIS land products were left in their native Sinusoidal projection and HDF-EOS format for analysis.

Table 1. Quality control criteria used for screening MODIS GPP data for 2001 and 2002.

QC flag description	Screening criteria
MODLAND_QC	< = 1
DEADDETECTOR	0
CLOUDSTATE	0 or 3
SCF_QC	< = 3

*A detailed explanation of these criteria can be found in Heinsch et al. (2003).

Identifying Agricultural Land Use

To achieve the objective of computing wheat yield for Montana and North Dakota, I isolated areas where wheat was planted by limiting the analysis to counties that reported $\geq$ 12,000 ha of planted wheat in 2001 and 2002. The MODIS land cover product was spatially subset to include only agricultural land use (figure 2), using a spatial subset derived from MODIS land cover Type 2 data (University of Maryland Classification) (Friedl et al. 2002). The Type 2 land cover is comparable to the International Geosphere-Biosphere Program (IGBP) global land cover data set (Hansen and Reed 2000).

Obtaining Wheat Yield Observations

Observed wheat yield was obtained from the United States Department of Agriculture (USDA) National Agricultural Statistics Survey (NASS). The NASS provides crop yield estimates through the Published Estimates Database (PEDB) (USDA 2003) (http://www.nass.usda.gov:81/ipedb/) for counties, states and crop reporting districts (climate districts). Yield data for individual counties are gathered using a census, thus the original yield data come from individual producers. Detailed reports on data accuracy and compilation techniques are available at USDA (2003) and USDA (2004). It was necessary to choose the all-wheat, dryland farming category because the MODIS Type 2 land cover product does not differentiate irrigated from non-irrigated agriculture or different kinds of wheat. This was not considered a problem in the analysis

because dryland farming comprises > 97 % and > 99.5 % of Montana's and North

Dakota's wheat crop respectively (USDA 2003). Furthermore, most irrigated fields

cover a much smaller spatial extent, rarely exceeding 65 ha.

The all-wheat yield category within each county for both states includes durum,

spring, and winter wheat as a weighted mean for each county based on their respective

proportion of area cropped. For example, in 2001, Teton County, Montana reported

plantings of 2,834, 21,458, and 20,041 ha of durum, spring, and winter wheat

respectively. Reported yield for these respective types of wheat were 1414.5, 1145.1, and

1414.5 kg ha^{-1}. As a weighted mean the final yield computed for Teton County was

1284.1 kg ha^{-1}.

Deriving Wheat Yield From GPP Estimates

Preliminary results indicated that net primary productivity (NPP) from MODIS

produced wheat yield estimates that were unrealistically low using the formulation

discussed here. Thus, gross primary productivity was used instead of NPP to estimate

wheat yield despite the fact that GPP does not account for respiratory losses. A potential

reason that NPP estimates produce low figures of wheat yield is that the default radiation

use efficiency (RUE) in the MODIS vegetation productivity algorithm is 0.608 g C MJ^{-1}

PAR (Heinsch et al. 2003), which is equivalent to 1.208 g biomass MJ^{-1} PAR since

biomass is approximately 50% carbon (Waring and Running 1998). This is just less than

half of the standard RUE (2.2 g biomass MJ^{-1} PAR) used in well known field level wheat

yield models such as SIRIUS (Jamieson et al. 1998), and that developed by Amir and

Sinclair (1990). These estimates of gross primary productivity were spatially subset to

the crop analysis mask and temporally integrated over an apparent growing season

defined as DOY 81-208, 81-216, 81-225, and 81-233.

Unlike previous studies (Labus et al. 2002), I elected not to use annual integration

for yield estimation, because it makes little sense to include GPP data from before mid-

March or after mid-September for wheat yield analysis in the northern great plains unless

the analysis focuses solely on winter wheat. Since spatially explicit information on date

of harvest was not available for counties or climate districts, it was assumed that all

wheat fields in Montana and North Dakota were harvested or physiologically mature by

21 August (DOY 233). Similarly, no spatially explicit data were available for time of

emergence, so it was assumed that winter wheat planted in the fall of the previous year

had emerged and was visibly green by March of the following year, although

photosynthesis at that time is negligible primarily due to temperature constraints.

Following the masking and temporal integration, GPP data were averaged over

three spatial domains including counties, climate districts, and entire states (figure 3).

Wheat yield was computed for individual counties, climate districts and states (Montana

and North Dakota) using a simple harvest index.

Gross primary productivity estimates from MODIS are given in kg C m^{-2}. These

units are easily converted to biomass estimates because carbon comprises roughly 50% of

vegetative biomass (Waring and Running 1998). At physiological maturity,

approximately 90% of the accumulated biomass of wheat is above-ground while the rest

is allocated to roots (Jamieson 1999). A review of past research (Fischer and Kohn 1966,

Puckridge and Donald 1967, Mcneal et al. 1971, Singh and Stoskopf 1971, Syme 1972,

Fischer and Kertesz 1976, Bauer et al. 1987, Rickert et al. 1987, Entz and Fowler 1988,

Austin et al. 1989, Martin and Kiyomoto 1989, Flood et al. 1995, Tacettin et al. 1995,

Moot et al. 1996, Wheeler et al. 1996) indicated that, on average, across many cultivars

and types of wheat (winter, spring, and durum), a harvest index of 38% can be used to

estimate the amount of grain present in above-ground biomass. This harvest index was

included in the wheat yield formulation:

$$Yield_{est} = \sum_{DOY=81}^{a} GPP_{DOY} * 2 * 0.9 * HI \tag{2}$$

where $Yield_{est}$ is the yield estimate (kg ha^{-1}), a is an arbitrary growing season end point

(DOY 208, 216, 225, or 233), GPP_{DOY} is daily gross primary productivity (kg C m^{-2}), two

is a conversion factor from carbon to biomass, 0.9 (90%) is the annual proportion of GPP

allocated to above-ground productivity, and HI is the harvest index of 38%.

Results and Discussion

In 2001, period 81-208 and 81-216 produced the highest level of agreement

between estimated and observed state level yields for Montana and North

Dakota,respectively. In contrast, period 81-225 produced the highest agreement in 2002

for both states (Table 2). These periods were established as the standard for subsequent

county and climate district analyses in this paper.

Table 2. Results of state level wheat yield estimates from MODIS GPP for Montana and
North Dakota in 2001 and 2002.

State	Year	Estimated yield(SE) kg ha^{-1}	Observed yield(SE) kg ha^{-1}	% Difference estimated-observed	Apparent Growing Season*
MT	2001	1520.9± (62.6)	1500.1± (105.6)	1	81-208
MT	2002	1475.8± (70.9)	1410.0± (91.1)	5	81-225
ND	2001	2092.8± (67.0)	2188.8± (141.4)	-4	81-216
ND	2002	1640.1± (41.1)	1700.8± (161.2)	-4	81-225

*The apparent growing season that provided the best relationship between estimated and
observed state level wheat yield for Montana and North Dakota.

County Level Yield Estimation

Linear regression demonstrated that county level wheat yield estimates from MODIS for Montana and North Dakota are only weakly related to observed yield (Table 3). However, in 2001, and to a lesser degree 2002, the strength of the relation between estimated and observed wheat yield increased with progressively longer apparent growing seasons (Table 3).

In both years of the study MODIS GPP produced wheat yield estimates that were generally too low at high levels of observed yield (figure 5). This is likely due to the low RUE discussed above. Gallatin county is a noteable outlier in 2001 and 2002. Yield estimates from MODIS for this county were 1751 and 1768 kg ha^{-1} for 2001 and 2002 respectively, while observed wheat yield estimates were 3516 and 3300 kg ha^{-1} over the same time period. Of all counties in Montana with $\geq$ 12,000 ha of planted wheat, Gallatin has the highest mean elevation of agricultural fields. Temperatures at higher elevation will be cooler, which is favourable for wheat especially during the grain filling process (Brocklehurst 1977, Sofield et al. 1977, Moot et al. 1996). This indicates a need for a variable growing season determined by air temperature instead of using the apparent growing season used by Labus et al. (2002) and the current study.

Table 3. Relationship (r^2) between estimated and observed county level wheat yield for Montana and North Dakota in 2001 and 2002.

State	Year	Apparent growing season (DOY)	r^2	p-value
MT	2001	81-208	0.33	0.001
		81-216	0.42	0.0
		81-225	0.43	0.0
		81-233	0.46	0.0
MT	2002	81-208	0.01	0.52
		81-216	0.22	0.006
		81-225	0.30	0.002
		81-233	0.33	0.000
ND	2001	81-208	0.04	0.410
		81-216	0.05	0.443
		81-225	0.06	0.266
		81-233	0.06	0.20
ND	2002	81-208	0.07	0.12
		81-216	0.13	0.51
		81-225	0.14	0.07
		81-233	0.16	0.06

The poor overall performance of the wheat yield model at the county level was not surprising because counties are the smallest spatial conglomerate for which the NASS provides observed wheat yield data and therefore are highly variable. The 2002 county level results of this study generally compare unfavourably with those reported by Doraiswamy and Cook (1995), who related observed yield in North and South Dakota to summation of NDVI across varying time frames in a retrospective, empirical fashion. In their study r-square values describing the relationship between estimated and observed county level yield ranged from 0.57 to 0.69 in North Dakota to 0.01 to 0.6 in South Dakota. In contrast to this study, Doraiswamy and Cook (1995), focused on spring wheat only, and utilized a spring wheat mask developed by Brown et al. (1993). Although the inclusion of a regionally applicable crop specific analysis mask would have likely improved county level results in this study, I limited the analytical inputs to test the

potential and practical limits of MODIS data alone. Similarly, meterological variables

such as growing season precipitation could have been included along with MODIS GPP

in a regression model designed to empirically estimate wheat yield, which would have

increased predictive ability.
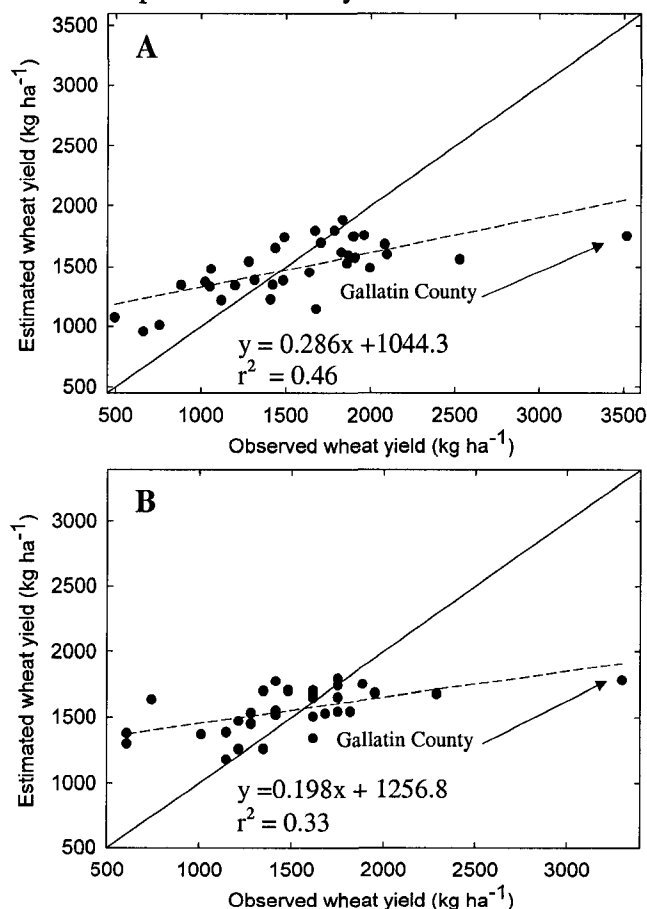
Figure 5. Observed versus estimated county level wheat yield (Kg ha^{-1}) for Montana in
2001 (A) and 2002 (B). The dashed line is a linear least-squares best fit
regression analysis. Gallatin County is the notable outlier. High yields are
observed in Gallatin County due to increased grain filling periods resulting from
high elevation fields.

Again, this would have defeated a major objective of this study, which aims to

move beyond statistical methods for estimating wheat yield from satellite data.

The poor correlation between estimated and observed county level wheat yield for

2001 and 2002 is partly due to high intra-and inter-annual variability in observed yield,

resulting from diverse growing conditions and anomalous meteorological events found throughout the study area. Unusual meteorological events resulted in extreme variability in the range of reported county level wheat yield (figure 6). The 2001 range in wheat yield in Montana has been surpassed only three times over the period from 1951 to 2002, while the 2002 range has been surpassed five times (figure 6). Similarly, the range in observed North Dakota wheat yield for 2002 has been surpassed only one time during the same period (figure 6). In 2001, yield ranged from 491.7 to 4135.7 kg ha^{-1} in Montana and 1414.5 to 3340.9 kg ha^{-1} in North Dakota. Reported yields in 2002 ranged from 538.9 to 3704.6 kg ha^{-1} in Montana and 606.2 to 2761.6 kg ha^{-1} in North Dakota.

Both years analysed for this study represent unusual conditions caused by atypical meteorological events. For example, in 2001, mid-season precipitation events of unusual intensity (> 400 mm in 48 hours) were unofficially recorded in some wheat growing regions of North Dakota, while other meteorological stations in the vicinity ($\leq$ 10 kilometers) may have received as little as 250 mm of total growing season precipitation (Edwardson 2003). These aberrant rain storms produced flooding conditions on a localized basis which led to crop failure in some areas of North Dakota (Edwardson 2003). Such variability in precipitation is critical to understanding potential sources of error in the county level wheat yield estimates, which are based on measures of above-ground vegetative productivity (Eq. 2).
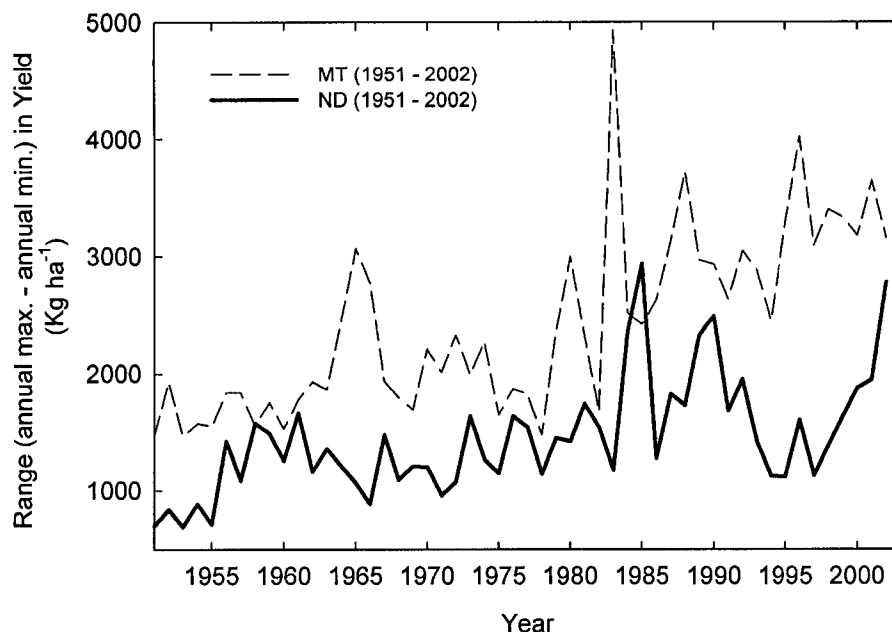
Figure 6. Range in county level wheat yield (kg ha^{-1}) from 1950-2002 for Montana and North Dakota.

For example, above average preciptation in the 2001 growing season produced increased vegetative growth in North Dakota, which is reflected in higher estimates of FPAR and may reduce vapor pressure deficit, a key component for determination of realized RUE. This, in turn, increased GPP as computed by the MODIS GPP algorithm. Using the wheat yield estimation logic presented in this paper (Eq. 2), any pixel exibiting higher GPP will have a commensurately higher yield estimate. However, as previously mentioned, some of the same areas which experienced high vegetative productivity also reported low yield. Crops, such as alfalfa or grass hay, whose yield consists of the vegetative parts can be easily and accurately related to satellite derived estimates of above-ground productivity. In contrast, crops, like wheat, whose yield consists of storage organs, depend on the grain filling rate and duration (Sofield et al. 1977) as well as efficiency of the vegetative apparatus to assimilate CO_2. Using remote sensing, grain crops can only be indirectly related to yield, using primarily remote sensing based

models, thus posing a serious constraint for estimating wheat yield (Benedetti and Rossini 1993).

Climate District Yield Estimation

There were 16 climate districts in the study area (figure 3), but only 14 of these were used for analysis due to low area of planted wheat in two of them. The mean size of climate districts within the study area was approximately 3.5 million ha compared with a mean county size of 320,000 ha. Climate district relationships between estimated and observed wheat yield were more tightly coupled than county level yields in 2001 and roughly equivalent in 2002 (figure 7). However, both climate district and county level wheat yields were either weakly related or not related to observed wheat yield in 2002. Longer apparent growing seasons from DOY 81-208, 81-216, 81-225, and 81-233 steadily improved the r-square between estimated and observed climate district wheat yields from 0.46 to 0.67 in 2001 and 0.0 to 0.33 in 2002.

Factors that prevented a good relationship between estimated and observed yield at the county level were also present for climate districts. These factors included relatively smaller spatial aggregation, abberrant precipitation leading to widely ranging wheat yield, and difficulty relating estimates of above-ground GPP to wheat yield. In addition, one inhibiting factor not previously discussed is the potential spectral contribution of other crops. North Dakota receives greater growing season precipitation statewide than Montana (figure 4), and therefore a more diverse suite of crops is grown including broadleaf, cereal and fodder crops. For example, in 2001, approximately 35% (2,562,348 ha) of all crops cultivated in North Dakota were broadleaf crops (canola, sugar beets, corn, soybeans, sunflower, and dry beans) wheat. In Montana,
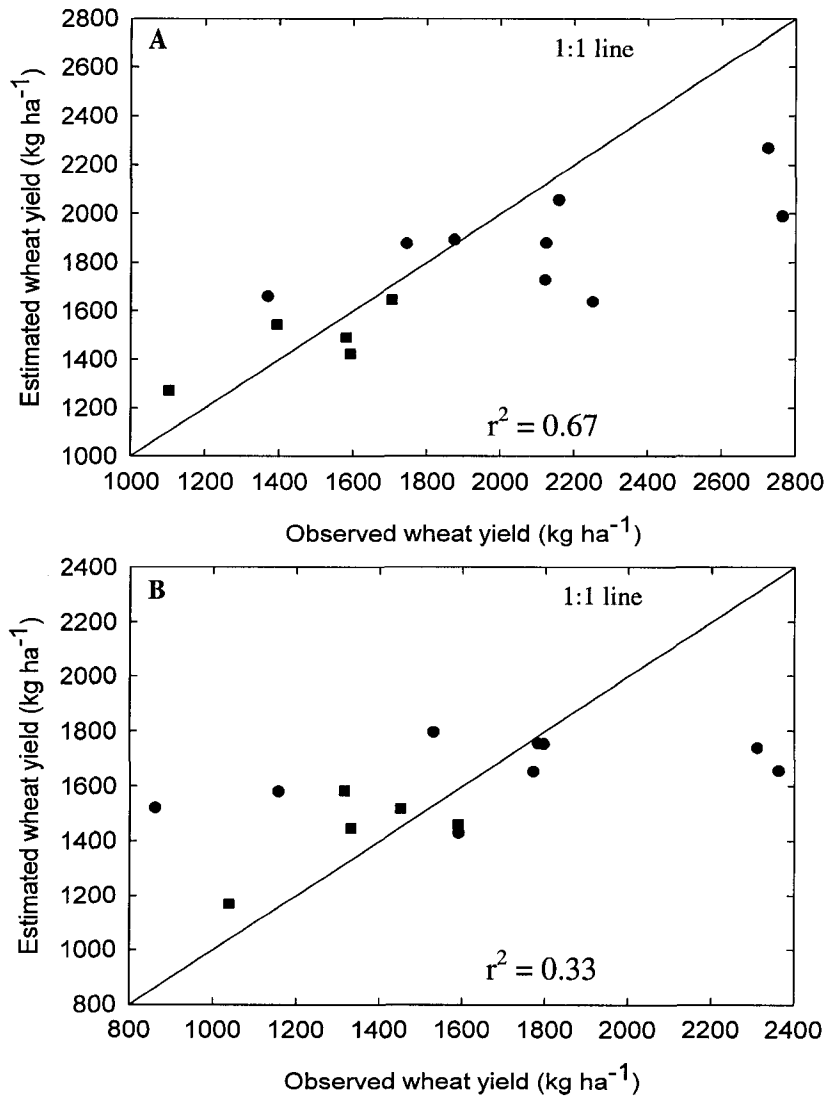
Figure 7. Relationship between estimated and observed wheat yield for climate districts with ≥ 12,000 ha of planted wheat. (A) 2001, and (B) 2002. ■, Montana and ●, North Dakota.

only 3.5% (89,635 ha) of the same broadleaf crops were planted compared with 93% (2,170,040 ha) of wheat. Since the MODIS land cover product does not distinguish among crop types, it is very likely that a portion of the spectral response (and thus FPAR and GPP) at a given pixel is dominated by crops other than wheat, especially in North Dakota. Although this has negative consequences for yield estimation, these can be

partially alleviated with a more appropriate analysis mask as demonstrated by

Doraiswamy and Cook (1995).

State Level Yield simulation

State level wheat yields provided the most favourable results, which indicates

good potential for use of MODIS GPP to estimate wheat yield for an entire state or region

of similar size. Estimated wheat yields for both Montana and North Dakota were

sufficiently accurate and never deviated more than ± 5% from actual yield for the

duration of the study (Table 2). These results are encouraging and compare favourably

with those of Doraiswamy and Cook (1995). In addition, the growing season and

subsequent harvest were estimated to be of longer duration in 2002 (Table 2), which

matches closely with crop reports issued by the NASS.

Identifying Practical Limits to Wheat Yield Assessment With MODIS GPP Data

While not accurate at smaller scales, MODIS GPP can be used with the simple

yield formulation shown in this paper for accurate statewide yield estimates. Perhaps

more importantly, the results of this study did reveal a suite of practical limitations that

appear to handicap wheat yield estimates from MODIS GPP, especially for smaller

geographic regions. The following practical limitations deserve careful consideration

prior to embarking on a research or managerial project aimed at using MODIS GPP for

deriving wheat yield estimates. These practical limitations fit within the following

categories: 1) sensor, 2) data and 3) wheat yield logic limitations.

Sensor Spatial Limitations

The MODIS provides the most state-of-the-art, globaly applicable satellite data

freely available. For regional or global applications the spatial resolution of MODIS GPP

provides a beneficial trade-off among spatial resolution, repeat cycle, and data volume. However, the standard GPP product is only available at 1-km^2 spatial resolution as eight-day summations. For smaller spatial aggregation analyses (e.g. counties and climate districts), there are limitations imposed by this 1- km^2 resolution. Clearly, most crops are not grown at regularly spaced, 1-km^2 intervals. In fact, many fields consist of intermittent crops and bare ground with wheat stubble (fallow), known as strip cropping. This means that computation of FPAR and, therefore, estimated GPP will include the effects of photosynthesizing wheat (or other vegetation), bare soil with wheat stubble and bare soil. The situation is further complicated by mis-registration errors between scenes, though theoretically, each pixel should be accurate within ± 0.1 pixels at two standard deviations (Running et al. 1994).

Data and Algorithm Limitations

The MODIS sensor was engineered, in part, to produce data for monitoring and documenting global biospheric health (Running et al. 2000). Among other things, this task requires timely global vegetation productivity estimates, which necessitates several noteworthy simplifying assumptions (Heinsch et al. 2003).

The following assumptions limits the ability of researchers to accurately and consistently estimate wheat yield for small geographic regions using the standard GPP product. First, the crop specific physiological parameters used to compute GPP do not vary with space or time. This means that although several cultivars of wheat may be grown within a single county, there is nothing in the MODIS GPP algorithm to account for varietal differences in physiological performance. Although, the actual maximum RUE of wheat declines significantly during the seed growth period of wheat (Amir and

Sinclair 1990) it is assumed to be constant for the entire growing season in the GPP algorithm. Second, GPP for a given pixel is dependent upon, among other things, FPAR, which is an eight-day composite product. This ensures that although GPP is calculated daily, the algorithm necessarily assumes that FPAR does not vary in a given eight-day period. Third, the MODIS vegetation productivity algorithm uses daily meteorological data including average and minimum temperature, vapor pressure deficit, and incident short wave radiation from the NASA Goddard Space Flight Center (GSFC) Data Assimilation Office (DAO) (Schubert et al. 1993). Collection 4 MODIS data (used in this study) use DAO inputs that are provided at 1° x 1.25° spatial resolution. Though these DAO data generally agree well with observed meteorology there are differences which can potentially induce innacurate productivity estimates, though the effects are probably less consequential for larger regions of aggregation. Finally, and perhaps most importantly, MODIS GPP estimates rely upon land cover data whose classification scheme does not differentiate among crop types.

Given these paremeters, especially in states such as North Dakota where many crop species are grown statewide, estimating wheat yield is challenging. For example, the MODIS land cover dataset used in this study did not agree well with observed planted area estimates of wheat (figure 8) and is likely a major reason for the disparity between estimated and observed wheat yield in this study. In addition, in Montana and North Dakota rangeland herbaceous vegetation begins greening-up at approximately the same time spring wheat is becoming established. Similarly, since spring wheat is cultivated in the spring, it matures about the same that summer crops such as corn, sunflower and soybeans are between peak leaf area and the start of senescence.
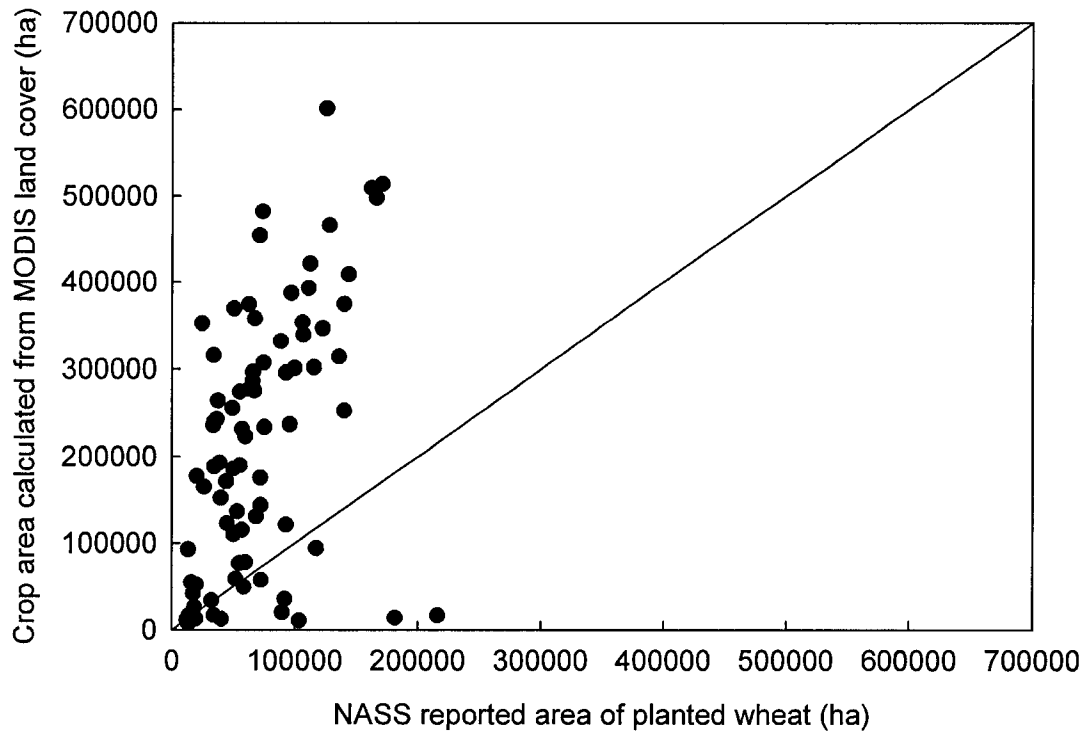
Figure 8. Observed area of wheat planted in 2001 for counties in Montana and North
Dakota with ≥ 12,000 ha of planted wheat versus crop acreage calculation from
type 2 MODIS land cover. ●,Counties of North Dakota and Montana.

Limitations of Wheat Yield Logic With MODIS GPP

Like the MODIS GPP algorithm itself, the wheat yield logic employed in this

paper (Eq. 2) relies on several necessary simplifying assumptions implemented due to

previously mentioned data limitations. Correct application of the wheat yield logic

requires determination of growing season length. The NASS provides reports that

indicate the proportion of the current year's wheat crop which is physiologically mature

or harvested. Unfortunately, however, these reports are provided on a statewide basis

only, and are of limited use for determining crop growth stage for smaller regions.

Without knowledge of growing season length, GPP summation (and therefore wheat

yield) will be over-or under-estimated.

During this study, state level yield estimates for North Dakota were found to be most accurate over the apparent growing season from DOY 81-216 and 81-225 in 2001 and 2002 respectively. However, in either year, GPP summation and resulting wheat yield computation one composite period before or after these dates decreased accuracy of estimates by at least $\pm$ 67 kg ha^{-1}. An objective of this research was to create a wheat yield estimation protocol that did not rely solely on empiricism, and instead computed above-ground productivity using a few simple relationships fundamentally linking GPP to above-ground biomass and yield. Specifically, the model assumes that by the end of the growing season, approximately 90% of the total biomass is above-ground. Further, grain yield is fixed at 38% of the above-ground biomass. Local meteorological conditions, especially the anomalous events of 2001 and 2002, likely caused significant deviation of grain and root allocation in wheat crops from the constants used in this study. Again, the impact of such phenomena was likely magnified for smaller geographic regions, as the results suggest.

The difficulties of estimating wheat yield using MODIS GPP are numerous. Thus, I propose several strategies that address some of the stated practical limitations to accurate wheat yield estimates, especially for smaller geographic regions. The following section describes three suggestions for improving wheat yield estimates for scientists willing to re-compute MODIS-derived productivity estimates using regionally specific inputs.

First, land cover schemes including different cropping practises can be used as an analysis mask for analyzing MODIS GPP data. Doraiswamy and Cook (1995) used the land cover scheme created by Brown et al. (1993) to delineate spring wheat, while Labus

et al. (2002) used the MAPS Atlas to delineate dryland from irrigated farming in Montana. Second, observed local meteorological data can be substituted for DAO data in the MODIS GPP algorithm for a more accurate depiction of local growing conditions. Incorporating local meteorology would also permit estimates of growth stage and length of growing season in a timely manner. In particular, the development of spring wheat is strongly linked to accumulated growing degree days (Baker et al. 1986, Amir and Sinclair 1990, McMaster et al. 1991) most commonly computed as:

$$\Sigma((T_{min} + T_{max})/2 - 0_i) \tag{3}$$

where T_{min} and T_{max} are the minimum and maximum daily temperature, respectively, and 0 is the base temperature (°C) for a given phenological stage over the crop cycle $(_i)$. Finally, the NASS provides reports at the year's end that summarize the dominant wheat varieties planted in each state. Although these data are only available for climate districts, these would be useful for improving wheat yield logic. For example, different cultivars may posess different physiological characteristics such as harvest index, root allocation of sequestered carbon, and response to thermal time. Using these characteristics, crop physiological parameters in the GPP algorithm could be modified to accommodate different varieties of wheat.

Summary

Neither county level or climate district aggregations of wheat yield estimates were sufficiently accurate. However, the state level analysis did provide sufficiently accurate results, thereby providing further evidence (in concordance with Chapter two) that the appropriate spatial domain for analyzing MODIS data is larger regions. Progressively larger regional averages provide more precise measures of vegetation productivity bases

on the results of Chapter's two and three. In addition, it makes little sense to develop field level wheat yield monitors driven by remote sensing data given the enormous amount of calibration and data requirements. Further, farmers are likely to have a very good idea about the potential yield of their crop, thereby reducing the need for field level wheat yield estimates.

Fortunately, the current study provides a yield estimation framework which, unlike its predecessors, does not require retrospective empirical relations to derive yield. The merit of this technique (Eq. 2) is a quick turn-around time, which, at most, is ten days behind current conditions. For example, since the standard MODIS vegetation product (and most other land products) are eight-day composites, and are available almost immediately after completion, yield estimates could be computed by the ninth or tenth day. This, combined with the fact that state level wheat yield estimates can be accurately estimated prior to complete statewide harvest makes MODIS GPP a valuable tool for deriving timely estimates of state level wheat yield.

This research represents a preliminary attempt to fundamentally link MODIS GPP to wheat yield in Montana and North Dakota while defining the practical limitations to this endeavor. The anomalous growing season conditions encountered during this study substantiated the definition of practical limitations to accurate wheat yield estimates. Chief among the limitations outlined in this paper were: (1) positional accuracy within and between successive MODIS GPP estimates, compared to a spatially dynamic, agriculturally dominated landscape; (2) spatially and temporally invariant physiological parameters in the GPP algorithm; (3) coarse resolution GPP and meteorological data; (4) insufficient land cover masks for delineating different crop types; (5) no current method

for determining growing season length without retrospective analaysis and, (6) lack of spatially explicit cultivar data, which called for broad assumptions regarding harvest index and root:shoot ratio.

The pattern in accuracy of wheat yield estimates from counties to entire states demonstrated that these practical limitations are magnified for smaller spatial domains. Although these limitations provided a significant barrier to accurate wheat yield estimates for smaller regions, strategies are available to move beyond these limitations. These suggested improvements which are beyond the scope of the current study are: (1) implementation of more appropriate and regionally specific analysis masks to delineate wheat from other crops; (2) inclusion of localized, observed meteorological data and; (3) adaptation of crop physiological parameters in the current GPP algorithm to more closely emulate observed physiological characteristics of commonly grown wheat varieties in the region of interest. These recommedations are implemented in Chapter four.

Acknowledgements

Literature Cited

Amir, J. and Sinclair, T.R., 1991, A model of the temperature and solar-radiation effects on spring wheat growth and yield. *Field Crops Research*, **28**, 47-58.

Austin, R.B., Ford, M.A. and Morgan, C.L., 1989, Genetic improvement in the yield of winter wheat: a further evaluation. *Journal of Agricultural Science, Cambridge*, **112**, 295-301.

Baker, J.T., Pinter, P.J., Regenato, R.J. and Kanemasu, E.T., 1986, Effects of temperature on leaf appearance in spring and winter wheat cultivars. *Agronomy Journal*, **78**, 605-13.

Bauer, A., Black, A.B. and Black, A.L., 1987, Aerial parts of hard red spring wheat. 1. Dry matter distribution by plant development stage. *Agronomy Journal*, **79**, 845-852.

Benedetti, R. and Rossini, P., 1993, On the use of NDVI profiles as a tool for agricultural statistics: The case study of wheat yield estimate and forecast in Amilia Romagna. *Remote Sensing of Environment*, **45**, 311-326.

Brocklehurst, P.A., 1977, Factors controlling grain weight in wheat. *Nature*, **266**, 348-349.

Brown, J.F., Loveland, T.R., Merchant, J.W., Reed, B.C. and Ohlen, D.O., 1993, Using multispectral data in global landcover characterization: Concepts, requirements and methods. *Photogrammetric Engineering and Remote Sensing*, **59**, 977-987.

Doraiswamy, P.C. and Cook, P.W., 1995, Spring wheat yield assessment using NOAA AVHRR data. *Canadian Journal of Remote Sensing*, **21**, 43-51.

Edwardson, S., 2003, Personal Communication: Agronomic specialist-Minn-Dakk Growers LTD., Grand Forks, ND.

Entz, M.H. and Fowler, D.B., 1988, Critical stress periods affecting productivity of no-till winter wheat in Western Canada. *Agronomy Journal*, **80**, 987-992.

Fischer, R.A. and Kertesz, Z., 1976, Harvest index in spaced populations and grain weight in microplots as indicators of yielding ability in spring wheat. *Crop Science*, **16**, 55-59.

Fischer, R.A. and Kohn, G.D., 1966, The relationship of grain yield to vegetative growth and post-flowering leaf area in the wheat crop under conditions of limited soil moisture. *Australian Journal of Agricultural Research*, **17**, 281-286.

Flood, R.G., Martin, P.J. and Gardner, W.K., 1995, Dry matter accumulation and partitioning and its relationship to grain yield in wheat. *Australian Journal of Agricultural Research*, **35**, 495-502.

Friedl, M.A., McIver, D.K., Hodges, J.C.F., Zhang, X.Y., Muchoney, D., Strahler, A.H., Woodcock, C.E., Gopal, S., Schneider, A., Cooper, A., Baccini, A., Gao, F. and Schaaf, C., 2002, Global land cover mapping from MODIS: algorithms and early results. *Remote Sensing of Environment*, **83**, 287-302.

Gupta, R.K., Prasad, S., Rao, G.H. and Nadham, T.S.V., 1993, District level wheat yield estimation using NOAA/AVHRR NDVI temporal profiles. *Advances in Space Research*, **13**, 252-256.

Hansen, M.C. and Reed, B., 2000, A comparison of the IGBP DISCover and University of Maryland 1 km global land cover products. *International Journal of Remote Sensing*, **21**, 1365-1373.

Hatfield, J.L., 1983, Remote sensing estimators of potential and actual crop yield. *Remote Sensing of Environment*, **13**, 301-311.

Heinsch, F.A., Reeves, M.C., Bowker, C.F., Votava, P., Kang, S., Milesi, C., Zhao, M., Glassy, J., Jolly, W.H., Kimball, J.S. and Nemani, R.R., 2003. User's Guide: GPP and NPP (MOD17A2/A3) Products NASA MODIS Land Algorithm V. 2.0, University of Montana, Missoula, MT.

Jamieson, P.D., 1999, Personal Communication with Dr. Pete Jamieson. New Zealand Institute of Crop and Food Research.

Jamieson, P.D., Porter, J.R., Goudriann, J., Ritchie, J.T., Keulen, H.v. and Stol, W., 1998, A comparison of the models AFRCWHEAT2, CERES-Wheat, Sirius, SUCROS2 and SWHEAT with measurements from wheat grown under drought. *Field Crops Research*, **55**, 23-44.

Labus, M.P., Nielsen, G.A., Lawrence, R.L. and Engel, R., 2002, Wheat yield estimates using multi-temporal NDVI satellite imagery. *International Journal of Remote Sensing*, **23**, 4169-4180.

Laguette, S., Vidal, A. and Vossen, P., 1998, Using NOAA-AVHRR data to forecast wheat yields at a European scale. *Agrometeorological Applications for Regional Crop Monitoring and Production Assessment*, 131-146.

Martin, P.N.G. and Kiyomoto, R.K., 1989, Assimilation and distribution of photosynthate in winter wheat cultivars differing in harvest index. *Crop Science*, **29**, 120-125.

McMaster, G.S., Klepper, B., Rickman, R.W., Wilhelm, W.W. and Willis, W.O., 1991, Simulation of shoot vegetative development and growth of unstressed winter wheat. *Ecological Modeling*, **53**, 189-204.

Mcneal, F.H., Berg, M.A., Brown, P.L. and McGuire, C.F., 1971, Productivity and quality response of five spring wheat genotypes, *Triticum aestivum* L., to nitrogen fertilizer. *Agronomy Journal*, **63**, 908-910.

Montieth, J.L., 1972, Solar radiation and productivity in tropical ecosystems. *Applied Ecology*, **9**, 747-766.

Montieth, J.L., 1977, Climate and efficiency of crop production in Britain. *Philosophical Transactions Royal Society of London*, 277-294.

Moot, D.J., Jamieson, P.D., Henderson, A.L., Ford, M.A. and Porter, J.R., 1996, Rate of change in harvest index during grain-filling of wheat. *Journal of Agricultural Science*, **126**, 387-395.

Puckridge, D.W. and Donald, C.M., 1967, Competition among wheat plants sown at a wide range of densities. *Australian Journal of Agricultural Research*, **18**, 193-200.

Rao, G.H., Gupta, R.K., Nadham, T.S.V. and Prasad, S., 1993, NOAA/AVHRR vegetation indices as district level wheat growth indicators. *Advances in Space Research*, **13**, 249-252.

Rickert, K.G., Sedgley, R.H. and Stern, W.R., 1987, Environmental response of spring wheat in the south-western Australian Cereal Belt. *Australian Journal of Agricultural Research*, **38**, 655-670.

Running, S.W., Justice, C.O., Salomonson, V., Hall, D., Barker, J., Kaufmann, Y.J., Strahler, A.H., Huete, A.R., Muller, J.P., Vanderbilt, V., Wan, Z.M., Teillet, P. and Carnegie, D., 1994, Terrestrial remote sensing science and algorithms

planned for EOS/MODIS. *International Journal of Remote Sensing*, **15**, 3587-3620.

Running, S.W., Thornton, P.E., Nemani, R. and Glassy, J.M., 2000. Global terrestrial gross and net primary productivity from the Earth Observing System. In Methods in Ecosystem Science, edited by O. Sala, R. Jackson and H. Mooney (New York: Springer Verlag), pp. 44-57.

Schubert, S.D., Rood, R.B. and Pfaendtner, J., 1993, An assimilated data set for Earth Science applications. *Bulletin of the American Meteorological Society*, **74**, 2331-2342.

Singh, I.D. and Stoskopf, N.C., 1971, Harvest index in cereals. *Agronomy Journal*, **63**, 224-228.

Sofield, I.L., Evans, T., Cook, M.G. and Wardlaw, I.F., 1977, Factors influencing the rate and duration of grain filling in wheat. *Australian Journal of Plant Physiology*, **4**, 785-97.

Syme, J.R., 1972, Single plant characters as a measure of field plot performance of wheat cultivars. *Australian Journal of Agricultural Research*, **23**, 753-759.

Tacettin, Y., Ozkan, H. and Genc, I., 1995, Relationships of growth periods, harvest index and grain yield in common wheat under Mediterranean climatic conditions. *Cereal Research Communications*, **23**, 59-62.

Tucker, C.J., Holben, B.N., Elgin Jr., J.H. and McMurtrey III, J.E., 1980, Relationship of spectral data to grain yield variation. *Photogrammetric Engineering and Remote Sensing*, **46**, 657-666.

United States Department of Agriculture (USDA)National Agricultural Statistics Service (NASS)., 2003, USDA Published Estimates Database. *http://www.nass.usda.gov:81/ipedb/*.

United States Department of Agriculture (USDA)National Agricultural Statistics Service (NASS)., 2004. Crop Production Reports, http://usda.mannlib.cornell.edu/reports/nassr/field/pcp-bb/2003/.

Waring, R.H. and Running, R.W., 1998, Forest Ecosystems: Analysis at Multiple Scales, (San Diego: Academic Press).

Wheeler, T.R., Hong, T.D., Ellis, R.H., Batts, G.R., Morison, J.I.L. and Hadley, P., 1996, The duration and rate of grain growth, and harvest index, of wheat (*Tritium aestivum* L.) in response to temperature and CO_2. *Journal of experimental Botany*, **47**, 623-630.

CHAPTER 4

INTEGRATING MODIS VEGETATION DATA WITH A MODEL OF SPRING
WHEAT GROWTH AND YIELD FOR OPERATIONAL USE OVER MONTANA

Abstract

The limitations to accurate wheat yield predictions outlined in Chapter three

provided the impetus to further this research hoping to improve the yield monitoring

system. In this light, a simple mechanistic model of spring wheat growth and yield was

developed for Montana using meteorological observations and MODIS FPAR within a

GIS framework. Predicted county level yields for 2001 through 2003 are compared with

observations for all counties with $>= 1820$ ha of planted wheat and $>= 50$ % spring

wheat. County level results are significantly enhanced over previous research but still

demonstrate the need for improvement in physiological parameter estimates and land

cover characterization throughout the region. State wide predictions were closely aligned

with state level observations and were indistinguishable ($P \leq 0.05$) from one another in

each year of the study. The improved model predicted ($P \leq 0.05$) 2001 wheat yield about

23 days in advance of maturity. This highlights the usefulness of the wheat yield logic

presented here for accurately characterizing large regions of wheat yield in a timely

fashion without the need for retrospective empirical analyses.

Introduction

Agriculture is the leading industry in Montana, currently providing nearly 2.3

billion dollars for the region in annual revenue. Montana ranks third in the United States

in spring wheat production (USDA and NASS 2004). From 2001 through 2003, spring

wheat comprised roughly 60 % of the total wheat crop in Montana. Thus, a regional

spring wheat monitor would be a beneficial tool for the agricultural industry for several

reasons. First, grain buyers would benefit by knowing the quantity of production

available for purchase, especially if the buyer is sourcing from a two to three county area.

Second, producer's benefit by knowing how their wheat yields compare to other regions,

which theoretically could help them fine-tune their management practices. Finally, early

assessment of potential yield reduction could improve expected yield predictions and

avert disaster. Once a monitor was created for Montana, it could potentially be applied to

other areas.

Traditionally, wheat yield models have been intricate, field-based simulators such

as CERES-wheat (Ritchie and Otter 1985) and SIRIUS (Jamieson et al. 1998). These

models essentially "grow" a wheat plant from emergence to maturity by simulating

complex physiological interactions between the wheat plant and surrounding

environment and have been used successfully for predicting crop yields at the field level

(Toure et al. 1994, Chipanshi et al. 1997, Jamieson et al. 1998). However, management,

weather, soil and crop genetic data (responsiveness to environmental stimuli) are usually

required to achieve accurate yield calculations. Such data are difficult if not impossible

to obtain for entire regions. On the other hand remote sensing has been investigated and

promoted as a means of providing information about crop growth (Badwhar

1980,Choudhury 1987,Manjunath et al. 2002) and yield (Weigand et al. 1979,Tucker et

al. 1980,Hatfield 1983,Laguette et al. 1998,Labus et al. 2002) while avoiding the use of

extensive inputs.

Relating Normalized Difference Vegetation Index (NDVI) from the Advanced

Very High Resolution Radiometer (AVHRR) empirically to yield has been one of the

most common applications of remote sensing data for regional monitoring. The NDVI

has been used widely for assessing crop condition and yield owed primarily to its

inherent link to photosynthetic activity (Choudhury 1987) and simplistic formulation:

$$(NIR - RED)/(NIR + RED) \tag{1}$$

where NIR and RED are the spectral responses for the near-infrared and red wavebands

respectively. In a similar study, Doraiswamy and Cook (1995) used accumulated NDVI

between heading and maturity to predict spring wheat grain yield in North Dakota using

empirical relationships. Unfortunately, application of these empirical models

(Brocklehurst 1977, Gao et al. 1993, Doraiswamy and Cook 1995, Labus et al. 2002) is

limited to regions and time frames for which the regression equations were formulated,

thereby reducing their value where timely information is needed. Further, as described in

Chapter three, unlike crops whose yield consists of above-ground production, wheat yield

is contained in storage organs, and is sensitive to adverse meteorological conditions at

critical growth stages, principally flowering and grain filling.

The creation and implementation of accurate, timely wheat monitors has been

limited and remains problematic because past studies have focused on empirical

retrospective analyses, which only permit inference rather than computation of grain

yield. More recently, however, Doraiswamy et al. (2003) successfully demonstrated the

potential for estimating wheat yield for regions (counties) by coupling satellite remote sensing data with soil characteristics and meteorological data in the EPIC (Erosion Productivity Impact Calculator) crop growth simulation model. In their study Doraiswamy et al. (2003) used AVHRR and Landsat Thematic Mapper (TM) to assess spring wheat production in North Dakota. Given the advancements of crop remote sensing technology, greater emphasis has been placed on exploiting the timely nature and regional perspective that satellite remote sensing offers.

Since the year 2000, the Moderate Resolution Imaging Spectroradiometer (MODIS) has been providing a suite of global vegetation productivity products. Chief among these used in this study is the fraction of photosynthetically active radiation absorbed by the plant canopy (FPAR). The MODIS FPAR product is provided as global, daily coverage at 1-km^2 spatial resolution. Few if any studies to date have utilized MODIS products for agricultural applications, partly due to the infancy of the MODIS data stream.

In Chapter three however, I constructed a wheat yield estimation protocol for Montana and North Dakota, which relied on gross primary productivity (GPP) estimates from MODIS. These GPP estimates can be used for computing the seasonal growth and final yield of wheat for large regions without the need for retrospectively constructing empirical relationships between remote sensing data and observed yield. Despite their utility for estimating yield of states, or similarly sized regions, the standard MODIS GPP eight-day product is not completely practical for constructing a near-real time functional wheat yield monitor due to the lack of growing season length determination. I discovered these and other practical limits to accurately estimating wheat yield from MODIS

products, which led to suggested improvements of inputs and model logic for producing

timely estimates of wheat yield in Montana. These suggested improvements were: (1)

implementation of more appropriate and regionally specific analysis masks to delineate

wheat from other crops; (2) inclusion of localized, observed meteorological data and; (3)

adaptation of crop physiological parameters in the current GPP algorithm to more closely

emulate observed physiological characteristics of commonly grown wheat varieties in the

region of interest.

The merit of applying these improvements is that if a few conservative

relationships are known for wheat varieties grown in a given region, yield can

theoretically be modeled in near-real time and potentially anywhere on earth. In light of

these observations, this paper seeks to improve the wheat yield estimation protocol

produced in Chapter three through implementation of the suggested improvements, with

the ultimate goal of devising a simple, mechanistic remote sensing-based spring wheat

yield model for Montana.

To achieve this objective I used a modified version of the core MODIS vegetation

productivity algorithm (Running et al. 2000,Heinsch et al. 2003) within the crop

modeling framework demonstrated by Amir and Sinclair (1991a). This system, hereafter

referred to as the combined model, was run for the years 2001 through 2003 using

localized meteorological observations and more appropriate crop physiological

parameters than those inherent within the standard MODIS productivity algortihm. Yield

estimates were subsequently masked with a high resolution landcover datset to limit

analysis to areas dominated by spring wheat production. This masking process is simply

a means of identyfiying which grid cells, or pixels, are spring wheat. County level wheat

yields were computed by aggregating each sub-county (pixel-level) prediction in a geographic information system (GIS). Estimated wheat yields were subsequently compared with observed spring wheat yields at county and state levels.

Background

Common modeling advice is to use the simplest model that meets the objectives (Brooks and Tobias 1996). Of the operational field level wheat yield models that I examined, the model constructed by Amir and Sinclair (1991a) seemed to be the most appropriate to integrate with MODIS derived FPAR. There are numerous theoretical advantages of using remotely sensed biophysical parameters as direct inputs to a crop growth model. First, it limits some of the need for management information, such as fertilization rates because this information is inherently linked to the crop physiological response and therefore the remotely sensed imagery. In addition, management, soils, environmental parameters, pest infestations and other influences are incorporated into the physiological response of the crop. To the extent that the vegetative response is reliably quantified via remote sensing, it can be used directly, without the need for retrospective calibration. Second, given that MODIS provides global coverage, models could be developed for nearly any region. Finally, there are few benefits for predicting wheat yield by including excessive detail (Brooks and Tobias 1996, Brooks et al. 2001) in regional crop models, particularly when the parameters cannot be reliably initialized.

With respect to the wheat yield model I adapted in this research, use of remote sensing inputs greatly reduced the complexity of the system. The danger, however, of oversimplification is that important aspects of the system may be omitted (Brooks et al. 2001). The original formulation by Amir and Sinclair (1991a) necessarily estimates LAI

using plant population and the number of leaves per plant. The ultimate function of this routine is to simulate leaf area development so that the amount of intercepted solar radiation can be estimated. This logic is deleted in the combined model because I use MODIS derived estimates of FPAR. This makes the daily, global MODIS data stream an attractive contribution to developing regional crop models.

The combined model portrayed in the current study is an improvement over that developed in Chapter three and the numerous empirical models (Hatfield 1983,Aparicio et al. 1999,Manjunath et al. 2002) in that it provides a mechanistic approach as outlined by Amir and Sinclair (1991a) through combination of important processes postulated to be taking place in the system. The model built by Amir and Sinclair (1991a) assumed no water or nutrient limitations, though other versions do (Amir and Sinclair 1991b). I made similar assumptions.

Because most (about 97 %) (USDA and NASS 2003) spring wheat in Montana is grown under rain fed conditions, moisture stress during the growing season is common, which cannot be ignored in any yield simulation system. Fortunately, despite the contentious use of vapor pressure deficit (VPD) as a direct attenuator of radiation use efficiency (RUE), the MODIS productivity algorithm does include a VPD control on RUE (discussed later). The VPD scalar serves as a reasonable proxy for moisture stress as an attenuator of stomatal aperture due to increased evaporative demand.

Study Area

Because there is no spring wheat mask currently available for Montana, I limited the analysis to all counties within Montana where greater than 50 % of the planted acreage of wheat is dryland farmed spring wheat and where the total planted spring wheat

acreage in 2001 through 2003 was greater than 1820 ha (USDA and NASS 2003) (Figure

1). The total spring wheat acreage grown in Montana was 1,295,325, 1,568,025 and

1,227,150 ha in 2001, 2002, and 2003 respectively. Because most wheat in Montana is

grown under rain fed conditions, the seasonal variability in yield is strongly linked to

rainfall fluctuations and a high range of variability, on the order of about 2300 kg ha^{-1} (38

bu ac^{-1}), between counties has been observed. The major wheat growing regions within

the study area are characterized by cold winters and hot, dry summers. Regional

precipitation during the growing season fluctuates (based on the 50-year mean) from 140-

270 mm. In 2001, favorable temperatures during June and July combined with above

average precipitation led to higher yields than in 2002 or 2003.
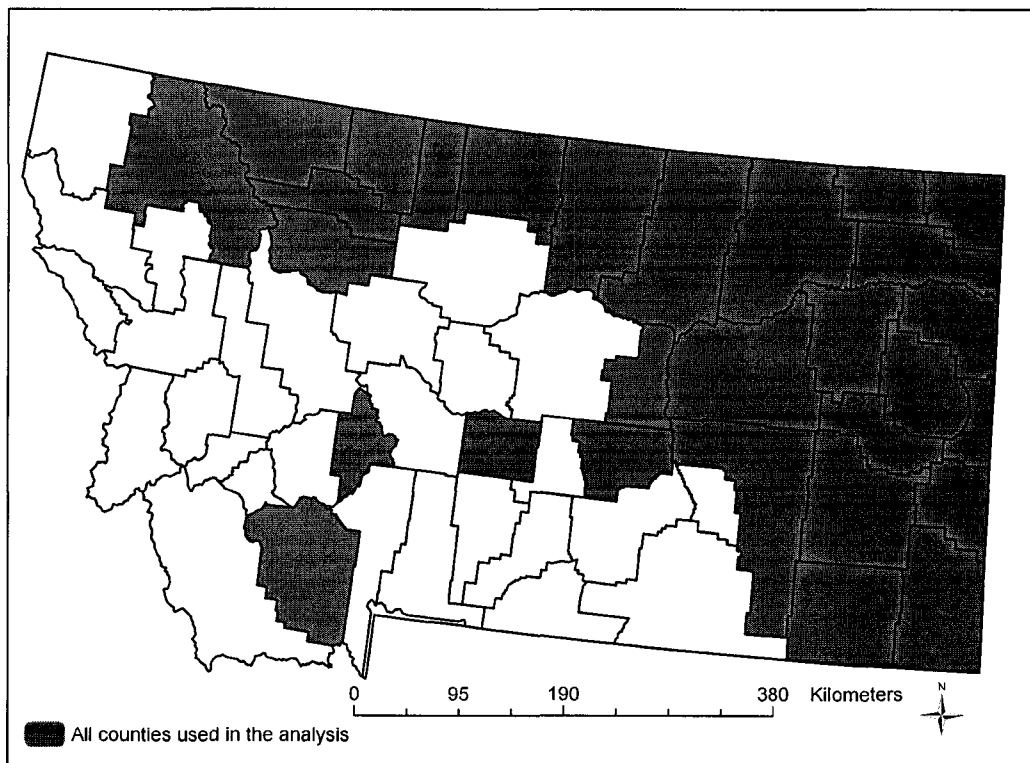
Figure 1. Counties of Montana with >= 1820 ha of dryland farmed spring wheat and >=
50 % of total wheat production as spring wheat.

Methods

The primary objective of this research was completed in two steps. First I modified inputs and parameters in the standard MODIS vegetation productivity algorithm. This was necessary because; 1) the standard algorithm has only a generic set of crop physiological parameters and no inherent phenology computation, 2) the meteorological data used in the standard algorithm are provided at 1° x 1.25° (Heinsch et al. 2003), which are too coarse for regional crop yield simulation models, and 3) the MODIS land cover does not distinguish wheat from other crops.

Second, the modified MODIS vegetation productivity algorithm was combined with a simplified spring wheat yield logic presented by Amir and Sinclair (1991a) to permit simulation of ontogenetic development and grain yield. The model by Amir and Sinclair (1991a) was simplified in the current study in order to facilitate extrapolating this model across the entire state and make integration of remote sensing parameters possible.

The combined model requires daily inputs of minimum and maximum air temperature, solar radiation, vapor pressure deficit, and FPAR. Three processes are simulated in the model including crop development, total biomass accumulation, and accumulation of biomass in the seed head.

Crop Development

The primary function of the crop development subroutine is for triggering significant physiological changes, which occur as a result of aging within the wheat plant. Developmental stages simulated are emergence, anthesis, and grain filling. Each stage is estimated by accumulated growing degree-days (AGDD) experienced by the crop in each period, computed as:

$$\Sigma((T_{min} + T_{max})/2 - 0_i) \tag{2}$$

where T_{min} and T_{max} are the minimum and maximum daily temperature, respectively, and

0 is the base temperature (°C) for a given phenological stage over the crop cycle $(_i)$. A

very strong relationship $(r^2 = 0.99)$ exists between AGDD and the Haun growth stage

(Edwardson and Watt 1987) and many studies have related AGDD to the development

and maturation of spring wheat (Angus et al. 1981b, Bauer et al. 1984a, Bauer et al.

1984b, 1985, Baker et al. 1986).

When planted in moist soil at a depth of about 38 mm in a proper seedbed it takes

an accumulation of 100 AGDD for the seedling to emerge (Bauer et al. 1984a). Thus in

the combined model, emergence is estimated to have occurred within 100 AGDD of the

seeding date (figure 2), which assumes proper soil moisture conditions. After emergence,

AGDD continues to accumulate and each successive growth stage is determined using a

phyllochron interval approach.

The phyllochron interval is the number of AGDD necessary to produce another

leaf on the spring wheat plant. Bauer et al. (1984a), demonstrated that commonly grown

cultivars of spring wheat on the Northern Great Plains had a phyllochron interval of

approximately 72 to 80 AGDD, though this can vary (Baker et al. 1986,Amir and Sinclair

1991a,Cao and Moss 1991,Mosaad et al. 1995). To account for some of this variability, I

chose a realistic value within the range of expected intervals for cultivars commonly

planted in this region. For all simulations, the phyllochron interval was held constant at

80. For example, using a phyllochron interval of 80, the end of main stem leaf growth,

assuming a standard eight-leaved variety requires about 640 AGDD

$(8 \times 80 \text{ AGDD leaf}^{-1})$.

The original model by Amir and Sinclair (1991a) introduced a variable time frame between the end of main stem leaf growth and anthesis. Three maturity classifications were recognized and accounted for as early, medium and late varieties requiring 370, 460, and 520 AGDD from the end of main stem leaf growth and anthesis respectively. In a more recent study, Sinclair and Bai (1997) modified these parameters to emulate aberrantly high wheat yield in China. This type of maturity classification was omitted from my model because it requires spatially explicit knowledge of which cultivars are grown in each county. These data do not exist for Montana though the NASS does publish the most common cultivar grown in some regions. To circumvent this problem, the time from the end of main stem leaf growth to anthesis was estimated using the relationship between AGDD and the Haun growth stage for anthesis (11.5) for common wheat varieties grown in the Northern Great Plains. Standard eight-leaved varieties in this region have completed flowering by about 884 AGDD (Bauer et al. 1984b). Such a generalization is necessary without knowledge of spatially explicit cultivar data. Doraiswamy et al. (2003) used a similar generic wheat crop approach in North Dakota by estimating that every field was mature at 1300 AGDD after emergence (base temperature $0°$) with apparently little if any deleterious effects on yield estimates.

The duration of the grain filling period is also strongly linked to air temperature (Sofield et al. 1977), but post-anthesis development is not a linear function of AGDD (Bauer et al. 1985). Bauer et al. (1985) studied grain growth of three spring wheat cultivars in five differing environments and found that the linear grain growth period ended 630 AGDD after anthesis, while Angus et al. (1981a) indicated approximately 650 AGDD were required. As a result, the linear grain filling period was estimated as in

Amir and Sinclair (1991a), where in all simulations, the duration of this period was held constant at 550 AGDD. Temperature exerts strong influence on the duration of the grain filling period, thus correct estimation of the timing of this event is critical (Jamieson et al. 1995a).

In the combined model the linear grain growth period begins after a 90 AGDD lag phase and is represented by a simple harvest index formulation (figure 2). During the lag phase small amounts of carbohydrates are mobilized and translocated to the seed head

MODEL Inputs
PAR
VPD
TMIN
TMAX
FPAR

End

Yes

No —— SGP >= 550

Day =sowing day —— No —→

Yes

No

No

SGP = SGP + AGDD

AGDD = TAVG - 0 °C
Haun Stage = AGDD / PHINT

grain biomass = BM * HI

HI = days * 0.011 + 0.1

AGDD >= 100

Yes
(emergence)

Yes

RUE = RUEmax * TMIN_scalar * VPD_scalar
RUEmax = 2.2 g biomass MJ⁻¹ PAR

AGDD > Anthesis + 90

AGB_{daily} = FPAR * PAR * RUE

BM = BM + AGB_{daily}

Abbreviations:
PAR   = Photosynthetically active radiation
VPD   = Vapor pressure deficit
TMIN   = Minimum daily temperature
TMAX   = Maximum daily temperature
FPAR   = fraction of absorbed photosynthetically active radiation
TAVG   = Average daily temperature
AGDD   = Accumulated growing degree days
RUE   = Radiation use efficiency
BM   = Biomass
HI   = Harvest index
AGBdaily = Above ground biomass(daily increment)

Figure 2. Flow diagram of combined model adapted from Amir and Sinclair (1991a) including data processing, model input and output.

followed by a constant rate phase of grain filling during which nearly 60 % of final grain weight is determined. Higher temperatures increase rates of grain filling but duration of grain filling most often decreases under warmer conditions (Wardlaw et al. 1980, Johnson and Kanemasu 1983, Nicolas et al. 1984, Wardlaw et al. 1989b, Wardlaw et al. 1995, Wheeler et al. 1996). The question then arises does the increased rate of grain filling compensate for the decreased duration? The answer is rarely. This is mainly because increasing rates of grain filling are not constant across all temperatures and reach a maximum around 30°C beyond which rate of dry matter accumulation decreases dramatically (Jenner 1974, Sofield et al. 1977). No explicit relationship linking heat stress to reduced grain yield has been included in the model. Instead, it is assumed that higher temperatures will increase the rate of ontogenetic development, thereby potentially limiting biomass accumulation by shortening the growing season and grain filling period.

Biomass Accumulation

Biomass accumulation is computed within a modified version of the MODIS productivity algorithm, which was spawned from the conservative relationship between absorbed photosynthetically active radiation (APAR) and primary productivity (NPP) first proposed by Montieth (1972 and 1977). This original logic, known as radiation use efficiency (RUE), has since been studied extensively (Gallagher and Biscoe 1978, Jamieson et al. 1995b, Kiniry et al. 1998, Sinclair and Muchow 1999a,b, Nouvellon et al. 2000) and used in crop simulation models (Amir and Sinclair 1991a,b, Jamieson et al. 1998, Brooks et al. 2001).

The maximum radiation use efficiency (ε_{max}) (i.e. without moisture or nutrient stress) currently used in common yield simulation models is 2.2 g of above-ground

biomass MJ^{-1} PAR (Amir and Sinclair 1991a, Jamieson et al. 1998). Consequently this ε_{max} was used in the current algorithm. This constitutes the first of several significant improvements made to the standard MODIS productivity algorithm for computing wheat yield.

In particular, the ε_{max} used in the standard algorithm (0.00068 kg C MJ^{-1} PAR) is designed to estimate carbon sequestration rather than biomass. Adjusting this ε_{max} to estimate biomass (biomass is about 50 % C (Waring and Running 1998)), still produces a figure (1.36 g biomass MJ^{-1} PAR) substantially lower than that used in this study. In addition, the MODIS productivity algorithm logic was designed for computing global carbon balance for crops and natural systems, which necessitates estimation of respiration components in addition to photosynthesis. Fortunately, the ε_{max} used in this study is essentially calibrated for predicting above-ground biomass, thus eliminating the need for complex carbon balance or allocation theory.

The ε_{max} is retarded by daily minimum temperature (TMIN) and VPD (figure 3). Use of VPD to attenuate RUE has been questioned (Sinclair and Muchow 1999a), especially for crops, however, the MODIS algorithm was designed for global implementation. Since VPD data are globally available on a daily time step (Atlas and Lucchesi 2000), they are used to attenuate the MODIS ε_{max} in conjunction with minimum temperature. I recognize that VPD as a direct forcing on ε_{max} may not be the most robust assumption (Sinclair and Muchow 1999a). However, VPD does work as a general scalar, and in many areas of the world, serves as the only readily available indicator of moisture conditions surrounding the plant canopy. In its' original formulation, the MODIS vegetation productivity algorithm was designed to estimate vegetation productivity on a

daily timestep for the entire globe, thereby requiring globally available meteorological data.

Thus, in the standard MODIS algorithm and the modified version used in this study, the daily estimated RUE is computed as:

$$RUE = \varepsilon_{max} * TMIN\_scalar * VPD\_scalar \tag{3}$$

In the combined model, daily biomass is calculated by:

$$AGB_{daily} = RUE * PAR * FPAR \tag{4}$$

Where AGB_{daily} is the daily estimate of above-ground biomass, RUE is the realized radiation use efficiency, PAR is photosynthetically active radiation, and FPAR is the fraction of photosynthetically active radiation absorbed by the plant canopy.

The FPAR used for this analysis is directly provided by MODIS. The MODIS offers a weekly (eight-day) composite estimate of FPAR for the globe as a regularly produced product. A quality assurance layer accompanies every FPAR file from MODIS. The quality assurance layer provides a means of screening all pixels that are not
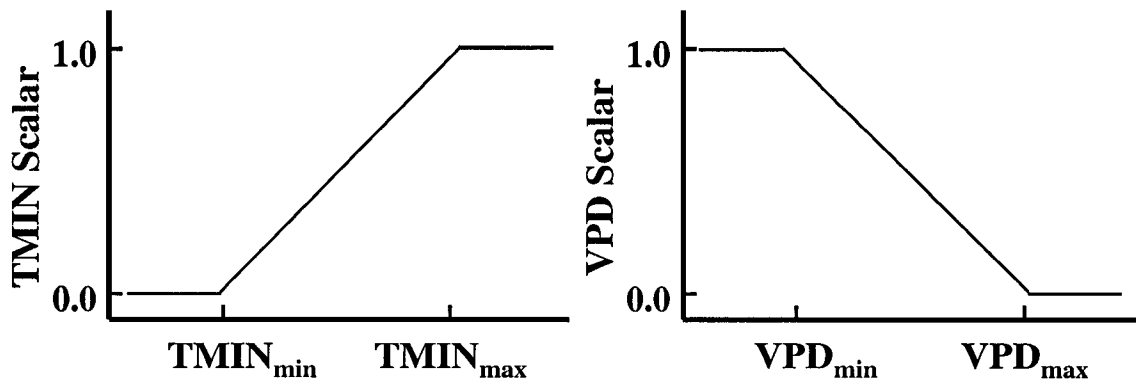
Figure 3. The TMIN and VPD attenuation scalars are simple linear ramp functions. VPDmin and VPDmax used in this study are 650 and 2500 kPa respectively, while TMINmin and TMINmax are -8 and 12.02 °C respectively.

desirable for analysis, either as a result of sensor and algorithm performance, atmospheric

conditions, or cloud contamination. Screening criteria used to filter FPAR used in this

study are included in Table 1. If any FPAR pixel did not pass the quality screening

criteria, its value was determined through linear interpolation between the previous

period's value and the next period to pass the screening process.

Table 1. Quality control criteria used for screening MODIS FPAR data for 2001 to 2003.

QC flag description[1]	Screening criteria
MODLAND_QC	$< = 1$
DEADDETECTOR	0
CLOUDSTATE	0 or 3
SCF_QC	$< = 3$

[1]A detailed explanation of these criteria can be found in Heinsch et al. (2003).

The FPAR time series for a given field (pixel) should capture ontogenetic decline

of the wheat crop. However, the model developed by Amir and Sinclair (1991a)

explicitly accounted for the loss of photosynthetic capacity of wheat as a result of

nitrogen translocation from the leaves to the grain by retarding the ε_{max} as a linear

function of time during the grain filling period. This effect was not simulated in the

combined model because the loss of photosynthetic capacity is theoretically inherent in

the spectral response of the crop, and thus the FPAR product.

Grain Growth

Using experimental field data, Amir and Sinclair (1991a) established a very

strong ($r^2 = 0.99$) relationship between time (days) since the start of the linear grain

filling period and harvest index in spring wheat. As a result, in concordance with Amir

and Sinclair (1991a), daily grain growth rate is calculated using a harvest index as a

linear function of time (days) since the start of the linear grain filling period estimated by:

$$HI = 0.01(\text{days}) + 0.1^1 \tag{5}$$

where HI is the estimated harvest index and days are the number of days since the onset

of grain filling. Though simplistic, this empirical formulation has a firm scientific basis

and thus provides a first approximation for rate of grain filling of spring wheat for a

region. Given the regional scope of this project, no data were available to calibrate a

more precise formulation for Montana, but evidence suggests that field data for

calibration will improve estimates of harvest index and therefore yield (Sinclair and Bai

1997). This is one of the fundamental limitations to regional modeling with limited

parameter variation. The implicit assumption with the current logic is that all spring

wheat cultivars grown in Montana have identical physiological responses to

environmental stimuli, principally temperature and radiation.

Meteorological Observations

The model requires daily observations of VPD (Pa), solar radiation (MJ), and

minimum and average temperature (C). Photosynthetically active radiation (PAR) is

estimated as 45 % of solar radiation. All meteorological observations are products of the

Surface Observation Gridding System (SOGS) (Jolly et al. 2004). The SOGS is a spatial

interpolation program based on kriging, which provides estimates of meteorological

variables at nearly any spatial resolution depending on station density, but for this study,

all observations were gridded to a 1-km cell resolution to match the spatial resolution of

the MODIS derived FPAR. The spatial resolution of SOGS data is a dramatic

improvement over the standard 1° by 1.25° DAO data used in the standard MODIS

vegetation productivity product. The National Climate Data Center (NCDC) operated by

---

[1] The Y-intercept is adapted and estimated from Amir, J. and Sinclair, T.R., 1991a, A model of the temperature and solar-radiation effects on spring wheat growth and yield. *Field Crops Research*, 28, 47-58.

the National Oceanic and Atmospheric Administration (NOAA), provided the primary data stream for the gridded surfaces used in this study.

Identifying Spring Wheat

The MODIS land cover schemes do not distinguish spring wheat from other types of crops. A diverse suite of crops including canola, sugar beets, corn, soybeans, sunflower, and dry beans are grown in Montana but these comprise only 3.5 % (89,635 ha) of all crops planted in 2001, compared with 93 % (2,170,040 ha) of wheat. Thus, to achieve the objective of computing spring wheat yield for Montana analysis was limited to counties that had greater than 50 % of spring wheat as a proportion of the total wheat crop and greater than 1820 ha of planted wheat in each year of the study. Unlike Chapter three, here I used the Montana GAP analysis instead of the MODIS land cover to identify agricultural lands.

The Montana GAP analysis (Fisher et al. 1998), contains a 90 meter spatial resolution image dataset depicting land cover types for the state. This was ultimately created from high spatial resolution (30-m) Landsat Thematic Mapper imagery. To further isolate areas of spring wheat, I chose the dryland-farmed land cover type (figure 4a). Due to the spatial resolution mismatch between the 1km FPAR, and 90 meter GAP analysis imagery, the GAP analysis image was resampled to 1-km using the aggregate function in ArcGis V. 8.2 (ESRI 2002). As a result of this process, raster cells that had greater than 80% coverage by the dryland farmed category were retained as the final mask (figure 4b). Essentially, the 80 % mask provided a solid sample using areas of the state that had a high probability of being spring wheat. In addition, based on past research, I assumed the 80 % mask would provide the most reliable results. Spring wheat

masks could be derived from MODIS reflectance data but this is beyond the scope of the current study and at 1-km resolution, use and overall accuracy of this mask would be limited as indicated by Doraiswamy et al. (2003). If an accurate spring wheat mask were developed for the region, it would likely improve yield estimates.

In Montana alternate cropping systems are common where a wheat field may be in production in one year but fallow the next. Since the GAP analysis was created over the period from 1994 to 1998 (Fisher et al. 1998) there is no means of determining if a field (or pixel) is fallow or in production. To facilitate this decision I relied on MODIS FPAR time-series. If the MODIS derived FPAR was less than five % for four periods during the growing season, it was assumed the croplands was fallow. In addition, since this study focused on dryland farmed spring wheat, spectral contamination by irrigated fields was avoided by not using a pixel whose FPAR was greater than 75 % for three periods (24 days). Varying these thresholds, however, made little difference in final yield calculations.
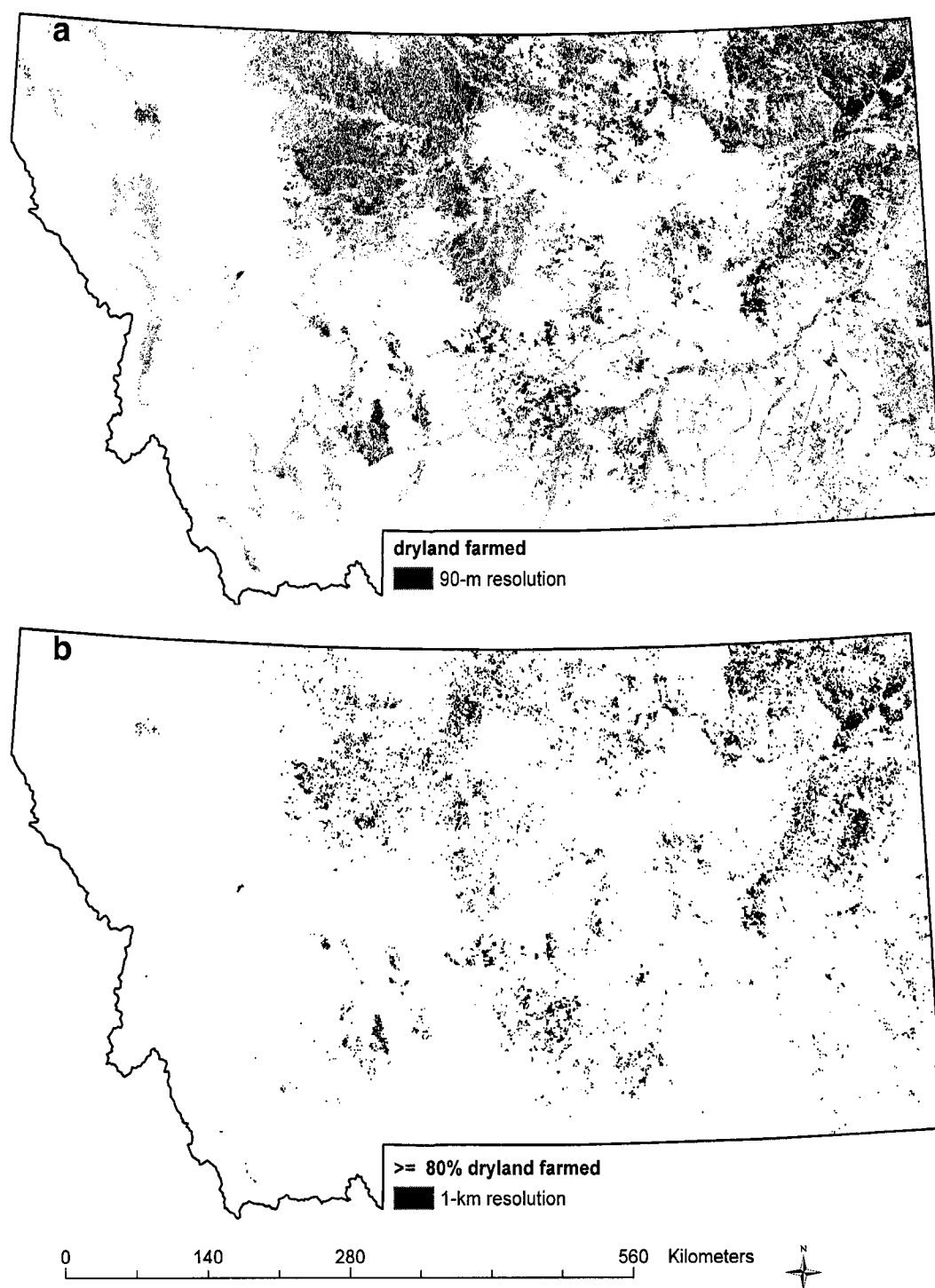
Figure 4. The Montana GAP analysis dryland farmed category (a) and product of the aggregation process at 1- km spatial resolution (b). The aggregation process results in a mask whose pixel values represent areas that had >= 80 % coverage by the finer resolution, original GAP analysis at 90-meter resolution.

Sensitivity Analyses

Sensitivity analyses were executed by first independently varying each of a set of model parameters and inputs. All analyses were performed using the 2001 meteorological data and MODIS FPAR data. After the initial analysis different climate scenarios were tested by varying a series of meteorological variables simultaneously. The aim of this analysis was to determine which model parameters and environmental variables were most responsible for determining yield in the model. This was accomplished by varying climate parameters in two ways. First, each daily meteorological input was varied by fixed amounts designed to emulate the expected range of natural variation in each variable (Table 2). Next I created realistic extreme climate scenarios by varying up to three parameters at a time. This was done so that the effects of climate on maturity and final yield could be emulated. This was a necessary step since hot days are generally associated with greater PAR and VPD. Finally, I varied physiological parameters across a range of realistic values that have been used in other studies.

Each variable was constrained to realistic limits observed in major wheat growing regions in Montana. The range of sowing dates between about 10 April and 30 May represents the extreme values for wheat in Montana (USDA and NASS 2004) that can normally be expected. Thus, sensitivity analysis was performed within this range of dates. For meteorological variables five randomly selected weather stations were chosen in major wheat growing regions of Montana and subsequently used to determine the mean and standard error of daily average and minimum temperatures and vapor pressure deficit. Only one station located at 48° north latitude, 105° west longitude, had daily

observations of solar radiation. At this latitude in Montana, a range of solar radiation was observed between about 33 and 2.5 MJ m^2 (14.9 and 1.1 MJ PAR m^2), while the SE was 4 MJ PAR m^2 day^{-1}. Thus PAR was constrained to be between 16 and 0.5 MJ m^2 day^{-1}. Additionally, VPD observations are rarely recorded in the field. As a result VPD was allowed to vary over the same range (as a percent) as daily average temperature, given the fundamental link between these parameters.

Table 2. Parameters used in the combined model for computing wheat yield and for sensitivity tests.

Parameter	Variable Name	Values used for wheat yield prediction[1]	Sensitivity Analysis Range[2]
Meteorological parameters			
Vapor pressure deficit (Pa)	VPD	Daily value	± 300
Daily incident PAR (MJ m^2 day^{-1})	PAR	Daily value	± 4
Daily average temperature (C)	TAVG	Daily value	± 6
Management parameters			
Sowing date (yearday)	SOWD	115	100-150
Physiological parameters			
Radiation use efficiency (g above ground biomass MJ^{-1} PAR)	RUE	2.2	1.224-2.5
Thermal time from sowing to emergence (AGDD base 0°C)	TTSE	100	85-160
Thermal time requirement for grain filling period	TTBE	550	383-633
Phyllochron Interval	PHINT	80	70 – 125
Rate of increase in harvest index	HISLOPE	0.01	0.68-2.07

[1]Unless otherwise stated, all estimated wheat yields in this paper were computed using these parameters.
[2]The practical limits to VPD are about 5000 Pa in much of Montana given the highest ever recorder temperature (47° C) and assuming a dewpoint of 26° C. VPD, TAVG, and PAR were constrained between 0 to 5000 pa, 0 to 37 (C), and 0.5 – 16 MJ^{-1} PAR respectively.

Average temperature between 1953 to 2003 at the five weather stations was about

16.1° ± 6 C (SE) (about 38%). This variation was constrained to a maximum of 37° C,

which is the maximum reported daily average temperature during the growing season.

Physiological parameters included in the sensitivity analysis were ε_{max}, thermal

time from sowing to emergence (TTSE), thermal time beginning to the end of the grain

filling period (TTBE), rate of increase in harvest index (HISLOPE), and the phyllochron

interval (PHINT).

The TTSE generally varies between about 100 and 150 AGDD (base temperature

0° C) (Bauer et al. 1984b,Jamieson et al. 1998). To be sure and encompass the full range

of expected variation TTSE was varied from 85 to 160 AGDD.

The TTBE for most cultivars should be between about 400 to 550 AGDD, though

Sinclair and Bai (1997) report estimates of TTBE as low as 340 AGDD (base temperature

8°C). The TTBE is difficult to characterize due to cultivar dependencies and the

disparate range of base temperature reported for calculating these figures, which are

between 0 and 8°C. To ensure the full range of this variation was captured, TTBE was

examined over the range between 383 and 600 AGDD (base temperature 0° C), which is

± 15 % of the values used by Amir and Sinclair (1991a) and Sinclair and Bai (1997).

In a similar manner, the rate of change in harvest index is also highly variable and

sensitive to environmental factors (Mcneal et al. 1971,Fischer and Kertesz 1976,Flood et

al. 1995,Wheeler et al. 1996). For example, warmer temperatures can result in smaller

grain weight at maturity because the increase in growth rate may be offset by the negative

effects of shorter grain filling periods (Sofield et al. 1977). A review of past studies

revealed a range in HISLOPE between 1.18 (Wheeler et al. 1996) and a low of 0.8 %

(Sinclair and Bai 1997). To ensure that the full range of expected variability was captured I tested the effects of HISLOPE over ± 15 % of this range (0.68 – 2.07 % day^{-1}).

Phyllochron intervals typically range between about 75 to 115 AGDD leaf^{-1}. To encompass the full range of this expected variation, the effects of phyllochron intervals were examined at 70 to 125 AGDD leaf^{-1} (base temperature 0°C).

The final physiological parameter analyzed in this sensitivity analysis was ε_{max}. As mentioned earlier, the ε_{max} used in the MODIS vegetation productivity algorithm is considerably lower than the value commonly used in field level wheat models. Two general factors lead to the discrepancy between the RUE used in the standard MODIS algorithm (Heinsch et al. 2003) and the value used in field level models.

First, the ε_{max} used in the MODIS vegetation productivity algorithm was calibrated to predict net primary productivity globally using coarse resolution meteorological data. This complicates the use of the MODIS RUE for predicting above-ground biomass, because it is calibrated to predict total carbon sequestration. To adjust the MODIS RUE for predicting above-ground biomass, I assumed a 10 % carbon allocation to the roots, resulting in a final ε_{max} of 1.224 g biomass MJ^{-1} PAR (1.36 x 0.9). Further, values of ε_{max} used in field level models are generally made responsive to fluctuations in soil moisture, which is not an option in a global product like the MODIS vegetation productivity algorithm. Second, given the limited information on crop distribution on a global basis, the MODIS RUE is an integrated estimate of ε_{max} for all crops, and thus does not differentiate wheat.

The upper level for ε_{max} has been directly quantified by Kiniry et al. (1998) as 2.5 g biomass MJ^{-1} PAR and used successfully by Sinclair and Bai (1997) to predict high

wheat yield in the Chaidamu Basin in Northwest China. Therefore, the sensitivity

analysis of RUE was constrained between 1.224 and 2.5 g biomass MJ^{-1} PAR.

Comparing Predicted and Observed Whea Yield

Model runs were conducted for 2001 through 2003 using the parameters outlined

in Table 2. The National Agricultural Statistics Survey (NASS) provides county and state

level spring wheat yield for all counties in Montana (USDA and NASS 2003). Observed

wheat yield was compared with modeled estimates of yield by computing correlation (r),

bias and mean absolute error (MAE) for each year during the study. State level yield

estimates were compared using paired t-tests (Zar 1995) to determine if differences

($p \leq 0.05$) exist between model estimated yield and observations from the NASS Published

Estimates Database (PEDB).

Yield Forecasting

I wanted to test the ability of the combined model to forecast potential yield. To

accomplish this, yield simulation were stopped in 12 increments of 50 AGDD prior to

simulated maturity. This process required that a constant harvest index value be used.

This is necessary because in the combined model, harvest index, and therefore grain

yield, is determined as a function of days since the beginning of grain filling. Thus, if the

analysis is stopped prior to grain filling, no harvest index can be calculated, which,

results in no grain growth simulated in the model. Given the success of the constant

harvest index of 38 % for predicting state level yield in Chapter three, this value was used

in the current analysis for investigating the use of the combined model to predict wheat

yield in advance of crop maturity. For example, the first simulation was stopped 600

AGDD prior to maturity. This was done for the year 2001. Each "shortened" simulation

was tested against yield observations for identical counties aggregated to the state level using a paired t-test after testing for homogeneity of variances using the F-ratio test (Zar 1995).

Results and Discussion

Sensitivity Analyses

The sensitivity analyses were done for two reasons. First I needed to understand the effects of dominant model components to facilitate interpretation of final results. Second, and perhaps more importantly, the sensitivity analyses provided insight to expected future yield based on regional meteorology, which can permit identification of critical biotic and abiotic thresholds beyond which crop failure or poor yield could be expected. The sensitivity analysis was performed for each pixel (field) in every county analyzed in this study. The pixel level predictions were then aggregated to county and state levels on an area weighted basis for reporting results. Mean state level prediction, root mean square error (RMSE), correlation coefficient (r) and the range are shown in Appendices. The RMSE, correlation coefficient, and the range were computed by comparing predicted and observed spring wheat yield for each county in the analysis.

Vapor Pressure Deficit

Sinclair and Muchow (1999a) argue that there is little background supporting the postulation that VPD directly controls RUE. In addition, they found in past studies by Pettigrew et al. (1990) and others generally fail to demonstrate a statistically significant relation between VPD and RUE. For example, Morrison and Gifford (1983) did not identify a response to VPD in maize, even at a high level of VPD (about 2.0 kPa). Dai et al. (1992), concluded that maize appeared to be insensitive to VPD up to 3.5 kPa.

Finally, most of the works citing the RUE response to VPD were measured in growth

chambers with high internal air mixing (usually up to about 4 m s^{-1})(Kawamitsu et al.

1993), which is generally greater than could be expected for a leaf in most crop canopies

where wind speed is usually 0.5 m s^{-1} (Lemon et al. 1971). This phenomenon results in

lower atmospheric vapor pressure on the leaf than would exist under the same VPD

conditions in the field (i.e. the VPD effect is exaggerated). It seems that across these and

other studies, a reduction in RUE does not start until approximately 2.5 kPa (Sinclair and

Muchow 1999a). These works can infer that use of VPD as a direct control on RUE is

flawed.

However, careful examination of these studies and critical arguments espoused by

Sinclair and Muchow (1999a), reveals that, most often, the effects of VPD on carbon

dioxide exchange rate and ultimately RUE are evaluated in very controlled environments

where water deficit is not a problem. Under these conditions it is clear that VPD is not a

major driver of RUE. But, in defense of MODIS vegetation productivity algorithm, it is

very challenging indeed to devise a better scheme given the global, daily requirements

and data constraints imposed in the productivity algorithm.

As a general scalar, use of VPD as an attenuator of RUE seems to work with

some level of certainty. For example, during the growing season for most wheat

producing areas in Montana, when VPD is high (especially for an extended period of

time) soil moisture is generally limiting. Use of VPD as a scalar for RUE necessarily

assumes that the leaf relative humidity is 100% and leaf temperature equals air

temperature. To the extent that these are valid assumptions, the use of VPD as a scalar of

RUE should work in dryland farmed environments when the goal is regional yield simulation.

Not surprisingly, the combined model is sensitive to VPD. Over the tested range of ± 300 Pa, estimated state level spring wheat yield varied from 808 to 1886 kg ha^{-1} across a range of planting dates from 10 April to 25 May. In all cases, increasing planting dates and increasing VPD lead to linear decreases in estimated grain yield (figure 5b). This is because RUE is attenuated in the algorithm as the cross product of the VPD and TMIN attenuation parameters (figure 3). I did not expect a non-linear effect on yield by VPD because only accumulated biomass is affected by changes in VPD.

Temperature

The effects of daily average temperature variation were larger in magnitude than VPD and non-linear (figure 5a). Temperature is the most pervasive environmental variable controlling developmental processes. Further, temperature extremes occurring during the periods of spikelet development, anthesis or grain filling can dramatically influence final grain yield (Haun Stages 4-5.5, 11-11.5, and > = 12 respectively). Spike size is a dominant component determining potential yield of spring wheat and is set ≅ 550 AGDD (Bauer et al. 1984a, Bauer et al. 1984b). High temperature during this period acts to significantly reduce the number of grain spikelets that will potentially produce a viable wheat kernel (Frank and Bauer 1996). Frank et al. (1987) found that during the Haun Stage between 4-4.5
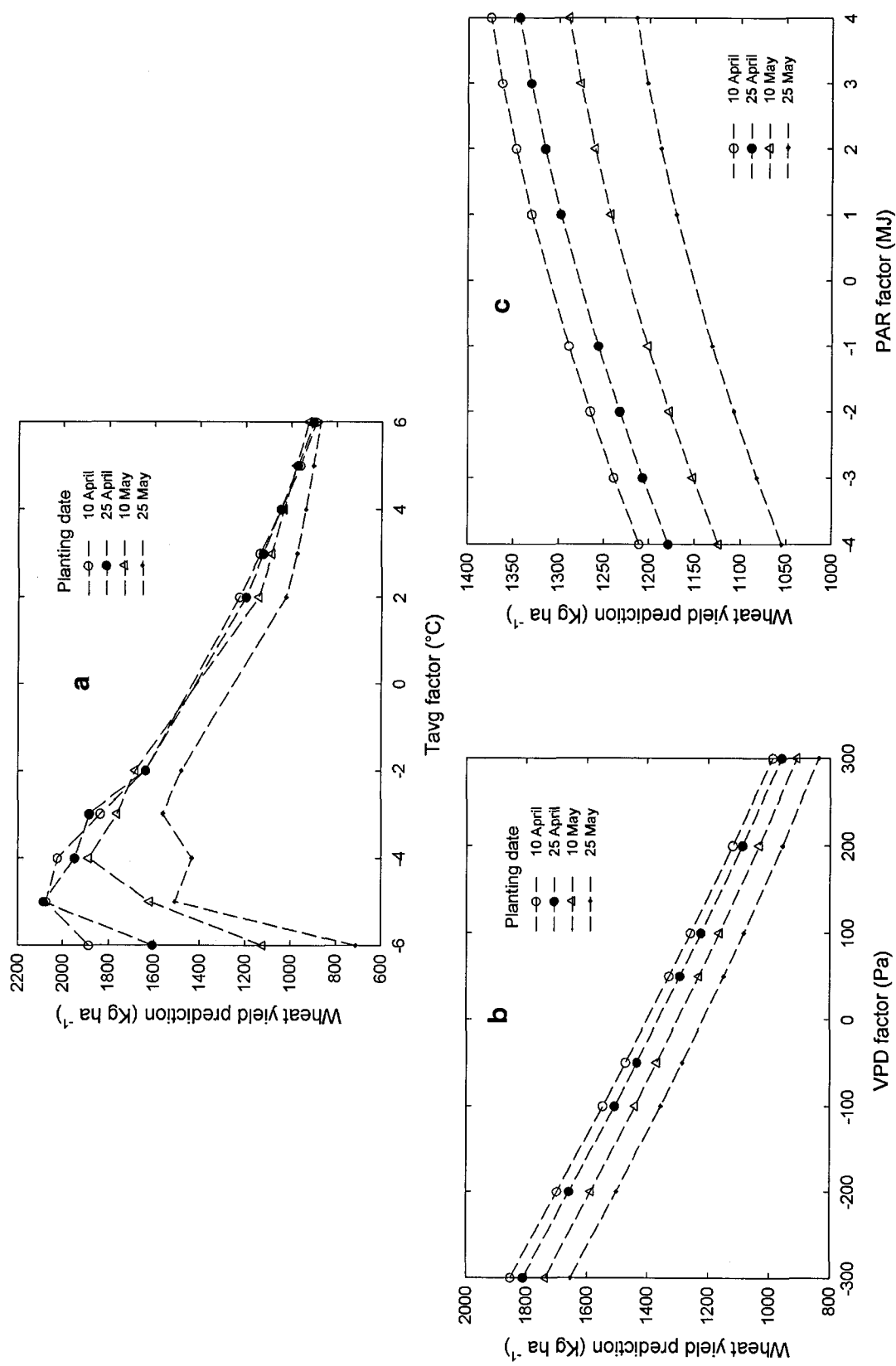
Figure 5. Effect of varying TAVG (a), VPD (b) and PAR (c) on spring wheat yield estimates over a series of four planting dates.

(time of formation of double ridge and terminal spikelet), every 3 degree rise in maximum daily air temperature decreased the number of spikelets per spike by 1. Due to the dependency of this relationship upon site specific factors, however, the combined model does not include a routine for heat induced yield reduction. Similarly, the combined model does not attempt to account for sterilization of florets as a result of high temperature during anthesis, though a clear effect exists (Saini and D. 1982, Al-Khatib and Paulsen 1984, Wardlaw et al. 1989a, Wardlaw et al. 1989b). In contrast, the combined model does implicitly account for the effects of temperature on grain filling via the harvest index.

The harvest index is a function of the rate and duration of grain filling, which is ultimately governed by air temperature. Cooler temperatures during the grain filling period produce higher yields both physiologically and mathematically in the model. Hence, in the combined model, air temperature effects the ontogenetic development, which in turn governs the time at which grain filling occurs. In this manner, if development occurs too rapidly, the grain filling period could start in July, the hottest month of the year. This has the inevitable effect of reducing yield. This phenomenon explains the non-linear nature of the estimated yield as a result of temperature variation in the sensitivity analysis (figure 5a).

Estimated state average wheat yield resulting from the sensitivity analysis of temperature was within the range of observed spring wheat yield in Montana from 1950 – 2003 (603 to 2479 kg ha^{-1}). Though the state wide average yield predictions are realistic, the range of variation in yield produced during the sensitivity analysis for each individual county was not (Appendices). These effects were erratic but explainable.

A decrease in average daily temperature of -6° C decreases the number of fields available for analysis, especially in high elevation areas. However, a decrease in average temperature of only -5° C (figure 5a and Appendix A) increases estimated yield, but also increases the range (Appendix E). Since the grain filling period is influenced principally by temperature, very high yields (> 3705 kg ha^{-1}) were predicted in some higher elevation areas because of greatly extended grain filling periods, and therefore harvest index values. These pixels were ordinated on the threshold between a lengthy simulated growing season, and not enough thermal time for completion of the growing season.

The sensitivity analysis of temperature reinforces its importance as a driver of yield. The interactive effects of temperature and planting date are also evident in Appendix A. For example, later planting dates can offset the effects of temperature to some degree (figure 5a) but this varies greatly on the timing of precipitation. Surprisingly, at progressively higher temperatures, planting date becomes less important as very low yields are estimated. This is demonstrated in figure 5a as the convergence of estimated yield curves for all planting dates.

Photosynthetically Active Radiation

The effects of PAR variation on estimated yield were predictably positive and slightly non-linear (figure 5c). The marginally curvilinear relationship depicted in figure 5c is due to the constraints on PAR observations between 0.5 – 16 MJ (Table 2). Interestingly, the simulated planting date had a slightly larger effect than PAR itself.

Effects of Simulated Climate Variation on Predicted Yield

The sensitivity of predicted yield to varying interactive climate scenarios was tested to see if thresholds could be detected beyond which, the model would predict

unrealistically high or low yield. This was important because in the dry summer climate

of Montana it is not realistic to assume increasing temperature without also increasing

VPD, unless air masses remain commensurately moist. Thus, the analysis simultaneously

varied PAR, VPD and TAVG across the range of expected climate variability in major

wheat growing regions of Montana. The results of this process reinforced my supposition

that as a regional wheat yield analysis tool, the combined model is quite robust. Running

the model with extreme climate scenarios (hot, dry and wet, cold) resulted in yield

predictions very near the highest and lowest yield ever recorded in Montana. From the

period of 1950 to 2003, the highest recorded state average spring wheat yield was 2490

kg ha^{-1}, while the lowest was 605 kg ha^{-1}. This compares remarkably well with the

estimated extremes of 2450 kg ha^{-1} and 600 kg ha^{-1} predicted during the climate variation

testing. Figure 6 reveals that the coolest and wettest conditions did not produce
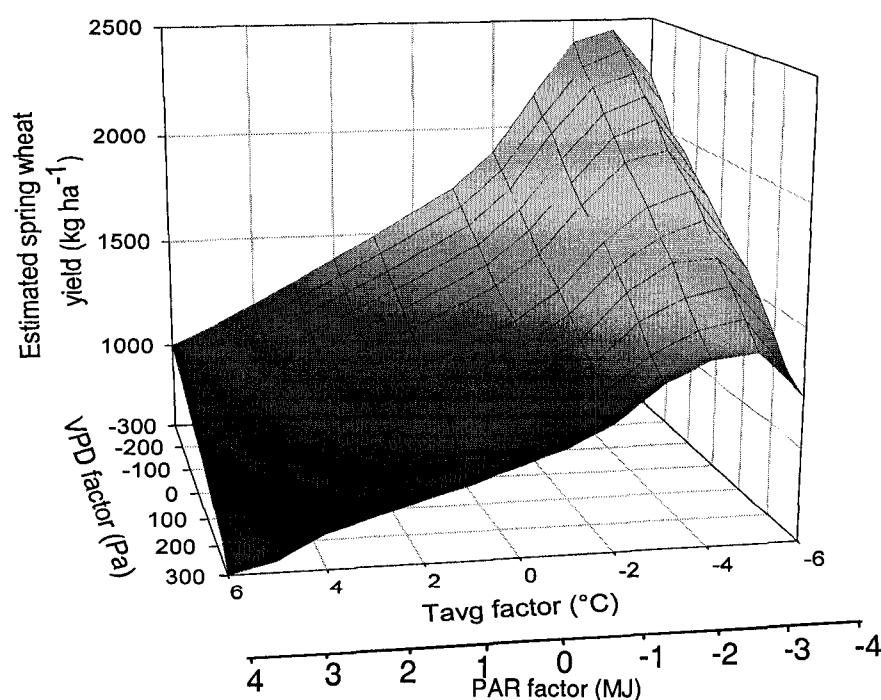
Figure 6. Effects of climate variation on estimated yield. Climate scenarios range from
hot and dry to cool and moist.

the highest yield. Indeed, it appears that a temperature decrease of 5° C, produced the highest yield. This is likely because at the lowest temperature, the extended grain filling period did not compensate for the reduction in growing season length and decreased photosynthesis early in the year as a result of cooler temperatures.

Although Montieth's formulation prescribes a linear increase in biomass, resulting from increasing PAR, grain yield does not follow this pattern. Figure 6 reveals that temperature is a much stronger determinant of grain yield than PAR. Even as PAR decreases, grain yield increases at progressively cooler temperatures. However, the high estimated yield may not be entirely realistic because at extremely low temperatures, planting dates are likely to be much later due to improper seedbed conditions. Indeed, as demonstrated in figure 5, low temperatures coincident with late planting dates may result in catastrophically low yield. In contrast, during hot dry growing seasons, the reduction in estimated RUE resulting from increased VPD more than compensates for increased PAR (figure 6).

Physiological Variables

Estimated yield was generally more erratically responsive to changes in meteorological conditions than to the array of physiological details examined. As expected, RUE and harvest index had the largest effect on yield. Of these two variables, varying harvest index had the largest effect on yield (figure 7) over the range tested. Of the other variables tested, TTSE had the smallest effect (figure 8) (Appendix B). Across all planting dates the response of yield to changes in TTSE, TTBE and PHINT was mostly linear (figure 8).
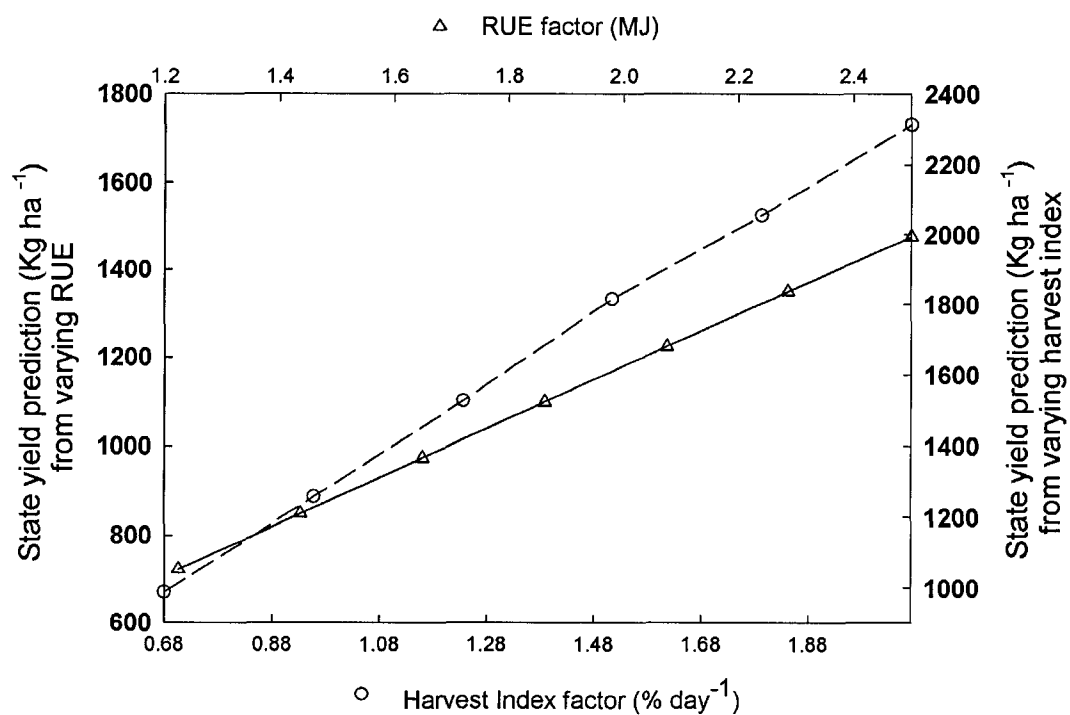
Figure 7. Effect of varying RUE and harvest index on estimated state average spring wheat yield.
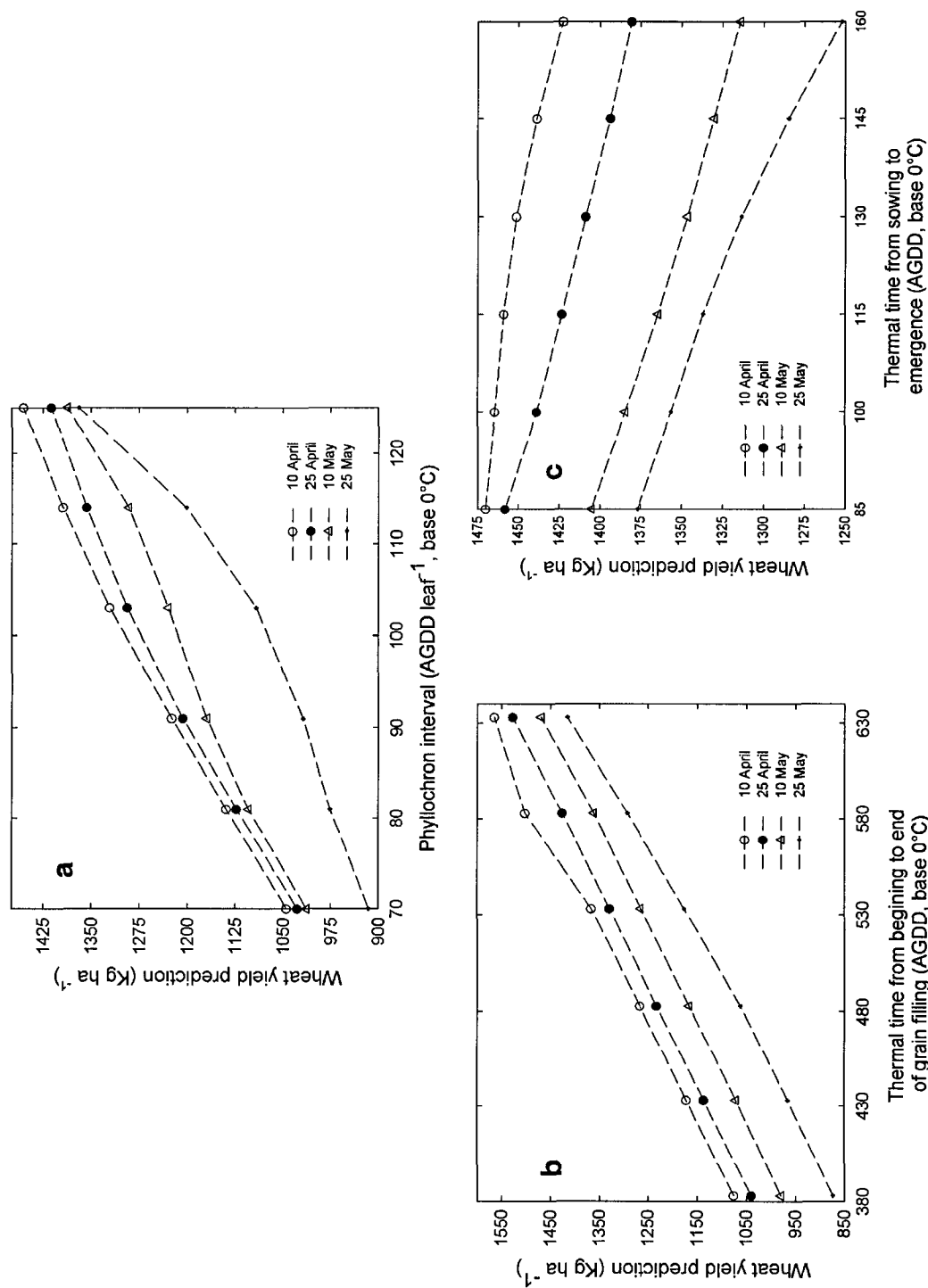
Figure 8. Effect of varying PHINT (a) TTBE (b) and TTSE (c) on estimated spring wheat yield.

Yield Simulation

The combined model produced state level wheat yields which closely matched the observed state level spring wheat yield computed from the same counties. To test for differences between means, I first ensured that the variances were equal between the years analyzed using the F-ratio test (Zar 1995). Indeed, there was no difference ($P \leq 0.05$) between the variances of predicted and observed wheat yield in any year of the study (Table 3). The t-tests indicated that in all years of the study, predicted wheat yield was indistinguishable from observed yield (Table 3). This was encouraging as it provides evidence that the combined model provides realistic and reliable yield information for large regions. Though similar conclusions were reached in Chapter three, the combined model is advantageous over the simple harvest index logic used in Chapter three for two major reasons; 1) The ability to emulate the effects of differing climate scenarios on yield and 2) The combined model has a dynamic and spatially unconstrained method for

Table 3. Variance, mean and associated F-ratio test parameters for demonstrating equality of variances ($P \leq 0.05$). Means were not significantly different ($P \leq 0.05$) in any year.

Year	2001		2002		2003	
Parameter	Observed	Predicted	Observed	Predicted	Observed	Predicted
Mean	1483	1429	1138	1294	1275	1245
Variance	370118	374873	346271	481696	11642	63350
F	1.0128		1.391		1.841	
P(F<=f)	0.4866		0.1983		0.056	
$F_{critical}$	1.882		1.905		1.882	
df	29		28		29	

computing expected maturity dates for each wheat field identified in the state. This is important for characterizing crop growth stage and expected yield in advance of the

harvest date. These factors make the wheat yield estimation protocol here a potentially valuable tool for predicting yield for large areas, in a rapid, unbiased manner.

Despite the capability of the combined model to accurately predict yield for large regions, it performs somewhat poorly at the county level. Figure 9 demonstrates the relatively poor relationship between predicted and observed spring wheat yield. The relationship was strongest in 2001, which corresponds to the results from Chapter three. With the exception of 2001, the results of this study compare unfavorably with results from a similar study by Doraiswamy et al. (2003) who integrated both TM and AVHRR data within the EPIC (Erosion Productivity Impact Calculator) crop growth simulation model.

The EPIC model utilizes a soil water balance model to control RUE, which is spatially parameterized using the STATSGO electronic soils data base (NRCS 2004). Doraiswamy et al. (2003) report extremely good results (r^2 between 0.8 – 0.96) by using remote sensing data to calibrate leaf area information over the period 1994 to 1998 in North Dakota. However, it is not clear if these coefficients of determination are computed from the 1 to 1 line or if they are the result of the best fit regression equation. If the former is true, the r-square reported by Doraiswamy et al. (2003) values could be substantially lower. In either case, the great success by Doraiswamy et al. (2003), has not been duplicated before or since, and it comes with great surprise that the system is not used operationally. It seems likely that if such a system were developed, it would have significant proprietary use and value.

One distinct advantage of the combined model used in this study over that used by Doraiswamy et al. (2003) is the fast turnaround time on the imagery for near-real time
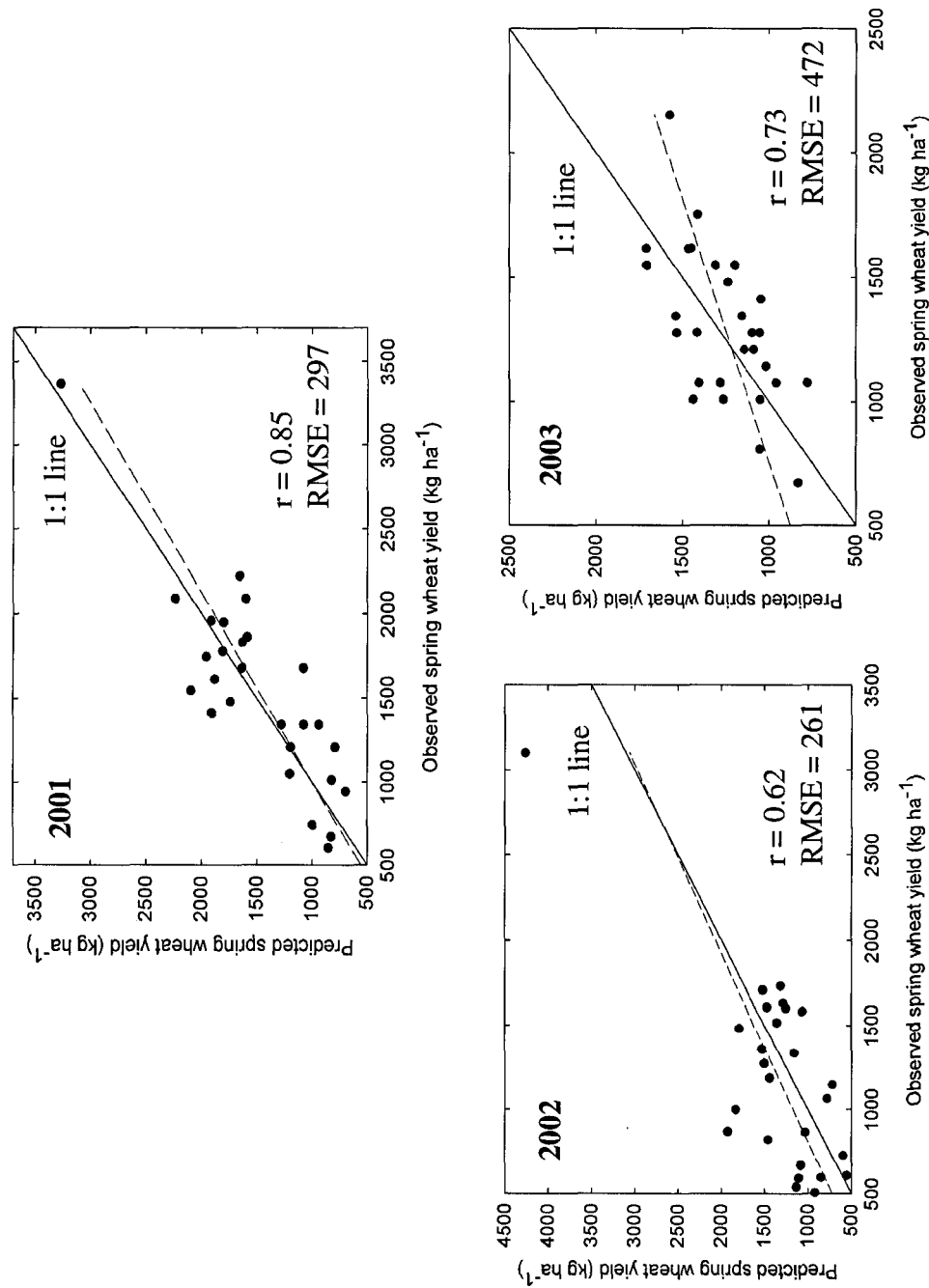
Figure 9. Predicted versus observed spring wheat yield for counties with >= 1820 acres of planted spring wheat. Regression models for 2001, 2002 and 2003 are $y = 0.887x + 114.03$, $y = 0.8983x + 270.94$ and $y = 0.4741x + 640.1$ respectively. Flathead County is the ubiquitous outlier in every year. High yield is observed in Flathead County because most spring wheat is grown in the northern portion of the county where snowfall and thus soil moisture is usually more abundant than in other counties.

117

yield estimates. For example, the standard eight-day composite MODIS FPAR/LAI

product can be ready to use about 10 days after acquisition of the first image in the eight-

day cycle. This means that a yield estimate can be produced within about 10 days behind

actual field conditions, which is in sharp contrast to empirical retrospective studies,

which require constant recalibration and are cumbersome for larger regions.

Yield Forecasting

The ability to forecast yield is an extremely desirable aspect of any yield

simulation model. The F-ratio test indicated that the variance between early predicted

wheat yield and observations were not significantly different ($P \leq 0.05$), thereby permitting

use of the paired t-test, for detecting differences (Appendix L.). When used with an

assumed harvest index of 38 %, the combined model predicted yield at least 550 AGDD

($p < 0.05$) in advance of actual maturity (figure 10).
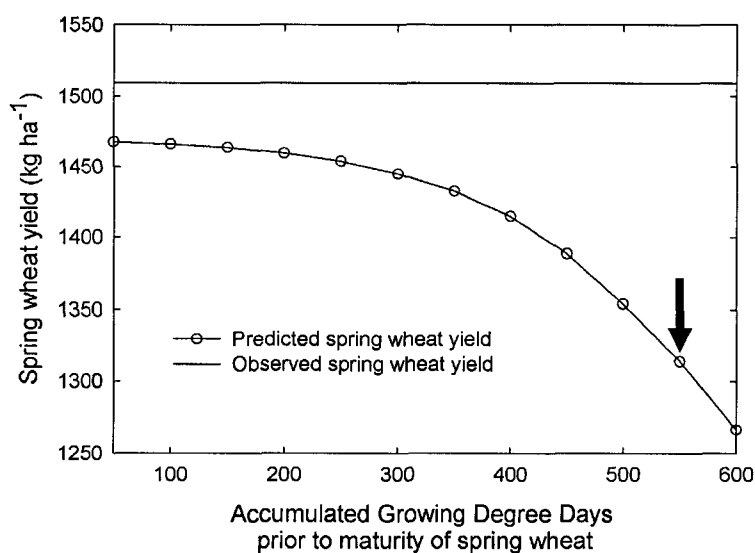
Figure 10. Results of yield forecasting procedure. Beyond the thick black arrow, yield
forecast is significantly different from observation ($P \leq 0.05$). Yield is statewide
average for counties analyzed in this study for 2001.

Assuming an average temperature of 23.89° C (75° F), this equates to about 23 days prior to maturity. This is extremely encouraging, because this methodology could be used to facilitate yield forecasting for large regions, and does not require knowledge of cultivar specific harvest index values.

Conclusions

The results of this study demonstrate a method of directly using MODIS derived FPAR with a simple mechanistic model for accurately computing regional wheat yield. Implementing the suggestions based on research presented in Chapter three improved the predictive ability of the combined model, making it more robust, yet sensitive to yield attenuating factors.

Incorporating the effects of temperature on final yield is an improvement over the logic presented in Chapter three and permits quite accurate yield estimates at the state level. In addition, if the daily average temperature drops by more than 5° C, catastrophically low grain yield can be expected when coupled with later planting dates. Given that the combined model is easy to use and requires little management information, it can be used as a tool to facilitate interpretation of broad scale wheat yield patterns.

Perhaps the largest benefit to others resulting from this project is the ease of operational use and the ability to potentially predict spring wheat yield for Montana about 23 days in advance. Hopefully, this model will be further refined and made ready for use in other areas with the caveat that it be used for regional predictions only.

I was slightly disappointed with the county level performance of the model except in 2001, especially since I have spent nearly four years developing these ideas. I contend however, that the accuracy and precision of yield estimates at a particular point is, for

some purposes, less useful than temporal trends of yield and a regional perspective. This is because; farmers generally know what the yield on their land is going to be, or sometimes even the entire county for that matter. But an individual is not going to have a good feel for how the entire region is doing, or perhaps more importantly, how their region of interest compares with other dominant wheat growing regions (i.e Sumner County, Kansas).

This is especially important from an international perspective where little information is available regarding crop performance, which leaves commodities markets and food banking organizations at the mercy of a foreign administrator who may not always be truthful. To this end, the combined model developed and validated as part of my research could be used as a tool for consistently characterizing the productivity and yield of large regions in an unbiased manner. In spite of this, there are obvious limitations and abundant opportunities for improving the logic and data streams available for this model.

The largest obstacles to producing consistently good county level yield estimates are proper land cover characterization and improved spatially explicit cultivar data. Doraiswamy et al. (2003) developed a spring wheat mask using a signature extension from TM to AVHRR data. Unfortunately, details regarding this process are lacking. I propose that a similar mask developed from MODIS 250-meter NDVI could significantly improve yield estimates. Such a mask, however, would likely require re-calibration each year to avoid fallow cropping systems in the analysis. Likewise, given the high sensitivity of yield to harvest index, improved knowledge of cultivar information should provide more reliable yield estimates for smaller regions. Other cultivar specific

information would easily improve the estimation of growing season length. Spring wheat varieties grown in Montana can vary in thermal time for maturity requirements by as much as 300 to 400 AGDD (about 16 days). This extra thermal time requirement could significantly alter the amount of simulated accumulated biomass, and grain yield.

The sensitivity analyses indicated that the combined model produces dependable results, for large regions, across a diverse suite of meteorological thresholds. This analysis combined with the observation that county level results were not as accurate as hoped give further merit to the idea that perhaps MODIS 1-km products are most suited for regional analyses and not necessarily for characterizing field-or-county level yield. This pattern was observed in Chapter's two and three as well.

Acknowledgements

Literature Cited

Al-Khatib, K. and Paulsen, G.M., 1984, Mode of high temperature injury to wheat during grain development. *Physiol. Plant,* **61,** 363-368.

Amir, J. and Sinclair, T.R., 1991a, A model of the temperature and solar-radiation effects on spring wheat growth and yield. *Field Crops Research,* **28,** 47-58.

Amir, J. and Sinclair, T.R., 1991b, A model of water limitation on spring wheat growth and yield. *Field Crops Research,* **28,** 59-69.

Angus, D.H., Mackenzie, R., Morton, R. and Schafer, C.A., 1981a, Phasic development in field crops 2. Thermal and photoperiodic responses of spring wheat. *Field Crops Research,* **4,** 269-283.

Angus, J.F., Cunningham, R.B., Moncur, M.W. and Mackenzie, D.H., 1981b, Phasic development in field crops 1. Thermal response in the seedling phase. *Field Crops Research,* **3.**

Aparicio, N., Villegas, D., Cassadesus, J., Araus, J.L. and Royo, C., 1999, Spectral vegetation indices as nondestructive tools for determining durum wheat yield. *Agroclimatology,* **92,** 83-91.

Atlas, R.M. and Lucchesi, R., 2000. File Specification for GEOS-DAS Gridded Output, Data Assimilation Office, Goddard Space Flight Center, Greenbelt Maryland.

Badwhar, G.D., 1980, Crop emergence date determination from spectral data. *Photogrammetric Engineering and Remote Sensing,* **46,** 369-377.

Baker, J.T., Pinter, P.J., Regenato, R.J. and Kanemasu, E.T., 1986, Effects of temperature on leaf appearance in spring and winter wheat cultivars. *Agronomy Journal,* **78,** 605-13.

Bauer, A., Fanning, C., Enz, J.W. and Eberlein, C.V., 1984a, Use of Growing Degree Days to Determine spring wheat growth stages. North Dakota State University Cooperative Extension Service, Fargo, pp. 1-10.

Bauer, A., Frank, A.B. and Black, A.L., 1984b, Estimation of spring wheat leaf growth rates and anthesis from air temperature. *Agronomy Journal,* **76,** 829-835.

Bauer, A., Frank, A.B. and Black, A.L., 1985, Estimation of spring wheat grain dry matter assimilation from air temperature. *Agronomy Journal,* **77,** 743-752.

Brocklehurst, P.A., 1977, Factors controlling grain weight in wheat. *Nature,* **266,** 348-349.

Brooks, R.J., Semenov, M.A. and Jamieson, P.D., 2001, Simplifying Sirius: Sensitivity analysis and development of a meta-model for wheat yield prediction. *European Journal of Agronomy,* **14,** 43-60.

Brooks, R.J. and Tobias, A.M., 1996, Choosing the best model: Level of detail, complexity and model performance. *Math. Comp. Modeling,* **24,** 1-14.

Cao, W. and Moss, D.N., 1991, Phyllochron change in winter wheat with planting date and environmental changes. *Agonomy Journal,* **83,** 396-401.

Chipanshi, A.C., Ripley, E.A. and Lawford, R.G., 1997, Early prediction of spring wheat yields in Saskatchewan from current and historical weather data using the CERES-Wheat model. *Agricultural and Forest Meteorology,* **84,** 223-232.

Choudhury, B.J., 1987, Relationships between vegetation indices, radiation absorption, and net photosynthesis evaluated by a sensitivity analysis. *Remote Sensing of Environment,* **22,** 209-233.

Dai, Z., Edwards, G.E. and Ku, M.S.B., 1992, Control of photosynthesis and stomatal conductance in *Ricinus communis* (Castor bean) by leaf to air vapor pressure deficit. *Plant Physiology*, **99**, 1426-1434.

Doraiswamy, P.C. and Cook, P.W., 1995, Spring wheat yield assessment using NOAA AVHRR data. *Canadian Journal of Remote Sensing*, **21**, 43-51.

Doraiswamy, P.C., Moulin, S., Cook, P.W. and Stern, A., 2003, Crop yield assessment from remote sensing. *Photogrammetric Engineering and Remote Sensing*, **69**, 665-674.

Edwardson, S.E. and Watt, D.L., 1987, GROWTH STAGE: Using growing degree days to predict the Haun scale of spring wheat. *Applied Agricultural Research*, **2**, 224-229.

Fischer, R.A. and Kertesz, Z., 1976, Harvest index in spaced populations and grain weight in microplots as indicators of yielding ability in spring wheat. *Crop Science*, **16**, 55-59.

Fisher, F.B., Winne, J.C., Thornton, M.M., Tady, T.P., Ma, Z., Hart, M.M. and Redmond, R.L., 1998. Montana land cover atlas, University of Montana, Missoula, MT.

Flood, R.G., Martin, P.J. and Gardner, W.K., 1995, Dry matter accumulation and partitioning and its relationship to grain yield in wheat. *Australian Journal of Agricultural Research*, **35**, 495-502.

Frank, A.B. and Bauer, A., 1996, Temperature, nitrogen, and carbon dioxide effects on spring wheat development and spikelet numbers. *Crop Science*, **36**, 659-665.

Frank, A.B., Bauer, A. and Black, A.L., 1987, Effects of air temperature and water stress on apex development in spring wheat. *Crop Science*, **27**, 113-116.

Gallagher, J.N. and Biscoe, P.V., 1978, Radiation absorption, growth and yield of cereals. *Agricultural Science*, **91**, 47-60.

Gao, B., Heidebrecht, K. and Goetz, A., 1993, Derivation of scaled surface reflectances from AVIRIS data. *Remote Sensing of Environment*, **44**, 165-178.

Hatfield, J.L., 1983, Remote sensing estimators of potential and actual crop yield. *Remote Sensing of Environment*, **13**, 301-311.

Heinsch, F.A., Reeves, M.C., Bowker, C.F., Votava, P., Kang, S., Milesi, C., Zhao, M., Glassy, J., Jolly, W.H., Kimball, J.S. and Nemani, R.R., 2003. User's Guide: GPP and NPP (MOD17A2/A3) Products NASA MODIS Land Algorithm V. 2.0, University of Montana, Missoula, MT.

Environmental Systems Research Institute, 2002, ArcGis, Redlands, CA.

Jamieson, P.D., Brooking, I.R., Porter, J.R. and Wilson, D.R., 1995a, Prediction of leaf appearance in wheat: a question of temperature. *Field Crops Research*, **41**, 35-44.

Jamieson, P.D., Martin, R.J., Francis, G.S. and Wilson, D.R., 1995b, Drought effects on biomass production and radiation use efficiency in barley. *Field Crops Research*, **43**, 77-86.

Jamieson, P.D., Porter, J.R., Goudriann, J., Ritchie, J.T., Keulen, H.v. and Stol, W., 1998, A comparison of the models AFRCWHEAT2, CERES-Wheat, Sirius, SUCROS2 and SWHEAT with measurements from wheat grown under drought. *Field Crops Research*, **55**, 23-44.

Jenner, C.F., 1974, Factors in the grain regulating the accumulation of starch. *BULLETIN*, 901-908.

Johnson, R.C. and Kanemasu, E.T., 1983, Yield and development of winter wheat at elevated temperatures. *Agronomy Journal*, **75**, 561-565.

Jolly, W.H., Graham, J.M., Michaelis, A., Nemani, R. and Running, S.W., 2004, A flexible, integrated system for generating meteorological surfaces derived from point sources across multiple geographic scales (accepted for publication). *Environmental Modeling and Software*.

Kawamitsu, Y., Yoda, S. and Agata, W., 1993, Humidity pretreatments affects the responses of stomata and CO_2 assimilation to vapor pressure differences in C_3 and C_4 plants. *Plant Cell Physiology*, **34**, 113-119.

Kiniry, J.C., Jones, J.A., O'toole, J.C., Blanchet, R., Cabelguenne, M. and Spanel, D.A., 1998, Radiation use efficiency in biomass accumulation prior to grain filling for five grain crop species. *Field Crops Research*, **20**, 51-64.

Labus, M.P., Nielsen, G.A., Lawrence, R.L. and Engel, R., 2002, Wheat yield estimates using multi-temporal NDVI satellite imagery. *International Journal of Remote Sensing*, **23**, 4169-4180.

Laguette, S., Vidal, A. and Vossen, P., 1998, Using NOAA-AVHRR data to forecast wheat yields at a European scale. *Agrometeorological Applications for Regional Crop Monitoring and Production Assessment*, 131-146.

Lemon, E., Stewart, D.W. and Shawcroft, R.W., 1971, The sun's work in a cornfield. *Science*, **80**, 371-378.

Manjunath, K.R., Potdar, M.B. and Purohit, N.L., 2002, Large area operational wheat yield model development and validation based on spectral and meteorological data. *International Journal of Remote Sensing*, **23**, 3023-3038.

Mcneal, F.H., Berg, M.A., Brown, P.L. and McGuire, C.F., 1971, Productivity and quality response of five spring wheat genotypes, *Triticum aestivum L.*, to nitrogen fertilizer. *Agronomy Journal*, **63**, 908-910.

Monteith, J.L., 1972, Solar radiation and productivity in tropical ecosystems. *Journal of Applied Ecology*, **9**, 747-766.

Montieth, J.L., 1977, Climate and efficiency of crop production in Britian. *Philosophical Transactions Royal Society of London*, 277-294.

Morrison, J.I.L. and Gifford, R.M., 1983, Stomatal sensitivity to carbon dioxide and humidity. A comparison of two C3 and two C4 grass species. *Plant Physiology*, **71**, 789-796.

Mosaad, M.G., Ortiz-Ferrara, G., Mahalakshmi, V. and Fischer, R.A., 1995, Phyllochron response to vernalization and photoperiod in spring wheat. *Crop Science*, **35**, 168-171.

Nicolas, M.E., Gleadow, R.M. and Dalling, M.J., 1984, Effects of drought and high temperature on grain growth in wheat. *Australian Journal of Plant Physiology*, **11**, 553-566.

Nouvellon, Y., Seen, D.L., Rambal, S., Begue, A., Moran, M.S. and Qi, J., 2000, Time course of radiation use efficiency in a shortgrass ecosystem: Consequences for remotely sensed estimation of primary production. *Remote Sensing of Environment*, **71**, 43-55.

Pettigrew, W.T., Hesketh, J.D. and D.B. Wooley, J.T., 1990, A vapor pressure deficit effect on crop canopy photosynthesis. *Field Crops Research*, **62**, 239-243.

Ritchie, J.T. and Otter, S., 1985. Description and performance of CERES-Wheat: A user-oriented wheat yield model. In ARS Wheat Yield Project, edited by W.O. Willis), pp. 159-175.

Running, S.W., Thornton, P.E., Nemani, R. and Glassy, J.M., 2000. Global terrestrial gross and net primary productivity from the Earth Observing System. In Methods in Ecosystem Science, edited by O. Sala, R. Jackson and H. Mooney (New York: Springer Verlag), pp. 44-57.

Saini, H.S. and D., A., 1982, Abnormal sporogenisis in wheat (Triticum aestivum L.) induced by short periods of high temperature. *Annals of Botany*, **49**, 835-846.

Sinclair, T.R. and Bai, Q., 1997, Analysis of high wheat yields in northwest China. *Agricultural Systems*, **53**, 373-385.

Sinclair, T.R. and Muchow, R.C., 1999a, Occam's Razor, radiation-use efficiency and vapor pressure deficit. *Field Crops Research*, **62**, 239-243.

Sinclair, T.R. and Muchow, R.C., 1999b, Radiation use efficiency. *Advances in Agronomy*, **65**, 265.

Sofield, I.L., Evans, T., Cook, M.G. and Wardlaw, I.F., 1977, Factors influencing the rate and duration of grain filling in wheat. *Australian Journal of Plant Physiology*, **4**, 785-97.

Toure, A., Major, D.J. and Lindwall, C.W., 1994, Comparison of five wheat simulation models in southern Alberta. *Canadian Journal of Soil Science*, 61-68.

Tucker, C.J., Holben, B.N., Jr., J.H.E. and III, J.E.M., 1980, Relationship of spectral data to grain yield variation. *Photogrammetric Engineering and Remote Sensing*, **46**, 657-666.

United States Department of Agriculture (USDA) National Agricultural Statistics Service (NASS)., 2003, USDA Published Estimates Database. *http://www.nass.usda.gov:81/ipedb/*.

United States Department of Agriculture (USDA) National Agricultural Statistics Service (NASS)., 2004. Crop Production Reports, http://usda.mannlib.cornell.edu/reports/nassr/field/pcp-bb/2003/.

United States Department of Agriculture (USDA) Natural Resources Conservation Service (NRCS) 2004, State Soil Geographic Database (STASGO).

Wardlaw, I.F., Dawson, I.A. and Munibi, P., 1989a, The tolerance of wheat to high temperatures during reproductive growth. 2 Grain Development. *Australian Journal of Agricultural Research*, **40**, 15-24.

Wardlaw, I.F., I.A. Dawson, P. Munubi and Fewster, R., 1989b, The tolerance of wheat to high temperatures during reproductive growth. 1

Survey procedures and general response patterns. *Australian Journal of Agricultural Research*, **40**, 1-13.

Wardlaw, I.F., Moncur, L. and Patrick, J.W., 1995, The response of wheat to high temperature following anthesis. 2. Sucrose accumulation and metabolism by isolated kernels. *Australian Journal of Plant Physiology*, **22**, 399-407.

Wardlaw, I.F., Sofield, I. and Cartwright, P.M., 1980, Factors limiting the rate of dry matter accumulation in the grain of wheat grown at high temperature. *Australian Journal of Plant Physiology*, **7**, 387-400.

Waring, R.H. and Running, R.W., 1998, Forest Ecosystems: Analysis at Multiple Scales, (San Diego: Academic Press).

Weigand, C.L., Richardson, A.J. and Kanemasu, E.T., 1979, Leaf area index estimates for wheat from LANDSAT and their implications for evapotranspiration and crop modeling. *Agronomy Journal*, **71**, 336-342.

Wheeler, T.R., Hong, T.D., Ellis, R.H., Batts, G.R., Morison, J.I.L. and Hadley, P., 1996, The duration and rate of grain growth, and harvest index, of wheat (*Triticum aestivum* L.) in response to temperature and CO_2. *Journal of experimental Botany*, **47**, 623-630.

Zar, J.H., 1995, Biostatistical Analysis, (Upper Saddle River, New Jersey: Prentice-Hall).

CHAPTER 5

CONCLUDING REMARKS

This final chapter is divided into two sections. The first section reiterates the original research questions and how the research presented here was used to answer them. The second section includes personal thoughts and suggestions for the next generation of similar research using MODIS data

Overall Research Conclusions

During the course of my Ph.D. research, I sought to answer four general questions: To what extent does MODIS vegetation data emulate trends in rangeland vegetation dynamics? Can wheat yield be accurately estimated for entire regions using only the MODIS vegetation product suite? If not, what changes can be made to the modeling environment and input data stream to improve yield estimates? and, what is the appropriate spatial domain for characterizing regional rangeland productivity and wheat yield from MODIS data?

Seeking to answer these questions, I have evaluated the potential use of MODIS vegetation data for characterizing productivity of both rangeland and agriculture landscapes. The results presented in Chapter's two through four revealed several noteworthy and unifying themes. The common threads linking these chapters are the methods used for aggregating data and identification of proper spatial scale of analysis. These themes were espoused at chapter and should help others who intend on using MODIS data for similar endeavors. Hence the purpose of this chapter is to provide brief concluding remarks and personal thoughts regarding the major findings of this dissertation.

The appropriate scale for evaluating remote sensing data ultimately depends on the question being asked. All geographic phenomena, particularly those linked to the biophysical properties of the earth's surface, are considered to be scale dependent. Scale dependence refers to situations where (1) representations of spatial patterns may be different when observed at different scales; (2) certain patterns and processes may not be observable at a particular scale or resolution; and (3) methods used to observe causal relationships between variables are affected by the scale of observations. I postulate that because all geographic phenomena are scale dependent, different conclusions may be drawn from using imagery with different scales and spatial resolution. This was a great lesson since, like others, I once believed it was necessary to have global, 1-meter resolution, hyperspectral data, twice daily to answer resource based questions. Indeed some questions cannot be properly addressed using broad-scale satellite spectral data without the use of supplemental ground based reconnaissance. However, the dominant theme conveyed in this dissertation is that, in general, increasing the spatial aggregation improves the relationships between measures of vegetation abundance and satellite remote sensing data.

In Chapter two, I first discovered this while trying to relate ETM+ NDVI to biomass observations with little success at the site and transect levels. Next, I aggregated both NDVI and biomass observations to the grazing allotment level. Still, relations were poor. As a final attempt I created Thiesson polygons around 12 weather stations within and adjacent to the Little Missouri National Grasslands and subsequently aggregated NDVI and biomass observations within these spatial extents. This level of aggregation (about 185,000 ha) provided suitable relationships between NDVI and observed biomass.

These findings were reiterated while analyzing MODIS PSN$_{net}$ data and even more so after evaluating inter-annual relations between NPP and growing season precipitation.

The results presented in Chapter two indicate that time integrated MODIS PSN$_{net}$ data can be used for analyzing inter-annual productivity differences of large regions. In addition, intra-annual productivity differences can be suitably evaluated especially during favorable years. In response the first and last of the four research questions outlined in Chapter one and above, MODIS data can be used for monitoring rangeland vegetation productivity with the following caveats: 1) Inter-annual variation can probably be more appropriately characterized than intra-annual differences, 2) Intra-annual differences are more easily detected during years with favorable growing conditions and 3) progressive spatial aggregation from the pixel level to large regions will provide more precise and reliable estimates of productivity. Based on these findings, I devised a testing procedure in Chapter three for evaluating the appropriate spatial aggregation of MODIS GPP estimates for computing wheat yield estimates in Montana and North Dakota.

Chapter three reveals that progressive aggregation from counties to climate districts to states greatly improves wheat yield predictions. The relationship between predicted and observed wheat yield at the county level was the strongest ($r^2 = 0.46$) in 2001, which is also the year of the strongest relationship between MODIS PSN$_{net}$ and observed above-ground green biomass in North Dakota. Subsequent aggregation to the state level produced wheat yield estimates which were never more than 5% different from observed yield. These results, in part, answer the questions "Can wheat yield be accurately estimated for entire regions using only the MODIS vegetation product suite?" and "What is the appropriate spatial domain for characterizing regional wheat yield from

MODIS vegetation data?". The research presented in Chapter three provides evidence that, indeed, MODIS GPP estimates can be used to accurately estimate wheat yield, but only for large regions (states). The poor ability of MODIS GPP for estimating yield at the county level provided the impetus for improving data inputs and model logic, which was discussed in Chapter four. These suggested improvements were (1) implementation of more appropriate and regionally specific analysis masks to delineate wheat from other crops; (2) inclusion of localized, observed meteorological data and; (3) adaptation of crop physiological parameters in the current GPP algorithm to more closely emulate observed physiological characteristics of commonly grown wheat varieties in the region of interest. These suggested improvements provided the motivation for Chapter four.

The improved model designed in Chapter four permitted more precise estimates of wheat yield at the county level than in Chapter three. However, the state level spring wheat yield predictions were, once again, the most impressive. In fact, at the state level, the combined model produced estimates of wheat yield which were impressively indistinguishable (P<0.05) from observations in all years of the study. Thus, I am quite confident that MODIS vegetation data can be used for accurately estimating state level wheat yield for spring wheat.

Personal Thoughts and Suggestions for Future Research

A suite of satellites has been used to measure and monitor biophysical constituents of the earth's surface, each exhibiting different characteristics. The MODIS sensor, however, is unique because it combines both the spatial and spectral resolution of several satellites on a single platform. MODIS exhibits greater radiometric resolution than traditional sensors providing a broader range of measurement and therefore

increased sensitivity to small changes in spectral reflectivity. The MODIS offers 36 spectral channels, as compared to 5 on the AVHRR instrument, 7 on Landsat TM or 8 on the Landsat Enhanced Thematic Mapper plus (ETM+). Although Landsat satellites offer greater spatial resolution they exhibit a revisit time of 16 days but with clouds, often yield only 2 to 3 scenes per growing season. In addition the MODIS offers multi-spatial resolution for different applications. Calibration of the sensor is performed on-board allowing adjustments to be made while in orbit. In contrast the AVHRR has no comparable on-board calibration. Another weakness of the AVHRR data is the lack of orbit timing control creating inconsistent overpasses and associated sun-angles. In addition, the MODIS earth location algorithm produces eight pieces of information and uses ground control points for instrument alignment. Earth location knowledge will be accurate within 0.1 pixels at 2 standard deviations for the 1- km bands. In addition to improved sensor characteristics and temporal and spatial resolution the MODIS data stream undergoes unprecedented processing and quality assurance tests before distribution. For example, spectral radiance data are cloud filtered, atmospherically and topographically corrected using sun and look angle information to yield an accurate surface reflectance. These procedures are part of the unique MODIS data processing system.

Does all this mean that MODIS vegetation productivity data are better for evaluating rangeland productivity and estimating wheat yield? Not necessarily. In the case of assessing rangeland biomass, large differences can be monitored with MODIS productivity but not necessarily "better" than with traditional methods. For example, early in the course of my Ph.D. research I evaluated both EVI and NDVI using the same

scaled biomass data set for 2001 that was explained in Chapter 2. I related NDVI and EVI to scaled above-ground green biomass over grazing allotments and Thiesson polygons (the same polygons used in Chapter 2). MODIS vegetation productivity was more related ($r^2 = 0.77$) than NDVI ($r^2 = 0.67$) during peak greeness. However, EVI was more related ($r^2 = 0.84$), indicating that there is probably a greater likelihood of describing spatial variation across the landscape using EVI. A testament to this is the relative lack of publications using MODIS derived vegetation productivity for evaluating differences across the landscape in either rangeland or agricultural environments.

To be fair, there are many more assumptions being made in the MODIS vegetation productivity formulation than in vegetation indices. What's more, if biomass estimates are required, use of NDVI or EVI could be more restrictive because regression formulations between biomass and these indices would probably have to be re-evaluated periodically and applied in a retrospective manner (which may or may not be an issue). In contrast, MODIS vegetation productivity provides an estimate of carbon sequestration, which to the extent that it is accurate, could be converted to biomass on the fly. I don't recommend this given the host of unknown landscape parameters needed but at least it is an option without a great deal of retrospect (about 10 days). Having said this, I must re-iterate that if the only monitoring objective is assessment of relative differences across the landscape, then vegetation indices might be a superior choice. Specifically, for most applications, MODIS 250 meter NDVI would be the most useful but this depends on the scope of analysis.

Though I did not explicitly compare AVHRR NDVI versus MODIS vegetation indices or vegetation productivity, I believe MODIS has cleaner and more consistent data

(mostly due to regularized preprocessing). Still, the argument has been made that we are no better off than we were 20 – 30 years ago. For example, despite the inherent improvements that MODIS data compared with other sources, MODIS is still limited by the same factors that beguiled its' predecessors. There are still limitations imposed by spectral mixture problems, atmospheric distortion, clouds and data processing. These factors among others still inhibit assessment of earth's biophysical properties.

For rangeland analysis, I propose three recommendations for future research. First, I would spend more time sampling fewer allotments rather than less time on more allotments. The important concept is to sample the entire productivity continuum, so the analyst should purposely sample high, low and moderate productivity allotments. For the actual sampling I would definitely recommend clipped plot data unless the entire field crew is quite experienced at ocular estimation. During the 2001 field season, I tried ocular estimates, digital camera and agricultural digital camera techniques. I found that the crew was too inexperienced for precise ocular estimates. The digital cameras were impractical because of cloudiness and because without a frame to hold the cameras steady, there is no way to ensure that the same area of ground is viewed with each picture taken.

Second, development of a MODIS 250 meter NDVI database for Montana with a variety of associated metrics would be a very valuable project. The associated metrics might be 1) phenology, 2) relative "greenness" and 3) departure from normal. Development of this type of project would be widely used and appreciated. These data will not really help a rancher unless they have the ability to act on it. What's more, the individual producer probably already knows what the condition of the vegetation is on

their pasture. However, information about the spatial variation in rangeland productivity would be quite helpful however, especially for insurance companies as it might help the adjustor focus resources on problem areas. The remotely sensed vegetation productivity could act as a layer in a series of redundant drought threshold indicators. The seasonal trajectory and inert-annual variance should quite easily fit into the role the risk management agency for drought assessment. Once again, I believe the area for aggregation should be large (larger than small ranches). I am not sure how large this should be because I have not evaluated the 250 meter product enough to know. But as a general measure of variability of vegetation "greenness" the MODIS 250 NDVI does offer promising opportunity. Third, more research at different scales of analysis must be conducted. For example, a re-analysis of allotment level relationships between MODIS data and scaled biomass could be conducted with a different sampling scheme. In addition, some logical ecological boundaries could be evaluated such as Bailey's Ecoregions.

For wheat yield analysis, larger spatial aggregates will provide better results but if more ancillary data are available, it is possible to evaluate smaller areas than those examined in this dissertation. As in the case of rangeland productivity analysis, other data streams may be just as useful. For example, In 2000, I used LAI/FPAR estimates from AVHRR to drive the MODIS vegetation productivity algorithm and came very close to the observed 1999 state level wheat yield using the simple harvest index approach used in Chapter 3. I only tested this for one year but the results were similar to those presented in this dissertation, which indicates that the improved technology MODIS offers has not necessarily improved our ability to answer research questions posed in this

document. However, the MODIS products are ready to use "out of the box" which eliminates the historic need for relating NDVI to the variable of interest. In short, the MODIS vegetation products do enable the researcher to focus more on the biological science and less on the remote sensing science.

Maybe yield is not the best target for analysis, though if future research was able to compute yield for smaller areas in advance of harvest it could potentially be incalculably valuable. The value would not be to the farmer but to the market speculator (which often times is a single producer), crop insurance agencies and grain buyers. In addition, such an analysis could help avert falsified yield statements by different countries as they barter for a better price during negotiation.

In reality, the research community is a long way from this type of program. If yield estimation for smaller regions (some level between counties and fields) becomes the objective of future research I have four suggestions organized in order of relevance. First, an accurate wheat mask must be created and an automated system for updating the mask should be in place. A decent mask could be created from MODIS because the surface reflectance data are consistent, multiresolution and atmospherically corrected.

Second, a water balance should be computed and used to attenuate RUE in place of VPD, but only if accurate soils and precipitation are available. I tried computing a water balance for wheat yield but the resolution of the STATSGO digital soils database is probably too course. In addition, there may not have been enough precipitation to reliably drive the water balance. Third, once the other components are in place, I perceive good potential for driving a simplified field level wheat yield simulation model with MODIS 250 meter FPAR. At some point however, estimating wheat yield using

remote sensing become uninteresting. For example, focusing on individual fields is of little help because a farmer already knows what the yield is and often times cannot do anything about it. On the other end of the spectrum if, for example, the level of analysis is the entire western united states, I am not certain that would be of much use either.

In closing, MODIS does offer an unprecedented data stream that will not answer all research questions relating to wheat yield assessment and rangeland productivity. However, I believe that the MODIS data stream has equipped researchers with a timely, objective data set that permits more focus on the biological science and less on the remote sensing science.

Appendix A

Mean wheat yield resulting from varying meteorology during sensitivity analysis.

Parameter	Planting date			
	10 April	25 April	10 May	25 May
VPD				
-300	1853.0	1811.4	1737.5	1653.9
-200	1698.2	1657.8	1586.7	1502.0
-100	1546.9	1508.1	1440.2	1355.8
-50	1472.8	1435.0	1368.8	1285.0
50	1327.9	1292.2	1230.2	1148.4
100	1257.3	1222.7	1162.9	1082.8
200	1119.6	1087.7	1032.6	956.1
300	987.7	958.7	908.4	836.5
Tavg				
-6	1885.9	1606.2	1122.0	711.0
-5	2075.8	2085.7	1619.3	1508.4
-4	2024.7	1948.3	1887.0	1434.6
-3	1836.4	1883.7	1762.9	1562.6
-2	1636.4	1636.4	1681.7	1479.6
2	1226.9	1197.9	1141.2	1022.1
3	1134.6	1121.1	1083.6	971.8
4	1042.1	1044.3	1030.1	934.5
5	958.7	969.9	976.1	902.0
6	889.4	899.6	922.5	870.4
PAR				
-4	1210.4	1178.4	1123.7	1054.5
-3	1239.0	1206.8	1152.0	1082.1
-2	1265.0	1232.7	1177.7	1107.4
-1	1288.6	1256.3	1201.3	1131.1
1	1329.7	1297.5	1242.7	1170.6
2	1347.1	1315.0	1260.3	1187.4
3	1362.1	1330.2	1275.6	1201.9
4	1375.0	1343.2	1288.7	1214.1

Appendix B

Mean wheat yield resulting from varying physiological parameters during sensitivity analysis.

Parameter	Planting Date			
	10 April	25 April	10 May	25 May
Parameter				
RUE				
1.224	778.6	758.1	722.4	676.2
1.437	914.2	890.1	848.2	793.9
1.649	1049.1	1021.5	973.4	911.6
1.862	1184.7	1153.5	1099.2	1028.9
2.075	1320.2	1285.5	1225.0	1146.7
2.287	1455.2	1416.9	1350.2	1263.9
2.5	1590.7	1548.9	1476.0	1381.6
HI_slope				
0.68	1068.4	1040.1	988.7	917.0
0.958	1356.3	1320.6	1258.1	1177.0
1.236	1644.2	1601.1	1527.5	1436.9
1.514	1955.5	1903.4	1815.3	1717.8
1.792	2214.3	2154.7	2055.7	1935.4
2.07	2498.9	2431.3	2313.9	2154.2
TTSE				
85	1470.1	1458.2	1405.3	1376.9
100	1464.4	1438.7	1384.6	1356.2
115	1459.1	1423.3	1364.4	1336.9
130	1451.3	1408.9	1346.5	1313.6
145	1438.7	1393.7	1330.1	1284.5
160	1422.8	1380.8	1314.3	1252.2
TTBE				
383	1076.0	1040.1	979.8	873.6
433	1171.8	1136.5	1071.2	966.0
483	1267.2	1232.8	1166.4	1062.1
533	1366.4	1329.3	1265.0	1176.0
583	1502.1	1425.9	1361.6	1293.0
633	1565.2	1527.3	1469.3	1415.6
PHINT				
70	1044.5	1027.6	1013.4	915.2
81	1139.3	1123.2	1104.5	976.2
91	1224.6	1207.4	1169.9	1018.7
103	1321.3	1293.9	1229.7	1092.4
114	1394.4	1357.4	1291.6	1201.6
125	1455.6	1412.2	1387.0	1369.2

Appendix C

Correlation between predicted and observed county level wheat yield after varying meteorology during sensitivity analysis.

Parameter	Planting Date			
	10 April	25 April	10 May	25 May
VPD				
-300	0.73	0.72	0.70	0.68
-200	0.72	0.71	0.69	0.67
-100	0.71	0.70	0.68	0.66
-50	0.70	0.70	0.68	0.66
50	0.70	0.69	0.67	0.65
100	0.69	0.68	0.66	0.65
200	0.68	0.68	0.66	0.64
300	0.67	0.67	0.65	0.63
Tavg				
-6	0.71	0.72	0.75	0.83
-5	0.71	0.71	0.75	0.75
-4	0.86	0.87	0.74	0.69
-3	0.80	0.79	0.85	0.74
-2	0.81	0.81	0.80	0.85
2	0.85	0.85	0.84	0.84
3	0.85	0.86	0.85	0.85
4	0.85	0.86	0.85	0.86
5	0.84	0.85	0.86	0.86
6	0.84	0.85	0.86	0.87
PAR				
-4	0.84	0.83	0.82	0.81
-3	0.83	0.83	0.82	0.81
-2	0.83	0.83	0.81	0.81
-1	0.83	0.83	0.81	0.80
1	0.83	0.82	0.81	0.80
2	0.82	0.82	0.81	0.80
3	0.82	0.82	0.81	0.80
4	0.82	0.82	0.80	0.79

Appendix D

Correlation between predicted and observed county level wheat yield after varying physiological parameters during sensitivity analysis.

Parameter		Planting Date			
		10 April	25 April	10 May	25 May
RUE					
	1.224	0.70	0.69	0.67	0.65
	1.437	0.70	0.69	0.67	0.65
	1.649	0.70	0.69	0.67	0.65
	1.862	0.70	0.69	0.67	0.65
	2.075	0.70	0.69	0.67	0.65
	2.287	0.70	0.69	0.67	0.65
	2.5	0.70	0.69	0.67	0.65
HI_slope					
	0.68	0.70	0.70	0.68	0.66
	0.958	0.70	0.69	0.67	0.65
	1.236	0.70	0.69	0.67	0.65
	1.514	0.70	0.69	0.67	0.65
	1.792	0.70	0.69	0.67	0.66
	2.07	0.70	0.69	0.68	0.67
TTSE					
	85	0.69	0.69	0.67	0.66
	100	0.70	0.69	0.67	0.66
	115	0.70	0.69	0.66	0.66
	130	0.70	0.69	0.67	0.66
	145	0.70	0.69	0.67	0.66
	160	0.70	0.69	0.67	0.66
TTBE					
	383	0.71	0.70	0.69	0.68
	433	0.71	0.70	0.69	0.67
	483	0.70	0.70	0.68	0.67
	533	0.70	0.69	0.67	0.66
	583	0.71	0.69	0.68	0.65
	633	0.69	0.68	0.67	0.65
PHINT					
	70	0.70	0.71	0.72	0.73
	81	0.71	0.72	0.73	0.72
	91	0.72	0.72	0.71	0.70
	103	0.72	0.71	0.70	0.68
	114	0.70	0.70	0.67	0.66
	125	0.68	0.68	0.66	0.63

Appendix E

Range of wheat yield predictions after varying meteorology during sensitivity analysis.

Parameter	Planting date			
	10 April	25 April	10 May	25 May
VPD				
-300	2129.0	2097.2	2042.0	1965.7
-200	2003.2	1969.3	1909.3	1814.2
-100	1874.9	1839.1	1775.8	1665.5
-50	1810.0	1773.5	1708.9	1592.7
50	1678.5	1641.0	1574.5	1449.4
100	1612.1	1574.5	1507.3	1378.9
200	1478.5	1440.8	1372.9	1239.8
300	1343.5	1306.1	1238.1	1103.7
Tavg				
-6	754.2	798.2	1301.7	229.5
-5	4178.5	3950.6	689.2	1135.3
-4	3002.0	3084.3	3490.7	620.1
-3	2323.6	2414.4	2526.7	2814.4
-2	1940.9	1940.9	2088.2	2057.9
2	1530.8	1548.7	1509.7	1310.1
3	1417.9	1434.1	1442.5	1232.9
4	1270.3	1344.0	1375.5	1188.5
5	1125.8	1226.6	1290.9	1158.8
6	1033.3	1111.7	1217.4	1119.7
PAR				
-4	1506.1	1474.6	1420.2	1322.9
-3	1551.8	1519.8	1464.2	1365.0
-2	1594.5	1562.3	1505.6	1404.4
-1	1634.6	1602.3	1544.7	1441.0
1	1707.6	1675.5	1616.0	1505.9
2	1739.5	1707.7	1647.2	1533.6
3	1767.4	1735.7	1674.6	1557.5
4	1790.2	1758.6	1697.1	1577.1

Appendix F

Range of wheat yield predictions after varying physiological parameters during sensitivity analysis.

Parameter	Planting date			
	10 April	25 April	10 May	25 May
RUE				
1.224	970.5	949.9	913.4	846.0
1.437	1139.4	1115.2	1072.4	993.3
1.649	1307.6	1279.6	1230.5	1139.8
1.862	1476.4	1445.0	1389.5	1287.1
2.075	1645.4	1610.3	1548.4	1434.3
2.287	1813.4	1774.8	1706.6	1580.8
2.5	1982.3	1940.1	1865.5	1728.1
HI_slope				
0.68	1336.9	1309.9	1258.1	1154.6
0.958	1690.9	1655.1	1591.3	1472.7
1.236	2045.0	2000.3	1924.6	1790.7
1.514	2432.1	2377.7	2289.0	2138.5
1.792	2753.1	2690.7	2591.1	2426.9
2.07	3107.0	3035.9	2924.3	2744.9
TTSE				
85	1807.3	1815.1	1745.0	1669.2
100	1806.0	1800.7	1721.9	1637.7
115	1808.4	1782.5	1704.4	1606.7
130	1805.7	1758.8	1695.4	1570.6
145	1795.0	1750.8	1677.8	1539.7
160	1770.9	1737.6	1664.9	1528.3
TTBE				
383	1345.8	1307.5	1268.3	1101.7
433	1465.2	1428.1	1374.6	1200.8
483	1583.1	1546.6	1486.9	1317.1
533	1708.4	1665.2	1603.6	1471.6
583	1345.8	1777.1	1718.9	1628.7
633	1941.3	1894.3	1847.6	1792.9
PHINT				
70	1257.0	1267.7	1328.3	1224.7
81	1398.1	1410.3	1461.7	1299.2
91	1523.0	1532.2	1545.2	1318.3
103	1664.8	1652.0	1584.4	1388.4
114	1743.8	1702.8	1643.4	1501.7
125	1765.3	1731.6	1736.1	1697.3

Appendix G

RMSE of wheat yield predictions after varying meteorological during sensitivity analysis.

Parameter	Planting date			
	10 April	25 April	10 May	25 May
VPD				
-300	559.1	556.4	576.8	617.1
-200	484.2	488.1	518.8	565.7
-100	435.9	446.8	487.3	541.1
-50	423.2	437.4	482.0	538.9
50	420.7	440.2	490.7	552.6
100	430.2	451.8	503.8	567.4
200	468.8	492.6	545.2	610.2
300	527.6	551.6	602.0	666.3
Tavg				
-6	1024.6	958.1	1322.4	1307.1
-5	1109.1	1111.8	1161.4	1128.2
-4	776.8	895.6	1134.4	959.5
-3	864.3	941.9	812.1	852.8
-2	643.6	643.6	763.8	699.0
2	355.6	377.8	419.1	484.4
3	380.4	387.4	422.4	486.7
4	423.4	420.2	437.2	492.6
5	475.5	463.7	460.3	504.3
6	521.0	511.5	491.5	520.4
PAR				
-4	411.8	434.1	485.1	546.0
-3	417.0	438.6	489.4	549.8
-2	425.1	445.9	496.6	556.3
-1	435.1	455.2	505.8	564.7
1	458.1	477.0	527.7	586.0
2	470.1	488.5	539.3	597.4
3	481.8	499.9	550.9	608.9
4	492.8	510.7	562.0	620.0

Appendix H

RMSE of wheat yield predictions after varying physiological parameters during sensitivity analysis.

Parameter	Planting date			
	10 April	25 April	10 May	25 May
RUE				
1.224	613.7	633.4	672.4	719.6
1.437	523.2	545.5	590.8	645.4
1.649	454.7	478.2	528.3	588.3
1.862	413.9	436.8	489.0	552.1
2.075	406.5	426.3	477.1	539.2
2.287	433.2	448.0	493.5	550.7
2.5	490.7	499.4	536.8	585.8
HI_slope				
0.68	440.9	463.7	513.3	576.5
0.958	409.3	427.8	477.1	537.9
1.236	527.0	534.2	571.2	620.5
1.514	754.1	745.7	757.8	806.7
1.792	989.9	969.6	966.4	965.0
2.07	1270.0	1239.5	1204.0	1121.8
TTSE				
85	440.8	459.1	509.1	549.3
100	437.3	456.0	504.2	542.1
115	433.2	451.9	503.5	532.6
130	428.0	447.2	501.0	527.2
145	424.5	444.8	496.3	529.2
160	421.6	442.0	491.6	535.8
TTBE				
383	425.3	456.7	503.4	584.8
433	401.7	428.2	475.9	550.2
483	397.1	416.4	464.4	523.4
533	410.0	426.9	476.0	533.3
583	425.3	456.1	489.7	563.0
633	495.7	511.1	534.4	619.1
PHINT				
70	436.4	442.4	447.4	506.7
81	393.9	400.4	408.1	483.4
91	372.3	379.6	406.9	488.7
103	374.5	393.8	428.0	500.8
114	415.7	429.5	478.9	534.1
125	479.7	480.5	541.9	639.8

Appendix I

Mean wheat yield resulting from differing climate scenarios produces during sensitivity analysis.

PAR	\-6	\-5	\-4	\-3	\-2	\-1	1	2	3	4	5	6	VPD
-4	2229	2450	2397	2147	1879	1710	1488	1388	1284	1181	1084	1001	-300
-3.5	2126	2380	2301	2074	1819	1656	1442	1347	1246	1147	1054	974	-250
-3	1988	2289	2232	2023	1762	1601	1395	1304	1208	1112	1023	945	-200
-2.5	1946	2206	2136	1927	1696	1545	1348	1260	1168	1076	990	916	-150
-2	1859	2126	2056	1848	1636	1488	1299	1216	1128	1040	957	886	-100
-1.5	1796	2014	1965	1779	1567	1430	1250	1171	1087	1003	924	855	-50
1.5	1639	1895	1829	1688	1485	1356	1185	1111	1033	955	881	816	50
2	1585	1803	1734	1613	1421	1294	1132	1062	989	914	844	783	100
2.5	1490	1677	1664	1546	1354	1232	1079	1013	944	873	807	749	150
3	1380	1599	1556	1463	1291	1171	1025	963	899	832	770	715	200
3.5	1263	1502	1463	1368	1224	1110	972	914	854	791	733	681	250
4	1217	1409	1385	1294	1144	1050	920	866	809	751	647	600	300

(TAVG)

Appendix J

Correlation (r) between predicted and observed wheat yield resulting from differing climate scenarios produces during sensitivity analysis.

PAR	TAVG												VPD
	-6	-5	-4	-3	-2	-1	1	2	3	4	5	6	
-4	0.50	0.50	0.75	0.66	0.68	0.70	0.74	0.75	0.75	0.66	0.74	0.74	-300
-3.5	0.51	0.50	0.75	0.65	0.68	0.69	0.73	0.75	0.75	0.75	0.73	0.73	-250
-3	0.53	0.50	0.76	0.64	0.67	0.69	0.73	0.74	0.74	0.74	0.73	0.72	-200
-2.5	0.53	0.51	0.74	0.64	0.67	0.68	0.72	0.73	0.74	0.73	0.72	0.72	-150
-2	0.52	0.53	0.75	0.64	0.66	0.68	0.71	0.73	0.73	0.73	0.72	0.71	-100
-1.5	0.53	0.50	0.74	0.63	0.66	0.67	0.71	0.72	0.73	0.72	0.71	0.71	-50
1.5	0.53	0.51	0.74	0.62	0.64	0.65	0.69	0.71	0.72	0.72	0.70	0.69	50
2	0.54	0.52	0.74	0.62	0.64	0.65	0.69	0.70	0.71	0.70	0.69	0.69	100
2.5	0.52	0.52	0.72	0.61	0.63	0.64	0.68	0.70	0.70	0.70	0.69	0.68	150
3	0.53	0.52	0.73	0.60	0.62	0.64	0.68	0.69	0.70	0.69	0.68	0.68	200
3.5	0.53	0.52	0.73	0.61	0.62	0.63	0.67	0.69	0.69	0.69	0.68	0.68	250
4	0.54	0.53	0.74	0.60	0.63	0.63	0.67	0.68	0.69	0.68	0.67	0.50	300

Appendix K

Range of wheat yield predictions resulting from differing climate scenarios produces during sensitivity analysis.

PAR	-6	-5	-4	-3	-2	-1	1	2	3	4	5	6	VPD
						TAVG							
-4	970	4412	3286	2534	2084	1924	1725	1589	1479	1352	1205	1089	-300
-3.5	930	4312	3216	2484	2047	1894	1700	1567	1460	1332	1187	1074	-250
-3	1094	4139	3142	2431	2008	1860	1673	1543	1438	1310	1168	1057	-200
-2.5	1102	4219	3065	2374	1965	1824	1643	1516	1414	1289	1147	1039	-150
-2	867	4113	2991	2315	1920	1785	1610	1487	1387	1265	1125	1020	-100
-1.5	886	3876	2900	2253	1872	1743	1575	1455	1359	1239	1101	1000	-50
1.5	871	3803	2842	2213	1846	1723	1561	1444	1349	1230	1094	995	50
2	891	3603	2742	2137	1786	1669	1514	1402	1310	1196	1064	968	100
2.5	732	3489	2634	2060	1723	1612	1465	1357	1270	1160	1032	940	150
3	678	3448	2534	1980	1659	1553	1414	1311	1228	1122	1000	911	200
3.5	670	3335	2478	1898	1592	1493	1360	1263	1184	1083	966	881	250
4	726	3081	2317	1815	1524	1430	1305	1213	1138	1042	850	880	300

147

Appendix L

RMSE of wheat yield predictions resulting from differing climate scenarios produces during sensitivity analysis.

PAR	-6	-5	-4	-3	-2	-1 (TAVG)	1	2	3	4	5	6	VPD
-4	1152	1328	1096	1048	701	529	328	288	296	329	379	430	-300
-3.5	1094	1293	1020	1007	678	519	334	302	314	350	401	452	-250
-3	1030	1227	943	979	674	511	343	318	335	373	425	475	-200
-2.5	1025	1187	891	922	638	505	355	336	357	398	449	499	-150
-2	1004	1175	820	879	630	502	370	357	381	423	475	523	-100
-1.5	979	1080	767	851	602	502	387	380	407	450	501	549	-50
1.5	971	1016	662	846	626	543	436	429	454	494	542	586	50
2	944	960	607	818	631	547	457	455	483	523	570	613	100
2.5	950	912	593	786	624	555	481	484	513	553	599	641	150
3	920	887	501	754	636	566	508	514	544	584	629	669	200
3.5	925	858	479	732	636	581	537	546	576	615	659	698	250
4	921	836	439	714	603	599	568	579	609	647	726	700	300

148

Appendix M

F-ratio test for predicted and observed wheat yield based on simulations for yield forecasting.

Parameter	AGDD (base temperature, 0°C) prior to maturity											
AGDD	50	100	150	200	250	300	350	400	450	500	550	600
$S^2_{predicted}$	517069	515427	512265	507795	501988	495858	488148	474677	455423	432133	405228	374524
$S^2_{observed}$	362762	362762	362762	362762	362762	362762	362762	362762	362762	362762	362762	362762
F	1.425	1.421	1.412	1.400	1.384	1.367	1.346	1.309	1.255	1.191	1.117	1.032
$P(F<=f)$	0.181	0.184	0.188	0.194	0.202	0.211	0.223	0.245	0.279	0.326	0.388	0.467
$F_{Critical}$	2.16	2.16	2.16	2.16	2.16	2.16	2.16	2.16	2.16	2.16	2.16	2.16
df	27	27	27	27	27	27	27	27	27	27	27	27

149